AEDC-TSR-06-T1

Developing a Data Set and Processing Methodology for Fluid/Structure Interaction Code Validation

Louis Deken, Thomas Tibbals, and James Reed
Aerospace Testing Alliance

Grady P. Saunders and Joseph Yen
Jacobs Technology Inc.

June 2007

Final Report for Period Oct. 2004-Sept. 2006

ARNOLD ENGINEERING DEVELOPMENT CENTER
ARNOLD AIR FORCE BASE, TENNESSEE
AIR FORCE MATERIEL COMMAND
UNITED STATES AIR FORCE

NOTICES

When U. S. Government drawings, specifications, or other data are used for any purpose other than a definitely related Government procurement operation, the Government thereby incurs no responsibility nor any obligation whatsoever, and the fact that the Government may have formulated, furnished, or in any way supplied the said drawings, specifications, or other data, is not to be regarded by implication or otherwise, as in any manner licensing the holder or any other person or corporation, or conveying any rights or permission to manufacture, use, or sell any patented invention that may in any way be related thereto.

Qualified users may obtain copies of this report from the Defense Technical Information Center.

References to named commercial products in this report are not to be considered in any sense as an endorsement of the product by the United States Air Force or the Government.

This report has been reviewed by the Office of Public Affairs (PA) and is releasable to the National Technical Information Service (NTIS). At NTIS, it will be available to the general public, including foreign nations.

DESTRUCTION NOTICE

For unclassified documents, destroy by any method that will prevent disclosure or reconstruction of the document.

APPROVAL STATEMENT

This report has been reviewed and approved.

CHARLES V. VINING
Technology Project Engineer,
Technology Division, Capabilities Integration Directorate

Approved for publication:

FOR THE COMMANDER

THOMAS P. FETTERHOFF
Chief, Technology Division
Capabilities Integration Directorate

REPORT DOCUMENTATION PAGE

Form Approved
OMB No. 0704-0188

PLEASE DO NOT RETURN YOUR FORM TO THE ABOVE ADDRESS

1. REPORT DATE (DD-MM-YYYY)	2. REPORT TYPE	3. DATES COVERED *(From – To)*
xx-06-2007	Final	Oct. 2004 – Sept. 2006

4. TITLE AND SUBTITLE
Developing a Data Set and Processing Methodology for Fluid/Structure Interaction Code Validation

5a. CONTRACT NUMBER

5b. GRANT NUMBER

5c. PROGRAM ELEMENT NUMBER

6. AUTHOR(S)
Deken, Louis A., Tibbals, Thomas F., and Reed, James A.
Aerospace Testing Alliance

Saunders, Grady P. and Yen, Joseph
Jacobs Technology Inc.

5d. PROJECT NUMBER
11012

5e. TASK NUMBER

5f. WORK UNIT NUMBER

7. PERFORMING ORGANIZATION NAME(S) AND ADDRESS(ES)
Arnold Engineering Development Center (AEDC/XR)
Arnold Air Force Base, TN 37389

8. PERFORMING ORGANIZATION REPORT NO.
AEDC-TSR-06-T1

9. SPONSORING/MONITORING AGENCY NAME(S) AND ADDRESS(ES)
Air Force Flight Test Center
Edwards Air Force Base, CA

10. SPONSOR/MONITOR'S ACRONYM(S)

11. SPONSOR/MONITOR'S REPORT NUMBER(S)

12. DISTRIBUTION/AVAILABILITY STATEMENT
Statement A: Approved for public release; distribution is unlimited.

13. SUPPLEMENTARY NOTES
Available in the Defense Technical Information Center (DTIC).

14. ABSTRACT
The purpose of the testing reported herein was to obtain data describing fluid and structural behavior (interaction of fluid on structure and of structure on fluid) in a controlled experiment in a systematic manner. These data are to be used for (a) validation of fluid/structure interaction (FSI) modeling codes and (b) to demonstrate a process for archiving and accessing the data. The approach, which uses two types of models (wing and tethered mass), was to obtain ambient upstream, wall, and downstream static and dynamic fluid pressures for the models in various dynamic conditions.

15. Subject Terms
fluid structure interaction, test data, models

16. SECURITY CLASSIFICATION OF:			17. LIMITATION OF ABSTRACT	18. NUMBER OF PAGES	19A. NAME OF RESPONSIBLE PERSON
a. report	b. abstract	c. this page			Donald J. Malloy
Unclassified	Unclassified	Unclassified	Same as Report	123	19B. TELEPHONE NUMBER *(Include area code)* 931-454-4112

CONTENTS

ILLUSTRATIONS

Figure

APPENDICES

Appendix

EXECUTIVE SUMMARY

The purpose of the testing reported herein was to obtain data describing fluid and structural behavior (interaction of fluid on structure and of structure on fluid) in a controlled experiment in a systematic manner. These data are to be used to (1) validate fluid/structure interaction (FSI) modeling codes and (2) demonstrate a process for archiving and accessing the data. The approach, which used two types of models (wing and tethered mass), was to obtain ambient upstream (wall) and static and dynamic downstream fluid pressures for the models in various dynamic conditions. For the airfoil, additional information was gathered on tip accelerations, surface dynamic pressures, and displacements of geometrically identical rigid and flexible airfoils oscillated mechanically, via an oscillation mechanism, and naturally, in the case of the flexible airfoil, in pitch (torsion) and flap modes over a range of low Mach numbers. The major benefit of this program is that it has provided realistic data that have the potential to:

- Simulate real structural behavior of aerosurfaces in flight
- Provide real-time structural deflection correction technique of test data during wind tunnel test
- Better predict structural behavior for the design of structures in a dynamic flow region

The program included the following major phases:

- Development of a survivable test article(s) that can be excited either by flow (naturally) or mechanically, at resonance
- Development of a mechanism to mechanically induce periodic oscillations of the test article
- Characterization of a test article (frequency response and displacements) using a shaker table for comparison to natural oscillations in the wind tunnel
- Validation of the structural model of a test article and the flow model of the tunnel
- Evaluation of test article response in the test cell (mechanically induced)
- Examination of differences in response plus excitation energy input to assess fluid damping characteristics
- Acquisition of detailed surface pressures for 1) a rigid airfoil in controlled-forced oscillation and 2) a flexible airfoil in natural (flow-induced) oscillation
- Development of a database and GUI to allow simple interaction with the data for analysis and comparison with fluid/structural models

The program was successfully accomplished and is reported herein. Chapter 1 presents the testing program using airfoils as the test article; Chapter 2 presents the program using the tethered-mass test article.

1.0 FLUID/STRUCTURE INTERACTION EXPERIMENTS FOR CODE VALIDATION

1.1 INTRODUCTION

The Air Force Test and Evaluation (T&E) centers at the Air Force Flight Test Center (AFFTC) and the Arnold Engineering Development Center (AEDC) have a continuing need to reduce flight vehicle development costs and to increase the safety and reliability of flight- and ground-test activities. Flight vehicle structural integrity is critical for test and operational pilot safety and can be predicted by computer simulations of flow-induced motions of aircraft structural components. Ground-test activities require high-fidelity estimates of test article movement and distortion. Fluid structural simulations can predict test article responses to fluid flow and increase confidence in test data reduction when distortions are present. These simulations can reduce concern about structural stability and fatigue in test article components and, in general, in facility support structures and rotating machinery blading. Both T&E centers require computational predictions of control-surface effectiveness on air-released flight-test vehicles and stores that are subject to mutual interference effects of deformations with the parent vehicle. These needs may be met with the advanced capabilities of modeling and simulation tools that will analyze deformations and/or motion of structures in high-dynamic-pressure flow regimes. Additionally, improved safety and structural integrity can be achieved by advancing modeling and simulation aeroelasticity tools to predict the deformations and fatigue of test articles and structures in flow environments, for both internal (as for engine structures) and external flows. Improved fluid structural interaction (FSI) capabilities can result in significant cost savings by providing critical flow-induced structural response or stress information for structural mechanical systems. This technology's prediction of aeroelastic structural performance of mechanical/structural systems can also support general, flow-induced operational maintenance and safety needs.

Acquiring an effective fluid/structure interaction (FSI) modeling and simulation capability requires expertise in both structural and CFD analysis techniques. Using the Modeling and Simulation Test and Evaluation Resource (MASTER) project, AEDC and AFFTC have formed a team to advance FSI analysis capabilities that can support a variety of Air Force programs. The purpose of this joint effort is to provide validated FSI analysis and simulation tools that are standardized across both AEDC and AFFTC test centers that, when completed, will be readily available for use in the T&E community. These tools will support test and evaluation of various DoD flight systems and help provide reliable simulations for aircraft and wind tunnel structural responses and loads under real test conditions. Capabilities of these tools include accurate prediction of aeroelastically induced deformations, modal frequencies and shapes, fluid flow pressures, temperatures, flow angularity, and Mach number, etc.

This section of the report covers a wind tunnel FSI test program conducted for the validation of the computational technology developed for AFFTC by the University of Colorado (U of CO) Center for Aerospace Structures. This technology, developed with Air Force Office of Scientific Research (AFOSR) funding, provides the framework for flutter and FSI prediction capabilities. It advances modeling and simulation tools to determine flow-induced deformations of a structure in a flow environment. The U of CO software was installed at AFFTC and AEDC for validation and transition to operational use at each center. Once the FSI technology is validated, it provides a modeling and

simulation capability that can help reduce cost and cycle time, predict flow-induced dynamic structural stability, and predict quality of test data for ground and flight testing. Although the U of CO technology is aimed toward the prediction of flutter onset during flight testing at AFFTC, it is readily adaptable to needs at AEDC and other centers. This technology supports fluid-structural interaction applications such as separation of flexible stores, test article support devices, general FSI modeling and simulations, and compressor and turbine blade analysis and simulations.

To ensure the accuracy of the U of CO technology, validation using flight-test data and test data from a wind tunnel controlled environment was required. The validation test data from an F-16 aircraft flight test were obtained by the Air Force Test Pilot School (TPS) located at AFFTC. Flight dynamic response data were collected from the F-16 configured with and without stores. The flight profiles flown by the aircraft represented accelerations to supersonic conditions and to elevated g-conditions that were designed to yield limit-cycle-oscillations (LCO) of some aircraft flexural modes. These data were used by the U of CO to validate fluid and structural F-16 model simulations of the test flights. This use also demonstrated an analysis approach that could be applied to these types of tests to clear a flutter envelope instead of a stabilized point-to-point clearance. This analysis validated the structural response of the F-16 in the flow environment, but it did not validate the fluid responses or the fluid-structural interaction of the flexible structure in the flow. The current approach can improve overall safety by providing the means to see frequency and damping trends and can provide correlations between flight-test and theoretical data. However, the flight tests do not validate the simulation of flow effects on secondary structural components downstream of the primary structure.

For successful completion of the validation process, fluid and structural interaction data in a controlled test environment are required. During the initial search for validation data, numerous test reports were available from wind tunnel tests performed at AEDC and other facilities. However, the data collected were focused on a specific purpose such as structural response or effects on the flow stream. For fluid structural interaction validation purposes, it's important that the data available represent concurrent detailed information about the response of the structure and its interaction with/on the fluid stream. Because of the lack of concurrent fluid-structural data, it was concluded that a test must be performed to build a database of reliable interaction data that could be used for validation of U of CO FSI codes. The flexible structural response desired was large deformations that could affect the fluid flow in an LCO condition. Additionally, the test article used must have sufficient flexibility to permit flow-induced LCO behavior at more than one flow condition and frequency. This report summarizes the FSI testing performed under the MASTER program to collect data from a controlled test environment for validation of the U of CO technology or other FSI codes as needed.

1.2. APPARATUS

1.2.1 General Description

A small wind tunnel fluid structure interaction test was developed to provide fluid and structural data to be used for FSI code validation purposes. The structural data collected included structural transient-flow-induced pressures on the surface and the corresponding deformations of the structure (either directly or inferred from embedded strain gages). For the fluid data, a rake of pressure transducers was used to record variations of flow pressures downstream of the flexible structure, and wall static taps in

the plane of the airfoil provided additional transient-pressure data. The structure developed for the FSI test included two airfoils, one classified as rigid and the other as flexible. The rigid airfoil provided data for a structure where flow-induced deformations can be ignored, and the flexible airfoil provided data where flexibility permits a structural LCO to occur naturally as a result of the fluid interaction with the airfoil. Additionally, the design provided the ability to force oscillations in the rigid airfoil so that test data could be obtained to benchmark the difference between forced rigid structural oscillations and flexible flow-induced structural oscillations. The design also provided data for validation of simulations for control surface effects on the flow. Important focus areas for the developed test program included instrumentation, data collection, airfoil properties, and other tunnel issues (sensitivities) associated with the test so that "true and reliable" fluid-structural interaction data could be collected. Test data thus obtained can then be used for comparisons with the predictions of the U of CO model simulations or other FSI codes for validation purposes.

1.2.2 FACILITY DESCRIPTION

The FSI test was performed in a small wind tunnel modified to provide for data acquisition of concurrent flow and structural interaction data at ambient conditions. A new test section was designed with a wing oscillation mechanism (WOM) that provided preset oscillation frequencies in either flap mode or pitch mode at preset angles of attack or flap angle for a rigid airfoil. This mechanism also serves as a mounting table for a flexible airfoil. Jacobs Technology Inc. (JTI) provided support in tunnel and test section design, modifications, fabrication, and facility operations to meet specified FSI requirements. The FSI experimental requirements for a rigid airfoil included the following capabilities:

Pitch frequencies..... 0 to 50 Hz

Angle of attack..... ± 20 deg

Flap frequencies..... 0 to 10 Hz

Flap angle..... ± 15 deg

Tunnel velocity ..... Up to Mach 0.5 Maximum

All tunnel segments were rectangular cross sections, and the test section inside dimensions were 14.5 in. wide by 16 in. high. The FSI tunnel consists of a 40-in. by 38-in. inlet followed by a smooth contraction in 51.0 in. to the 14.5-in. by 16.0-in. test section. The geometry for the contraction contour is shown in Table 1.The diffuser sections transition from the test section to a 30-in. by 30-in. section in an acoustic corner just upstream of the tunnel fans. The wall slopes are 2.27 deg in elevation and 2.52 deg in the plan views. The basic structure was plywood with a Plexiglas® test section and a fiberglass contraction section. All joints were sanded flush or at a minimum had a backward step of no more than 1/16 in. Two fan configurations were used during testing. For Mach numbers up to 0.3, a single fan was used. To achieve Mach numbers between 0.2 and 0.5, two fan units were installed in parallel. The tunnel geometry is shown from the inlet through the diffuser sections in Figs. 1 and 2.

A CFD analysis of the wind tunnel was performed using the CFD code NXAIR to provide a basic model for other analysts and to satisfy concerns about flow uniformity near the inlet because of its close proximity to other facility walls inside the wind tunnel building. A report describing the CFD analysis and the results is contained in Appendix A.

1.2.2.1 Jacobs Technology Inc. Test Facility

The FSI testing was performed at the Jacobs Technology Inc. (JTI) Fluid Dynamics Laboratory (FDL) at the Tullahoma, TN office location. The FDL is a multipurpose laboratory where experimental testing is performed and where field measurement equipment is built, checked out, and housed.

From FY02 through FY06, JTI has supported the FSI program from development through final data acquisition. The descriptions below briefly summarize the work performed under FSI support and test contracts.

During the initial contract, JTI designed and procured the wind tunnel ductwork for the single-fan wind tunnel circuit arrangement. They also designed the WOM to drive a rigid airfoil in both pitch and flap modes in the wind tunnel test section.

After completion of the design, JTI also procured the WOM and installed the WOM and wind tunnel components. The first set of experiments was performed on a rigid airfoil without instrumentation and on the first flexible airfoil built by the University of Tennessee Space Institute (UTSI), which was designed to flutter without mechanically forced oscillations. JTI technicians also installed surface pressure instrumentation in an instrumented rigid airfoil.

After testing had been performed with a single-fan configuration to a Mach number of 0.3, the JTI wind tunnel was modified to a parallel two-fan arrangement to increase the test section Mach number capability to 0.45. The instrumented rigid airfoil, as well as various flexible airfoil designs, was then tested to a Mach number of 0.45.

After the initial testing of the various airfoils, an exhaustive test matrix was completed for various flexible airfoils. A flexible airfoil with onboard telemetry built by UTSI was also tested. JTI supported data analysis by providing a data analysis capability to reduce the copious amount of data generated. After completion of the data reduction code, project reports were written to summarize the FSI test support.

1.2.2.2 Wing Oscillator Mechanism (WOM) Design

A mechanism was designed to oscillate a rigid airfoil at various pitch and flap angles and at various frequencies. The basic concept is shown in Fig. 3. It is essentially a simple harmonic motion oscillator with provisions for speed control and balancing. The design of a WOM provides for rigid airfoil oscillation capabilities to simulate twisting [wing pitching or angle-of-attack (AoA) oscillation] and flapping vibration modes for measurement of airfoil surface pressure distributions.

The WOM capabilities are 4 to 14 deg at 0 to 10Hz for the flap mode, and 4 to 20 deg at 0 to 45 Hz in the pitch/AoA mode. The frame of the shaker was designed to be rigid with a first natural frequency of 120 Hz to ensure that resonance of the table was not excited. To accomplish this, the frame was anchored to the laboratory floor with sleeve-type Hilti

concrete anchors. A set of mechanical interlocks allows the shaker pushrod to drive the test article shaft about the pitch or flap axis, but not simultaneously. Pitch/flap angle adjustment is provided by a variable position plate on the drive motor flywheel. Changing the position of the plate varies the stroke of the pushrod, thereby changing the pitch/flap angle. A variable-frequency drive (VFD) was used to control the oscillation frequency of the test article. Photos of the shaker table apparatus installed in the test section are shown in Figs. 4a and b.

1.2.2.3 Wind Tunnel Design (One Fan)

The original wind tunnel design used a single fan to produce test section Mach numbers around 0.3. The flow entered the wind tunnel stilling chamber through an open bellmouth inlet and FOD screen. There the flow was conditioned by a honeycomb with an L/d of 16 and two 57-percent open area screens. The flow was then fed through a "picture frame" rectangular contraction to the 14.5-in.- wide, 16-in.- high, 42-in.-long test section. A 12-in.- long test section extension downstream held the ATA 9-probe rake. A series of three pyramidal diffuser sections transition from the 14.5 by 16 test section to a 30-in.-square cross section. The flow then enters the acoustic corner. The corner is lined with perforated sheet with 12-in.-thick annular insulation and acoustic turning vanes. Downstream of the corner is an inline silencer. The duct then transitions to the fan inlet. The fan is a 125-hp Twin City 400-HIB that exhausts to atmosphere. A sketch of the single-fan wind tunnel circuit is shown in Fig. 5.

1.2.2.4 Wind Tunnel Design (Two Fans)

The two-parallel-fan circuit increases the Mach number capability of the wind tunnel circuit to a maximum of 0.45. The ducting from the bellmouth inlet through the last pyramidal diffuser section (30-in.-square outlet) was identical to the single-fan circuit layout. All new 1/8-in.-thick galvanized steel ductwork was installed from the last wooden diffuser section to the fans. A diffusing square-to-round transition was installed downstream of the last pyramidal diffuser to transition from a 30-in. square to a 48-in. diameter. Attached to the transition exit was an inline centerbody-type silencer. The flow was then turned through an acoustic corner. The acoustic corner was similar in design to that for the single-fan circuit. The perforated ducting of the flow path was transitioned to square so that equal-length acoustic turning vanes could be used. The pressure shell was circular for strength and stiffness under external pressure loading. A tee was installed downstream of the corner to split the flow between the two fans. Transition ducting was then installed downstream of the tee to the inlets of both fans. A sketch of the parallel fans setup is shown in Fig. 6.

1.2.2.5 Facility Instrumentation

JTI provided the pressure and temperature instrumentation and controls necessary to control wind tunnel Mach number, fan speed, or test section velocity. The facility pressure system consists of a high-accuracy MKS® absolute pressure transducer and two high-accuracy MKS differential pressure transducers. The MKS system was also used early in the test program to take empty section pitot-static survey measurements. A Pressure Systems Inc. (PSI) pressure measurement system was also provided to take slow-response pressure measurements. The PSI system was used to take static pressure measurements on the vertical wall of the test section and on the instrumented rigid airfoil, and total pressures on the ATA-provided traversing rake in conjunction with

dynamic pressure measurements made by the AEDC Computer-Assisted Dynamic Data Monitoring and Analysis (CADDMAS) data system. All PSI system measurements were sent to the CADDMAS system via Ethernet connection and recorded by the CADDMAS. A TSI hot-wire anemometer system was provided to take empty test section velocity and turbulence survey measurements. Data from the pitot-static and hot-wire surveys are presented in the Test Section Survey Data section. Details of the instrumentation and control system hardware are discussed in the following sections.

a) LabView® Code - The LabView code was used to read the wind tunnel pressure measurement data and control the fan RPM set point. The test section total and dynamic pressures were read into the program, and the Mach number calculated, by:

$$M = \left[\frac{2}{\gamma - 1} \cdot \left[\left(1 - \frac{q}{p_t} \right)^{\frac{-(\gamma-1)}{\gamma}} - 1 \right] \right]^{\frac{1}{2}}$$

where q is simply the difference between total and static pressures ($q = p_t - p$). The analog set point signal to the fan was then adjusted using a standard proportional-integral-derivative control algorithm. For simplicity, one fan acts as master and one as slave, where one receives a signal at a fixed proportion to the other (called the "following ratio"). The proper following ratio was found when the percentage of maximum power of the two fans matched at the maximum Mach number test point.

b) MKS Transducers - MKS® Model 698 differential pressure transducers were used to measure the gauge pressure of the total and static pressure probes and the test section dynamic pressure. The transducers have a 0- to 100-torr range, a resolution of 1 x 10^{-6} of full scale, and a manufacturer's listed accuracy of 0.05 percent of transducer reading. An MKS® Model 690 absolute pressure transducer was used to measure test section total pressure. The absolute transducer has a 0-to-1000 torr range, a resolution of 1 x 10^{-6} of full scale, and a manufacturer's listed accuracy of 0.05 percent of transducer reading. Both transducer models have a 10-KHz low-pass filter.

c) Pitot-Static Probes – A United Sensor® pitot-static probe was used to take total and static pressure measurements in the test section. The probe had a 0.25-in. OD with a hemispherical head, a 0.088 in.-diam total pressure orifice, and four diametrically opposed 0.033-in.-diam static pressure orifices located 1 in. aft of the probe nose. The probes' shank lengths (parallel to flow) were 3.5 in. (14 diameters). The test section probe height (normal to flow) was 24 in.

d) Flow Angle Probe - A United Sensor® three-dimensional directional probe, P/N DA-250-24-CD, was used to measure flow angularity fluctuations in the test section. The primary sensing orifices are 0.031-in. in diameter drilled through to a 0.032-in. diam by 1.5-in.-long passage. This passage then transitions to a 0.047-in. passage through the rest of the probe. The overall probe diameter is 0.25 in., and overall length is 24 in.. The primary sensing orifices are located in a

small wedge machined into the 0.25-in.-diam body of the probe. The apex of the wedge is truncated to form a flat-nosed wedge. A third sensing orifice is located in the nose of the wedge. During testing, the primary sensing orifices, on opposite sides of the wedge, were both connected to the MKS sensor and recorded simultaneously.

e) PSI 8400 System - The PSI 8400 system was used to measure the "steady-state," or low-frequency response, static pressures on the test section inboard wall and the instrumented rigid airfoil, as well as the total pressures on the ATA rake. These measurements were taken in conjunction with the high-frequency response data taken by ATA's CADDMAS system. The PSI system consists of the system processor (SP), pressure calibration units (PCU), scanner digitizer units (SDU), and an ESP-64 pressure scanner. The overall accuracy of the PSI 8400 system is ± 0.05 percent of full scale, or ± 0.2 in. water column (15 psi full scale).

i) System Processor - The SP provides all control and data reduction functions for the System 8400 with a 32-bit microprocessor, a VME bus, parallel processing, and firmware programs. The SP is connected to the host computer via a GPIB interface. The host computer, the lab PC, uses the JTI-developed TestView® to interface the user to the SP, issue all high-level commands, and direct the flow of data within the system.

ii) Pressure Calibration Unit - The PCU is a general purpose, digitally controlled, pneumatic calibration source and/or pressure generator. The PCU controls the porting of run and calibration reference pressures and the flow of scanner control pressures. The module consists of pneumatic valving and control elements plus two main circuit boards.

iii) Scanner Digitizer Units - The SDU performs analog-to-digital conversion of the analog signal from the pressure scanners. Data from each scanner pressure port are received via the scanner interface and converted to 16-bit digital raw data words.

iv) ESP-64 Pressure Scanner - The ESP-64 pressure scanner is a pressure transducer per port sensing device with online calibration designed for multipressure measurement applications. The scanner consists of 64 silicon pressure transducers whose analog outputs are multiplexed within the scanner. The analog outputs are amplified via an internal instrumentation amplifier to provide a full-scale output of ± 5 VDC nominally. The scanner also features a calibration valve that allows the transducers to be calibrated online. When placed in the "calibrate" position, all pressure transducers are manifolded to a common "calibrate" port to allow calibration pressures to be applied simultaneously to all transducers.

f) TSI Hot-Wire Anemometer - A TSI® IFA 300 Constant-Temperature Anemometer System was used to obtain the velocity components of the turbulence in the test section. The TSI system utilizes constant temperature x-film probes. The samples were acquired at 20 KHz with a 300-Hz analog low-pass filter. A LabView code was used to acquire and analyze the hot-wire anemometer data.

1.2.2.6 Test Section Survey Data

a) Pitot-Static Probes - Total and static pressure surveys were performed early in the test program to quantify test section flow quality. Several survey tests were performed on both the vertical and horizontal centerlines in the instrumentation box just aft of the test section. The instrumentation box floor is located where the base of the traversing total pressure rake was affixed during normal testing. The total and static pressure profiles for the vertical and horizontal centerlines at Mach 0.3 are shown in Figs. 7 and 8. There was a slightly more predominate static pressure gradient toward the floor than there was toward the ceiling, as shown in Fig. 7. The test-section-to-instrumentation-box fit was subsequently checked, and a discontinuity was measured. It was found that there was a 1/16-in.-high forward-facing ramp ¾ in. long on the floor and a 1/64-in.-high forward-facing ramp 1-1/2 in. long on the ceiling. An inviscid potential-flow solution was then found for the vertical survey, and this situation shows a similar trend as the experimental data. The potential-flow experimental survey comparison is shown in Fig. 9.

b) Flow Angle Surveys - Flow angle data were taken in the test section at two longitudinal locations. The upstream location was 13-1/2 in. downstream of the test section leading edge. The downstream location was 29 in. downstream of the test section leading edge. Probe ports were located in the ceiling of the test section; therefore, only pitch angle (horizontal plane relative to longitudinal axis) data were taken. Data were taken both with the ATA total pressure rake installed and with the rake removed to investigate the effects of the rake on flow angle. The rake, when installed, was moved to its farthest downstream position. A jig was fabricated to prevent the flow angle probe from rotating during the course of a survey. The probe was first “zeroed” by rotating the probe until the indicated flow angle was zero at the test section centerline. The flow angle jig was then installed. The data reported herein are from the flow angle relative to the test section longitudinal centerline. Figures 10 and 11 show the pitch angle relative to the test section center for Mach 0.25 and 0.4 with the rake installed and removed, respectively. The relative pitch angle is higher near the floor, as would be expected because of the nonuniformity of the floor caused by the shaker table mechanism bulge in the center of the test section. There also appears to be a slight flow angle increase caused by the presence of the total pressure rake.

c) Hot-Wire Surveys - Hot-wire anemometer surveys were conducted on the vertical centerline 13-1/2 in. downstream of the test section leading edge and at an angle such that the survey line passed through the centerline at the test section ceiling and the inboard-side wall/floor corner. The latter are hereafter referred to as the diagonal surveys (although they do not actually subtend the diagonal of the test section) and were performed to investigate the test section corner flows. A sketch of this test setup is shown in Fig. 12. Surveys were performed at both orientations for test Mach numbers of 0.12 and 0.2. The diagonal surveys were facilitated by the manufacture of a replacement plug for the ceiling probe port with an angled split to produce the desired probe angle to reach the inboard corner. The axial velocity profiles for the vertical and diagonal surveys are shown in Figs. 13 and 14, respectively. It is easily seen that the velocity deficit increases rapidly toward the corner. The axial and lateral turbulence intensity levels on the vertical centerline at Mach 0.2 are shown in

Figs. 15 and 16. Likewise, the axial and lateral turbulence intensity levels on the diagonal survey at Mach 0.2 are shown in Figs. 17 and 18. As expected, the turbulence intensity levels are markedly increased in the corner flow regions. It should be noted that the turbulence intensity is higher in the corner flow region partly because of an increase in fluctuating velocity in conjunction with a decrease in mean local velocity.

1.2.3 Test Article Descriptions

1.2.3.1 Basic Airfoil Design

The test articles for this test consisted of the following:

- Noninstrumented rigid airfoil
- Instrumented rigid airfoil
- Several noninstrumented flexible (elastomer) airfoils
- Instrumented flexible airfoil

All of these test articles were of a common airfoil cross section, which was derived from extrusions built by the U.S. Navy (Patuxent River, MD) for the Airborne Icing Tanker spray array system being developed by AFFTC. The airfoil shape is a modified NACA-0020 airfoil with reduced leading-edge radii and the maximum thickness moved aft along the chord for drag optimization (see Fig. 19). The length of all airfoils was 11.2 in. with an added 0.25-in. clearance between the test section floor and the bottom of the airfoil. The chord length of the airfoils was 4.5 in., with the geometry shown in Fig. 19. The cross-sectional geometry of all airfoils (rigid and flexible) were fabricated geometrically the same. Basic airfoil instrumentation included accelerometers in the airfoil cap, pressure transducers on the surface of the airfoil, strain gages on the structural bands inside the flexible airfoils, and a vibrometer to determine deformations at the top of the airfoil (see the instrumentation subsection, 1.2.4, for more details).

The rigid airfoils are made of 6061-T6 aluminum, and the flexible elastomer airfoils are made of Por-a-mold 2020 (Hyperlast North America) with internal metal straps to stiffen the structure and control the natural frequency. The elastomer material properties are shown in Fig. 20 (see Appendix B for nomenclature), and a complete report of the material characterization tests is included as Appendix B.

The instrumented and noninstrumented rigid airfoils were used with the WOM to obtain fluid/structure interaction data under controlled frequency and displacements in pitch and flap oscillation modes. The WOM apparatus was designed by JTI and installed at the center of the test section floor to provide preset oscillation frequencies and angles in either flap (as in a wing changing its dihedral angle) or pitch (as in a wing changing its AoA) modes. The oscillation apparatus also served as a mounting platform for the flexible airfoils. The rigid airfoils were excited within the following capabilities:

Pitch frequencies..... 0 to 50 Hz

Angle of attack..... ± 20 deg

Flap frequencies..... 0 to 10 Hz

Flap angle..... ± 15 deg

The noninstrumented flexible airfoils were used to validate the design of the test article with respect to its ability to naturally flutter within the constraints of the wind tunnel operating envelope. The instrumented airfoils, because of their manufacturing expense, were used only to refine the data set from other test articles with dynamic surface pressures. The basic test article dimensions are shown in Figs. 19 and 21.

1.2.3.2 Flexible Airfoil Design

The flexible airfoils (also called *flex wings*) were designed to ensure that they would undergo steady natural oscillations (torsional flutter) within the constraints of the wind tunnel operating envelope, yet last long enough to allow steady fluid/structure interaction data to be gathered over a variety of Mach numbers within the range of the wind tunnel (Mach numbers 0.0 through 0.43). To accomplish this, it was necessary to minimize stress concentrations of the cantilever mount to minimize fatigue, satisfy the stiffness requirements for the frequencies of interest, and dampen the structure to prevent divergent oscillations. To simplify the design, it was assumed that a basic skeleton could be produced of a specific stiffness that would meet the natural frequency desired and that, because of its mass distribution, covering it with a flexible elastomer would only slightly shift the frequency downward, while simultaneously adding enough damping to prevent rapid fatigue failure. Airfoil torsional flutter equations (Ref. 1) were used to determine the stiffness. Figures 22 and 23 are MathCAD pages illustrating the calculations made to design the flex-wing skeleton. In Fig. 22, cylindrical rods are used as the stiffness member, while in Fig. 23, flat, rectangular bands (straps) are used as stiffness members. (Note that data from Ref. 2 were used in the Fig. 23 calculations.) Figure 24 illustrates a typical flex-wing skeleton for a strap configuration. The flat bands were an evolution of the original design, which started with the solid cylindrical rods. However, the flat bands were selected following rapid fatigue failures during tests on a shaker table and in the wind tunnel because of the stress riser induced in the rods by contact with the base. The flat bands were a close enough match for the stiffness of the cylindrical rods that desired frequencies were essentially preserved. The flat bands also provided excellent fatigue resistance, which resulted in their survival throughout the test program.

The overall lengths of the flex wings are identical to the rigid airfoils. The spring steel band thicknesses were selected to meet stiffness requirements for the frequencies of interest. The bands were placed in the outermost leading- and trailing-edge cavities in the airfoil extrusion base, and they were held rigidly in the base by cross pins and JBWeld® epoxy. The opposite ends of the steel bands were held rigidly in the end cap by two No. 4-40 socket-head cap screws (SHCS). The base was then attached to a 5/8-in. OD by 1/4-in. ID hollow shaft for interfacing to the WOM. The ¼-in.-diam central hole in the shaft allowed for the accelerometer and other instrumentation cables from the test article to pass outside the wind tunnel in a sealed manner.

To fabricate the flex wings, molds were fabricated for casting the elastomer onto the skeleton. Figure 25 illustrates the molds developed for casting the elastomer. (The first telemetry-based six-channel instrumented wing is shown).

Before the airfoils were tested in the wind tunnel, the flex wings were evaluated in both skeletal and poured elastomer form on the AEDC shaker table located at UTSI. Figure 26 illustrates a flex-wing skeleton on the shaker table. (Shown is the first six-channel instrumented version, the circuit board being held in by temporary cable ties, since the elastomer holds the board in the final configuration. The shaker axis is in/out of the plane of the picture.)

Spectra obtained from the shaker testing provided the possible frequencies of oscillation to be expected in the wind tunnel. While only the first bending and first and second torsion modes could be excited in the wind tunnel, the shaker tests were performed through 200 Hz and in two configurations. The shaker table configurations varied only with the orientation of the blade relative to the shaker axis. The first shaker table configuration is shown in Fig. 26. The second configuration was with the flex-wing skeleton rotated 45 deg about the 5/8 shaft to help excite the torsional modes. Figure 27 shows spectra for typical skeleton and poured flex wings.

It is obvious from the above plots that the elastomer shifted the dominant modes downward in frequency and damped the higher resonances, but the first few modes were still available for investigation in the wind tunnel. Also note that the torsion modes are accentuated with the elastomer.

1.2.4 Test Instrumentation

Pressure and accelerometer instrumentation was installed in the test section wall to determine its rigidity and to determine static pressure variations resulting from the test article oscillations, and this instrumentation was installed in the airfoils (rigid, and one flexible) to determine loads and response. Also, a 9-probe total pressure rake was placed downstream of the airfoil for wake surveys. The tunnel wall statics, airfoil surface pressures, and 9-probe rake utilized high-response (10-KHz) transducers. The airfoils also had internal accelerometers to obtain wingtip G-loads and displacements, and these motion measurements were supplemented with an optical vibrometer for measuring tip and midspan vibration frequencies and deflections. Facility instrumentation also provided averaged steady-state parameters that included Mach number, tunnel static pressure and temperature, barometric pressure, ambient temperature, motor speeds, oscillation frequencies and angles (pitch or flap), 9-probe rake position, etc. Figure 28 illustrates the wall statics and 9-probe wake survey rake mounted in the test section. The 9-probe rake was designed and built in-house and is moved fore/aft to discrete, detented (each inch) positions via a cable/crank mechanism. Figure 29 illustrates the horizontal and vertical probe rake configurations used for testing.

All data were acquired on a portable CADDMAS system, which was developed by AEDC, although it is now proprietary to EDAS, Inc., via a CRADA technology transfer to industry. The CADDMAS is a block-driven common clock data acquisition system for real-time, time- and frequency-domain processing and was operated at a sampling rate of 9766 Hz. The CADDMAS provided online, instantaneous spectral and time-domain plots and datapoint strip chart history plots for all parameters (up to 48 analog and 24 TCPIP-based, facility-transferred parameters), with all parameters time-synched. [Analog channels have analog to digital (A2D) on a common clock, with the TCPIP parameters tagged to the analog data blocks.] Figure 30 illustrates a typical CADDMAS display during testing.

1.2.4.1 Instrumented Rigid Wing

The rigid instrumented wing was intended to provide surface pressures as a function of airfoil pitching and flapping under controlled conditions. Thirteen high-response (10-KHz) button transducers were embedded in the surface of the wing as shown in Fig. 31. Wiring for the transducers and cap accelerometer and tubing for the 0.020-in. static taps below each transducer were routed out the hollow support tube to the CADDMAS.

1.2.4.2 Instrumented Flexible Wing

The flexible instrumented wing was intended to provide detailed leading-edge surface pressures as a function of airfoil natural torsional oscillation to better determine the location of dynamic stall. Twelve high-response (10-KHz) absolute 0.063–in. barrel transducers were mounted in the modified cap and plumbed to the flex wing's leading-edge porting strip located one chord from the top of the cap, as shown in Fig. 32. Wiring for the transducers and band strain gages was routed to a miniature data acquisition circuit board located in the top of the wing. The embedded data acquisition system had 16 signal-conditioned channels to acquire data from the twelve transducers, two on-circuit-card accelerometers, and two strap strain gages. The digitized data were transmitted to CADDMAS over a single Cat-5 cable routed with power lines through the hollow support shaft.

1.2.4.3 Vibrometer System

A PolyTec laser vibrometer was used to supplement the other instrumentation for all flexible test articles. The intent was to provide explicit velocities and displacements for various locations of the flex wing.

The laser vibrometer was originally a single-point system subsequently upgraded to provide multipoint scanning capability. The vibrometer has a movable mirror to position the beam at any desired location on the flex wing. Figure 33 illustrates the vibrometer setup as used for this test, while Fig. 34 illustrates a typical measurement pattern on the flex wing. The vibrometer system is capable of providing relative velocity and displacement measurements for up to 512- by 512-point measurement arrays with a ±20 deg scan field in the x and y directions. Depending on the distance to the object to be measured, this translates to very high spatial resolution. An in-house-written code provided the capability to use airfoil coordinates as measurement inputs by calibrating the system based upon position from the object and known scan angles. The vibrometer utilizes a modulated helium-neon laser beam focused on a target with the reflected beam captured by the laser head and compared to a portion of the original modulated beam. The vibrometer measures velocity of a target from the Doppler frequency shift of the reflected light and displacement from the phase shift.

1.2.4.4 Blade and Cone/Cable Displacement Camera

The displacement camera was first used for the tethered mass experiments (see Section 2), but because of its success it was also used for the final series of testing using the instrumented flexible airfoil. The displacement camera was mounted above and downstream of the airfoil, and spot markers were placed on the top of the airfoil cap (see Figs. 35 and 36). ATA-developed software provides for time-based coordinate extraction from the video frames based on camera field of view, aperture, magnification,

and geometry of the camera setup. Any distinct point or edge in the video frame can be referenced, and the data extracted, as it moves in time from frame to frame in the video. The spots were applied to the airfoil cap to provide these distinct points for accurate data extraction and allow for detection of torsional modes. The data extracted could then be Fourier processed to obtain a frequency spectrum for the various modes of oscillation. This video acquisition process was accomplished using a PhotonFocus MV-1024-160 link-based camera. This camera has a 1024 by 1024 focal plane array with 8 bits of data per pixel that can be sampled at 147 frames per second (fps). During the tethered-mass testing, the camera was operated at 100 fps, with a variable zoom lens that allowed settings from 25 up to 125 mm. During the instrumented flexible airfoil testing, the camera was operated at 100 fps with a variable zoom lens that allowed settings from 17 mm up to 150 mm. The camera image was recorded to disk at 100 fps using a Matrox Helios PCI-X framegrabber and a hard-disk RAID array to provide data storage that could handle the approximately 100-MB per second data throughput.

1.3 TEST DESCRIPTION

1.3.1 Test Conditions

Test conditions were specified according to the following parameters:

- Mach number
- Rigid or flex blade
    - Rigid blade flap mode, degrees, and frequency
    - Rigid blade pitch mode, degrees, and frequency
- Pt probe location

Calibrations were performed before each day's first run and as-required afterwards. Ambient pressure and temperature were not controllable, since the tunnel has an ambient inlet, but these conditions were recorded.

A table showing wing type and date of test is provided in Appendix C. For additional information on test conditions, the run log for all data points is contained in Appendix D. The run log includes entries for date, time, datapoint number, angle of attack, Mach number, frequency, mode, hot-wire anemometer (HWA) probe position, velocity, and comments.

The angle of attack for a blade could be set to fixed positions of 0, 4, 8, 12, 16, or 20 deg.

Mach Number Range: For the rigid blade, the Mach number range was from 0.0 to 0.25 in 0.05 increments. For the flexible blades, the Mach number was set in the range from 0.0 to approximately 0.25, depending on how the blade was reacting to the flow. For investigation of the blade response, the Mach number was varied by a small increment of 0.01.

For the rigid blade, the mode was either pitch or flap. For pitch mode, rotation was about the chord centerline from hub to tip with the blade mounted vertically in the test section. The blade frequency was generally 0 (fixed AoA), 10, 20, 30, or 45 Hz.

For flap mode, rotation was about the blade hub at the test section floor from side to side in the test section (lateral oscillation) at a fixed angle of attack. The blade frequency in general was 0 (fixed dihedral angle), 3, 6, or 10 Hz.

The hot-wire anemometer (HWA) data were recorded with no blade mounted in the test section. The hot-wire anemometer was calibrated for velocities from 20 to 80 m/s in 10 m/s increments (66 to 262 ft/s in 33 ft/s increments). Data were taken at velocities of 10, 40, and 70 m/s (33, 131, and 230 ft/s). The HWA position varied from approximately -4 in. to 11 in. from the test section leading edge. The positive direction is downstream from the test section leading edge.

1.3.2 Test Procedure

The normal test procedure consisted of the following:

1. Power up instrumentation, computers, and tunnel operating system
2. Set up vibrometer to look at area of blade desired
3. Check data acquisition computer to ensure it is set up correctly with date and data point. Also, make sure it is in mode to take data and increment datapoint number correctly.
4. Set blade to angle of attack desired
5. Check transducer zeros
6. Take air-off data point
7. Set tunnel conditions for first data point
8. Set blade parameters and rake position desired for data point
9. Take data
10. Check datapoint file to ensure data were actually acquired
11. Set parameters for next data point

1.3.3 Data Reduction

1.3.3.1 Data Processing

Matlab® programs and scripts were developed for the management, processing, and display of the experimental data recorded for the FSI study. These tools provide a convenient and efficient means for retrieving the experimental data matching any desired test condition in the experimental test matrix. Together with the data reduction

software, the experimental data become an easily retrievable database that will be used for code verification of an FSI solver.

1.3.3.2 Introduction

There are two types of test articles; rigid (or solid) airfoils and flexible airfoils. The former are motion-controlled to disturb the freestream flow, while the latter are driven to motion by the flow. For the disparity of physics involved, the test conditions differ significantly.

In the rigid-airfoil study, the airfoil is set to either torsional or flapping motion at different oscillatory frequencies. Different freestream Mach numbers and preset angles of attack are also included in the test matrix. Moreover, the test matrix also accounts for different positions of the wake flow survey rake, traversable in the airfoil downstream. A combination of these parameters must be used to locate a specific experimental data set.

In the flexible airfoil study, the airfoil motion (flutter) is driven by the flow. Continuous Mach number sweep is applied to study the incipient and subsequent flutter motion. Moreover, continuous-position sweep of the wake flow survey rake is also performed. There is no stationary set of test conditions. Also, the airfoil motion in torsional, flapping, or combined modes is dependent on the transient test condition. Moreover, the resulting vibration may be nonstationary (nonperiodic over the period of data recording) where the frequency component or components are time dependent.

For either case in the study, the instrumentation's signals are sampled at a fixed sampling frequency of about 10 KHz. The high-resolution data involve a large amount of data storage space. In general, the flexible airfoil study requires much more storage because of the continuous sweep of Mach number or rake position for longer time periods for the flutter motion observation.

For the differences in test conditions and data storage requirements, two customized sets of data reduction software were developed for compatibility and efficiency. However, either software would work on the recorded data of a similar format, as explained below.

1.3.3.3 Recorded Data Structure

Each data file consists of a group of test conditions representing combinations of different variables. In all data files, two major blocks of information are recorded (header blocks and data blocks), as shown in Fig. 37. A header block, located at the start of the data file, contains the following data recording information:

- File name
- Sample rate
- Number of channels
- Data block size
- Start time

- Recorded time
- Recorded block and exported data information including
  - Number of channels
  - Start time
  - End time

The data block begins with a header row that identifies the data record channels. This is followed by the actual recorded data in columns showing the record time, sampling time interval, and different measurements from the data acquisition channels. Because of the large data size, text editor software, such as Excel (as shown in Fig. 37), will truncate a data file, limiting the scope of access to only a portion of the recorded data.

In the experiment, 48 or more channels of data were recorded. A data channel may have been used to record different signals over the course of the experimental program. The identification of the recorded data is documented in the test log of the experiment. The temporal data are stored in blocks of 4096 rows (records) each. Each test condition includes a number of blocks and may include a partial block. The actual number of blocks varies depending on the data recording time period.

In the experiment, the data acquisition system yields digitized signal in counts, and the information of the counts to engineering units is stored in the C++ binary data format. The current work applies CADDMAS first to generate the data in engineering units in CSV (comma separated value) files, and then to convert the CSV files to Matlab binary files. The conversion is made to achieve a consistent and efficient environment for data management and processing in the Matlab program.

1.3.3.4 Design of Data Reduction Software

The development of the data reduction software is to provide a convenient and efficient tool for retrieving the experimental data matching any desired test condition in the experimental test matrix. The Matlab program and scripts tools by MathWorks were used for the software development. An integrated software implementation is made through graphic user interfaces (GUIs) based on the software facility in Matlab, which was used for data management, processing, and visualization.

The data reduction software operates on the Matlab binary data files, which must be converted from the original CSV files. Because of the large file sizes, the time-consuming conversion process is made separately from the implementations of the GUI functions. The file conversion involves only a format exchange. The completeness of the original data is carefully preserved so that all the recorded information is retrievable. The language scripts of the Matlab program are used to implement the conversion.

As discussed above, separate developments of data reduction software are desired for the rigid and flexible airfoils. These involve different designs of the GUIs and data reduction implementations, which are described in the following sections.

1.3.3.5 Description of Rigid Airfoil Software

The GUIs for the rigid airfoil perform several functions including the following:

- Receive input test condition for experimental data file search
- Activate search function, and return and export the matched file or files
- Receive selection of data file for display
- Receive selection of data channels from the selected data file for display
- Analyze the temporal data in Fourier transform
- Display data in time trace or frequency spectrum
- Provide help information

Also, the GUIs can:

- Receive a user-supplied data file
- Process and display the user data for comparison

These functions are available in the GUI window based on choosing an airfoil motion, an angle of attack, a Mach number, a vibration frequency, and a survey rake position from the corresponding pull-down menus, as shown in Fig. 38, to find data files matching the search criteria. A continuous cascading filtering method was applied for convenient input selection, and this method is explained in the following paragraph.

The continuous cascading filtering process is such that the selection of a parameter (angle of attack, Mach numbers, vibration frequencies, and survey rake positions) will activate a complete search in the test matrix for all available data points matching the parameter. The remaining parameters can be used to refine the search further. When each of the four parameters is chosen, the search for the matched data files can be activated by the action button “Click for search.” The status of the search result will be reported as shown in Fig. 39.

The input reception region can also be used to import a user-supplied data file. The user data, such as a computer simulation result, can be compared to the experimental data. Once imported, the user data can be processed and overlaid in the display window for visual comparison. The user data can be matched, timewise, with the experimental data using the time offset option.

The result of a search for experimental data is shown in Fig. 39. The upper right-hand corner of the figure shows the pull-down menu containing the data points that matched the search criteria. Simultaneously, all these files are exported to the working directory to be used for additional analysis. These output file(s) retain the same file names of prefixes as the data recording files to indicate the origins of the extracted data.

Multiple data channels can be selected for analysis in either a frequency spectrum or a time domain. The original identifications of all the data channels are maintained to provide easy identification with the test logs. The data channels can be referred to the locations of measurement in a graphic, as shown in Fig. 40. Figure 41 shows a data point with two channels in the time domain, while the frequency spectrum is shown in Fig. 42 for the same data. The plot window also displays the mean, standard deviation, and number of data points. Other display options are available under “Tools” on the main menu. An example of a zoom-in on the data is shown in Fig. 43. Figure 44 shows a text window that provides additional information on the GUI functions.

1.3.3.6 Description of Flexible Airfoil Software

The implementation of the flexible airfoil GUIs includes several main functions such as the following:

- Receive selection of data file for display
- Receive selection of data channel from the selected data file for display
- Display data in time trace and time-frequency waterfall contours
- Provide help information
- Enable adding external data (e.g., computer simulation solution) for comparison in display
- Enable processing and displaying multiple channels of experimental data for comparison

Figure 45 shows the flexible airfoil GUI window, where the main data reduction functions can be seen. In the GUI windows, two time-trace plots of the recorded data are designed to illustrate the flutter response (such as the accelerometer data) subject to a control parameter (such as Mach number). However, any recorded parameters can be chosen for display. The sketches showing the data acquisition locations are also available from the GUI window, as shown Fig. 46. An example of the time-trace plots is illustrated in Fig. 47. To speed up the data importing and/or to avoid out-of-display-memory error, a data re-sampling option is available. However, this does not reduce the number of data samples. Such a reduction would cause an aliasing effect in the frequency analysis of other GUI functions.

Figure 48 shows the frequency analysis of sample data using wavelet and Fourier (bottom-right) transforms. The analysis is performed on the data within the time interval specified as shown in the time-trace plots. By default, the maximum frequency range is displayed, and a smaller frequency range can be shown by adjusting the axes display. Several options to the frequency analysis are available. These options are explained in the help functions (push buttons denoted by a question mark) wherever applicable in the GUIs.

A user-supplied data file, such as a computer simulation result, can be imported for separate analysis and/or comparison with the data of interest from the FSI experiment. The user file needs to be in the CSV format and in column order for different channels or

parameters. The detailed requirement is available in the GUI help function ("Info" button). One parameter of the time-trace data can be displayed with or without overlay of the experimental data. The frequency analysis can be activated, which will preserve the bottom-right display window for the user data. Either the wavelet or Fourier transform can be chosen for the frequency analysis. Figure 49 shows the wavelet analysis of sample experimental and sample user-supplied data.

Figure 50 shows the primary software instructions. Several complementary "Help" descriptions are also available in the GUIs next to the applicable subjects, which are not repeated here.

1.4 SUMMARY

An experimental program has been conducted for acquiring data on the interaction of fluid-on-structure and structure-on-fluid. A description of the test facility test-peculiar items and the various wing models has been provided. These wing models included a rigid wing, several wings made of a flexible elastomer material, and a flexible elastomer wing with an embedded telemetry package. (The telemetry package included blade surface pressures, two accelerometers, and a strain gage.) These wings were made such that the stiffness of the various wings was varied. Both steady-state and dynamic data were acquired during the test program. The rigid-wing data were acquired in both torsion mode and bending mode at set angles of attack, Mach numbers, and frequencies. The Mach number for the flexible airfoils was varied until the wing went naturally into either torsion mode or bending mode.

The data gathered during this test program are archived on an external USB hard drive. These data are available on need-to-know basis.

Jacobs Technology Inc. (JTI) where the wind tunnel was located, also developed data access tools based on the Matlab program. Data analysis is still ongoing. Comparison to predictions using the University of Colorado Fluid/Structure Interaction CFD code has not been accomplished because of computer platform/code compatibility issues. This effort will continue into FY07 using project carryover funds.

2.0 AIRFOIL TETHERED-MASS MODELING APPROACH AND VALIDATION EXPERIMENTS

2.1 INTRODUCTION

There are several instances when it is necessary for an aircraft to tow a device behind it. Such requirements range from towing targets to towing trailing wire antennas to launching gliders. Figure 51 illustrates a towed device.

For safe applications of towed devices in flight, understanding and predicting the dynamics of the cable and the stability of the towed device are crucial. Consequently, there is a need to model the cable dynamics of a tethered mass. To this end, experiments were conducted to investigate the phenomena with respect to the tethered-mass center of gravity (CG) position vs. stability and tethered-mass weight compared to cable-mass distribution and length. The major goals of this program were threefold: first, develop of a stable model with appropriate instrumentation and flexibility for cable and CG changes; second, obtain towed-device and cable dynamics data that could be used

for model validation; and third, generate and implement a novel modeling methodology that allows for evolution of the model from simple to complex configurations and analyses. This report documents the experiments performed to date and the data that were gathered. The preliminary cable dynamics modeling scheme is discussed in Ref. 3.

2.2 DESCRIPTION OF EXPERIMENTS

The experiments were to be performed in small, inexpensive wind tunnels at the University of Tennessee Space Institute (UTSI) and Jacobs Technology Inc. in Tullahoma, TN (JTI). Consequently, the tethered-mass problem had to be scaled to meet the constraints of these tunnels, which have test sections that are 20 in. wide by 14 in. high by 42 in. long and 14.5 in. wide by 16 in. high by 36 in. long, respectively. Scaling was such as to allow for an embedded instrumentation package and for the tethered mass to be lifted from the tunnel floor as the tunnel velocity increased. It also allowed significantly large displacements/oscillations without the tethered mass hitting the tunnel walls. Figure 52 illustrates the model in the UTSI wind tunnel. The experiments gathered data for the cable and model oscillations as a function of airspeed (0 to 460 ft/s, or 0 to 0.42 Mach) and cable length, including the transients of lift-off and set-down of the model on the tunnel floor. For the most part, data were gathered for ramps in Mach number, since this allowed capturing all the excited modes with minimal file sizes. However, some steady-state points were recorded to capture details about a specific cable/model oscillation mode.

2.3 TETHERED-MASS DESCRIPTION

A cone shape was selected as the tethered-mass shape since the drag characteristics are well documented in Hoerner, Ref. 4. A commercial plastic model rocket nose cone was used for the skin of the cone. The skeleton of the cone was designed to hold a telemetry instrumentation package, batteries, and a drag measurement beam. Figures 53 and 54 illustrate the cone model details.

The cone is a standard tangent ogive with a surface line described by a second-order curve fit given by

$$y = -0.0092x^2 - 0.0052x + 1.0495,$$

where y is the radius dimension and x is the length, with the origin at the aft center of the model. The resulting caliber is approximately 5.0, with a diameter of 2.10 in. and the nose trimmed to length, as shown in Fig. 54, to allow the passage of the tether string through the cone. The cone is symmetric with the revolution of this line forming the three-dimensional (3D) surface. The C_D is estimated per Hoerner to be approximately 0.20. The rigid skeleton of the tethered mass is made of aluminum. The CG was located at approximately the middle of the length of the tethered mass by balancing the model with lead weights in the nose, sandwiched between the batteries. The material used for the cable ranged from common construction layout line string with a mass-per-length of 0.418 g/ft and a stiffness of 3540 lbf/in. to small-diameter (0.062–in.) wire rope with a mass-per-length of 0.0213 lbm/ft and a stiffness of approximately 5800 lbf/in. The cables were marked every 2 in. so that cable displacement data could be obtained with a video system.

2.4 INSTRUMENTATION DESCRIPTION

The tunnel at UTSI had no facility instrumentation, and the velocity was based on motor control frequency corrected for the inlet ambient conditions. The JTI tunnel was heavily instrumented to obtain model wake pitot and wall static and dynamic pressures, as well as ambient conditions. Within the cone was a small, six-channel data acquisition system that was telemetry based to extract the data without affecting the cable stiffness, with additional communication wires. The data acquisition circuit board had two built-in accelerometers to measure accelerations perpendicular to the circuit board. Two more accelerometers were added on a separate circuit board arranged perpendicular to these (see Fig. 55). Therefore, nose and tail motion could be discerned in the vertical and horizontal planes of motion. The cone was balanced so that it would always roll and remain in a given orientation such that the data would be consistently acquired and the accelerometer positions in space would be known. The accelerometers were capable of measuring ±50g's. A video system was used to capture the motion of the cable and model. This system consisted of a PhotonFocus MV-D1024-160 camera attached to a Matrox Helios frame grabber to capture 1024- by 1024- by 8-bit images at 100 frames/s. These images were recorded to a hard drive disk array in real time for lengths of 15, 30, or 60 s, depending on the datapoint conditions. The images were analyzed using National Instruments LabView and IMAQ tools to perform pattern matching on parts of the tethered mass and on the string/cable that was used to suspend the model in the wind tunnel. Measurements were taken with the camera prior to wind tunnel operation to determine the number of pixels per inch at a particular lens setting, which provided the capability to determine the amount of oscillation movement of the tethered mass and cable. This information was then processed to provide a set of X-Y pairs for each pattern matched in a particular image.

2.5 DATA SET DESCRIPTION

The data were acquired via a telemetry receiver connected to the AEDC CADDMAS, which provided the merging of the telemetry data from the model and facility parameters for the wind tunnel conditions. The CADDMAS telemetry data (used at both facilities) were acquired at a sampling rate of 4000 Hz, and the CADDMAS was used for the JTI tunnel pitot and wall static and dynamic pressures where acquired at 9766 Hz. The raw analog-to-digital converter (A2DC) counts were stored in separate files for each data point. Online in real time, the accelerometer and rope tension data could be viewed in time and frequency domains. While the CADDMAS data are stored in a proprietary format, there is a free viewer available from Experimental Design & Analysis Solutions (EDAS) at their website (http://www.edasinc.com/downloads.html). Figure 56 illustrates the online plots and the type of processing available with the data viewer. Video data were also acquired at a rate of 100 Hz and were synchronized with the start of the CADDMAS data point. These video-recorded data can be processed to obtain the displacements of marked positions on the tether cable and on the edges of the model. Figure 57 illustrates a typical cable dynamics plot from the video data. A spreadsheet describing the data points taken during this testing is included in Appendix E.

2.6 DISCUSSION OF PHENOMENA OBSERVED AND EXPERIMENT CONCERNS

The experiments produced some interesting results. Some of these results are difficult to describe without an accompanying video. To the extent possible, these more interesting results are summarized below.

1. Based upon the tension measured in the cable, the basic model drag was determined to be 265 gm (0.58 Lbf). For the dynamic pressure involved and assuming a planform area, this results in a CD_{plan} of approximately 0.086, which does not agree with Hoerner for any reference area based on base area results in a CD_{base} = 0.345 or based on wetted area results in CD_{wet} = 0.027.

2. The cable was essentially straight and formed an angle of approximately 8 deg for 247 ft/s airspeed. However, the string showed a slightly reversed catenary shape (hyperbolic cosine), indicating that the lift per unit length was greater than the weight per unit length. For the wire rope cable, the catenary was more typical since the lift per unit length was less than the weight per unit length.

3. The model would generally lift from the floor at M = 0.168 or ~182 ft/s and would set back down at M = 140 or 154 ft/s, speeds which are consistent for both wind tunnels.

4. The slope of the cable in these experiments indicates that the model is reacting to forces that are lift-dominant, not drag-dominant. Therefore, the model is actually flying for the range of Mach numbers examined. This may not be the case for a true full-scale flight tethered mass, especially at high Mach numbers.

5. While the cone was essentially stable following lift-off from the tunnel floor, rolling about the floor before lift-off caused the model to have a rolling motion at initial lift-off that sometimes caused the cable to wind up and oscillate torsionally as a result of residual cable torque and the absence of damping in the torsional direction. This rolling motion was more evident with the string than with the wire rope cable. A bearing was later installed at the cable attachment point to eliminate this residual torque at lift-off.

6. At higher airspeeds a coning motion was observed where the model tended to orbit about the forward end of the tube through which the cable was inserted. As speed was increased, this coning grew to the point of the model hitting the tunnel walls, in which case the data point was aborted and the speed reduced or the cable retracted through its mounting tube to regain a stable model flight configuration.

7. At high Mach numbers (>0.38), the cone would eventually get lifted near the top of the tunnel and become very stable and then start violent oscillations and fall back down to a more normal tunnel position (approximately mid-height) with just minor oscillations in a coning manner. As the open tunnel had no detectable anomalies, it is conjectured that the tube support wake could be causing this phenomenon. This will be investigated further when testing continues.

8. As the cable was stiffened (swapped from a string to a miniature wire rope), the stability of the model diminished.

9. As the length of the cable increased, the stability of the model diminished.

10. As the length of the cable decreased, the model would lift off at a lower airspeed, as expected, since a higher initial AoA was established because the cable partially supported the model.

In these experiments, which were the first of what is hoped will be a series of experiments, several lessons were learned that indicated technical concerns with the experiments. Nevertheless, from a cable dynamics model validation viewpoint, the data obtained in these experiments are considered valuable and therefore should be qualified appropriately. Experimental concerns are listed below.

1. Scaling was determined more on the basis of available hardware and tunnels than on a true aerostructure scaling methodology. Because there were no data related to the length, mass, and stiffness of any specific tow cables, no attempt was made to scale the cable in a true structural sense. In addition, it should be noted that the model size and shape were dictated merely by convenience and did not represent any specific device.

2. Since scaling was ignored, the position of the center of gravity relative to the attachment point may not represent an actual flight-towed vehicle; this parameter should be evaluated in future testing.

3. Effects of the cable support sting on cable and model dynamics need to be identified and separated from the data to allow direct model comparisons.

4. Proper determination of model-only aeroperformance would qualify the data and provide a better estimate of data accuracy and uncertainty.

2.7 SUMMARY/CONCLUSIONS

This effort generated cable dynamics and tethered-mass dynamics data for the purpose of simulation validation. While the program was a small and very focused effort, the data generated are of reasonable quality for the intended purpose. Several lessons were learned, and some unique observations will contribute significantly to any follow-on programs along these lines.

2.8 RECOMMENDATIONS FOR FURTHER WORK

Based upon the limitations of this program and lessons learned, the following recommendations for follow-on experimentation are made:

1. This experiment and future experiments should be compared to actual tow-vehicle data for validation of scaling.

2. Tethered-mass stability as a function of CG position, drag, and Mach number should be investigated to augment this database.

3. A tethered-mass launch apparatus should be developed to simulate extension of the device in flight, as if from a captive-carry position on the aircraft.

4. The chaotic dynamics of the tethered-mass should be investigated and quantified as a function of cable stiffness/mass

REFERENCES

1. Fung, Y.C., *An Introduction to the Theory of Aeroelasticity*, Dover Publications, Inc., New York, 1993.

2. Alexander, Blake, *Practical Stress Analysis in Engineering Design*, 2nd Edition, Marcel Dekker, Inc. New York and Basel, 1990.

3. Lawrence, F. Clark and Tibbals, Thomas F., "Development of a Motion Simulation for a Segmented Cable and Towed Body," 2006 International Aircraft-Stores Compatibility Symposium XIV, April 2006.

4. Hoerner, Sighard F. *Fluid-Dynamic Drag: Practical Information on Aerodynamic Drag and Hydrodynamic Resistance*. Hoerner, Midland Park, NJ, 1965.

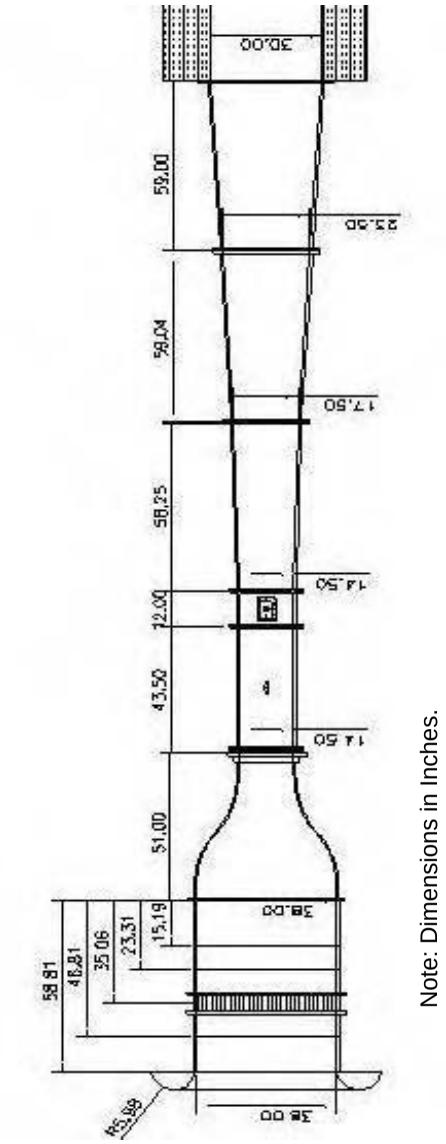

Note: Dimensions in Inches.

Figure 1. FSI Tunnel Plan View Inside Dimensions

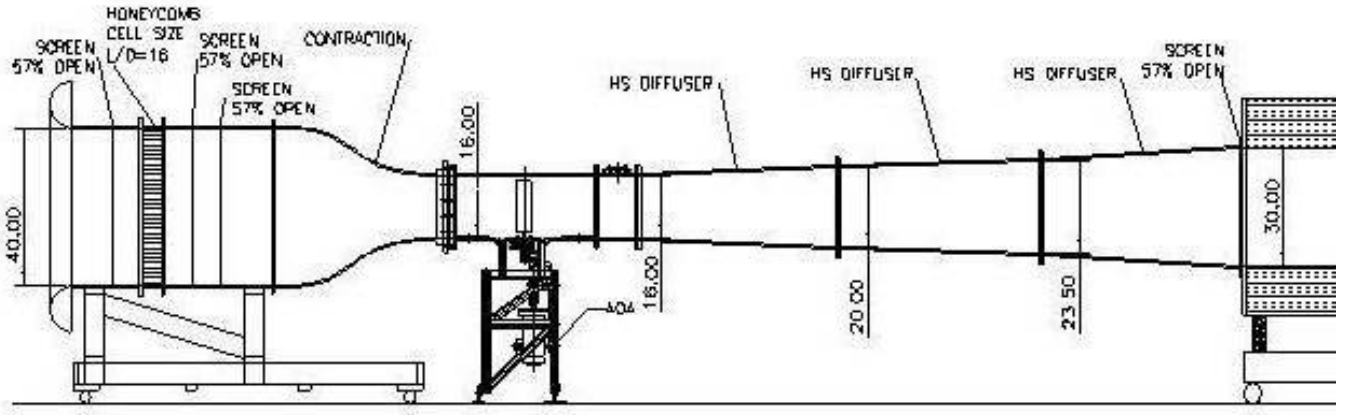

DIMENSIONS IN INCHES.

Figure 2. FSI Tunnel Elevation View Inside Dimensions

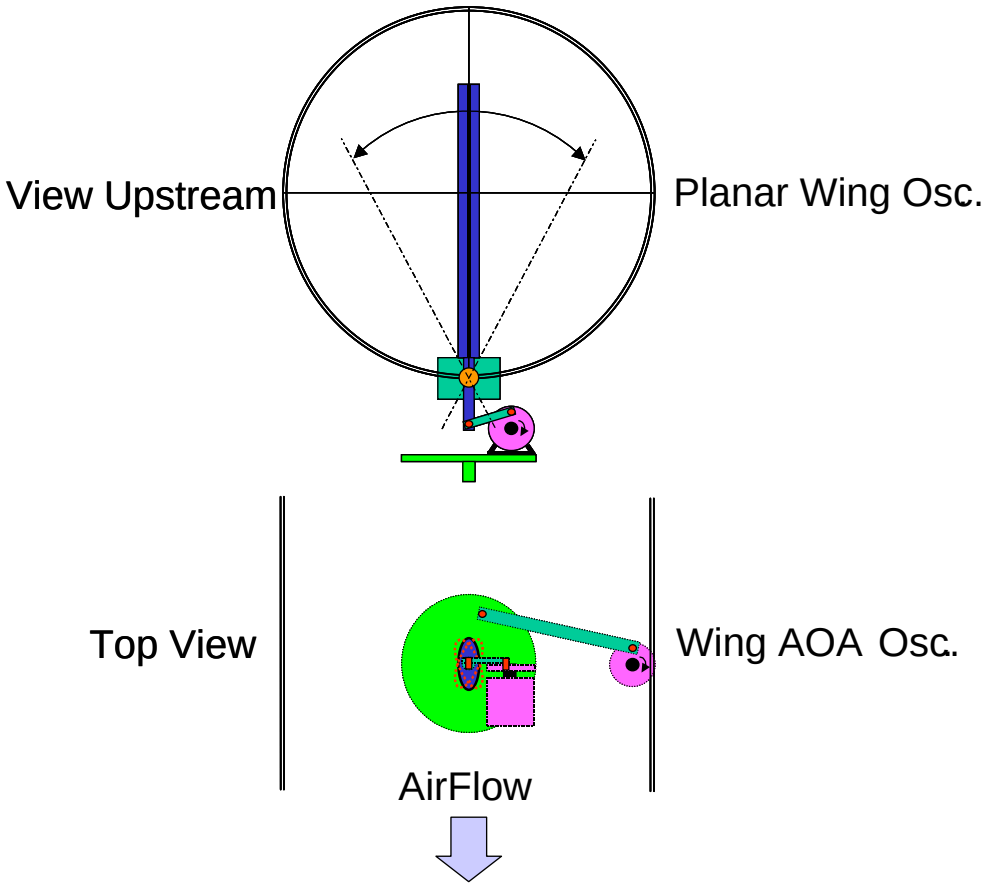

Figure 3. Wing Oscillation Mechanism (WOM) Concept

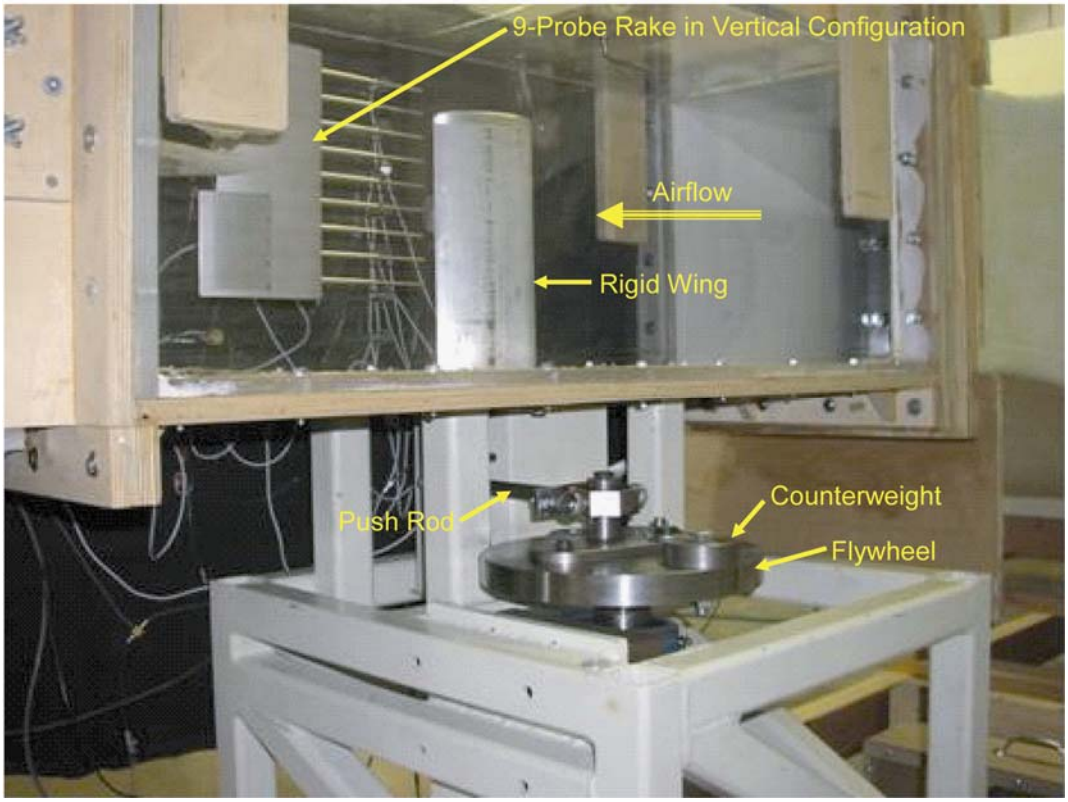

a. Quarterly View—Aft Looking Forward

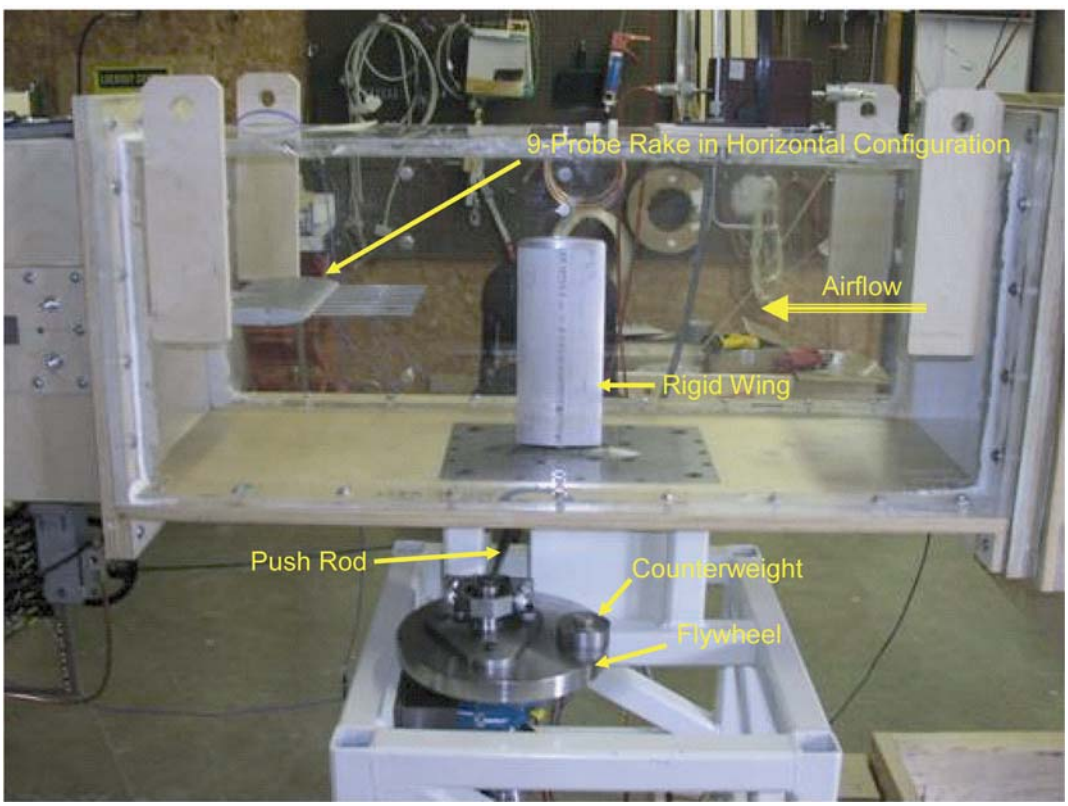

a. Side View

Figure 4. JTI Wind Tunnel Test Section with Wing Oscillation Mechanism

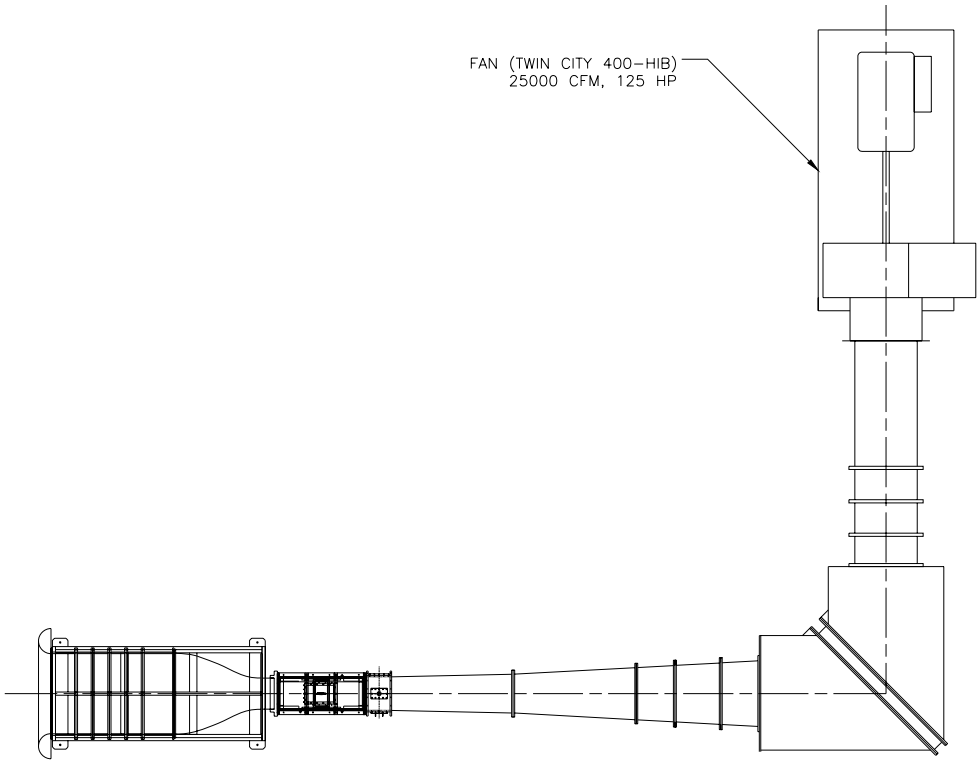

Figure 5. Single-Fan Wind Tunnel Circuit

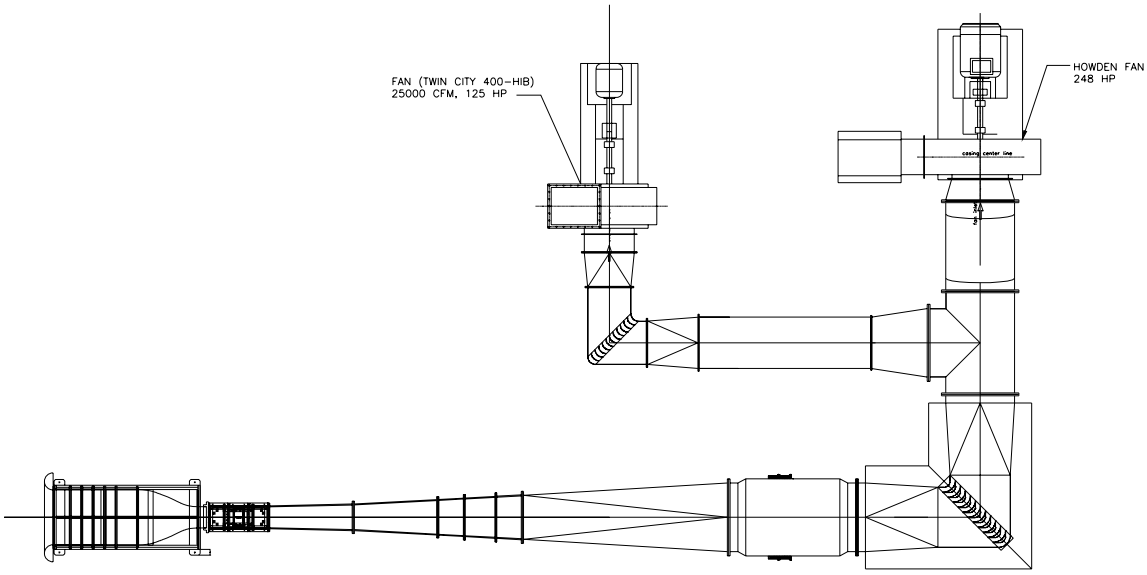

Figure 6. Dual-Fan Wind Tunnel Circuit

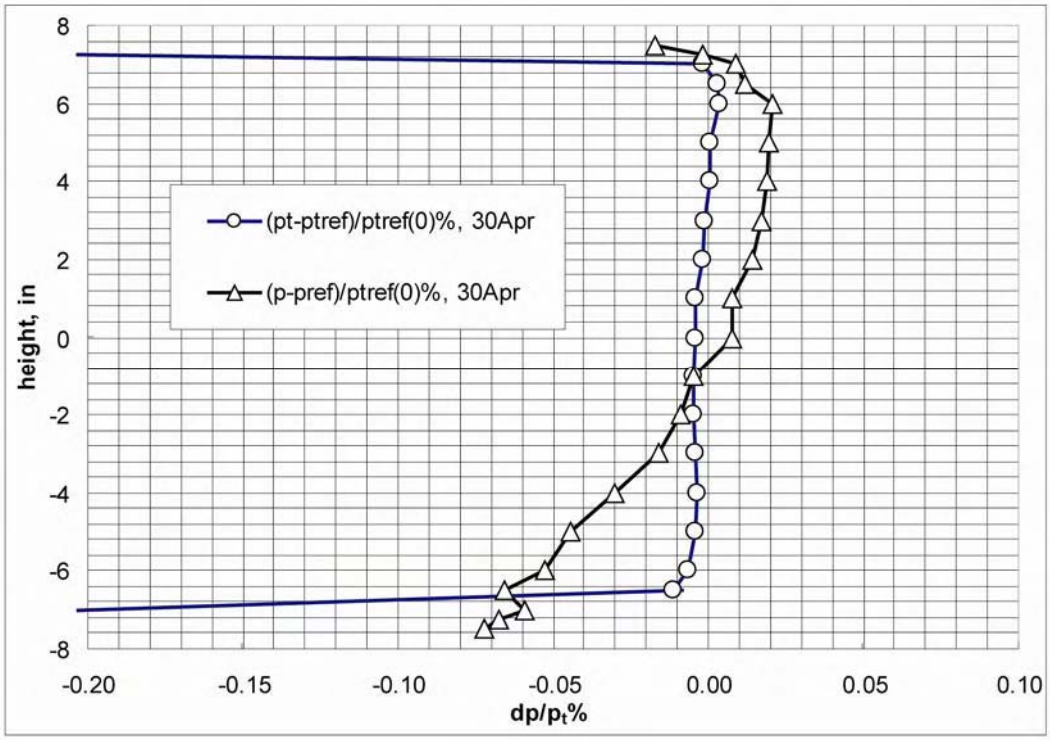

Figure 7. Pitot and Static Pressure Profiles on Tunnel Vertical Centerline

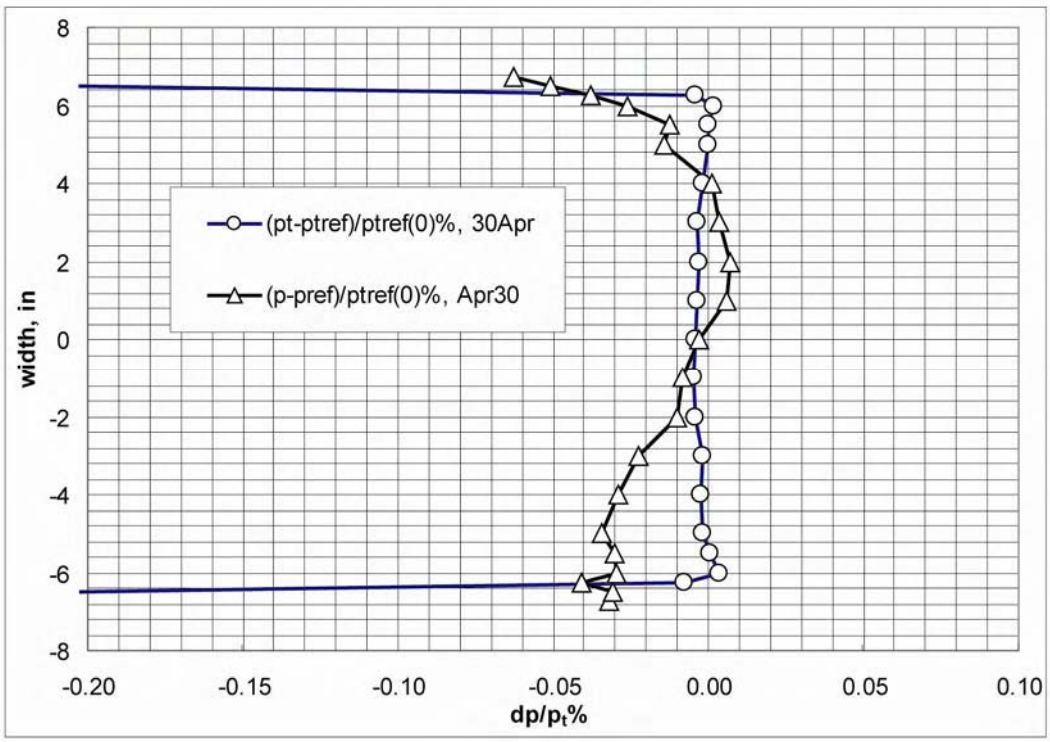

Figure 8. Pitot and Static Pressure Profiles on Tunnel Horizontal Centerline

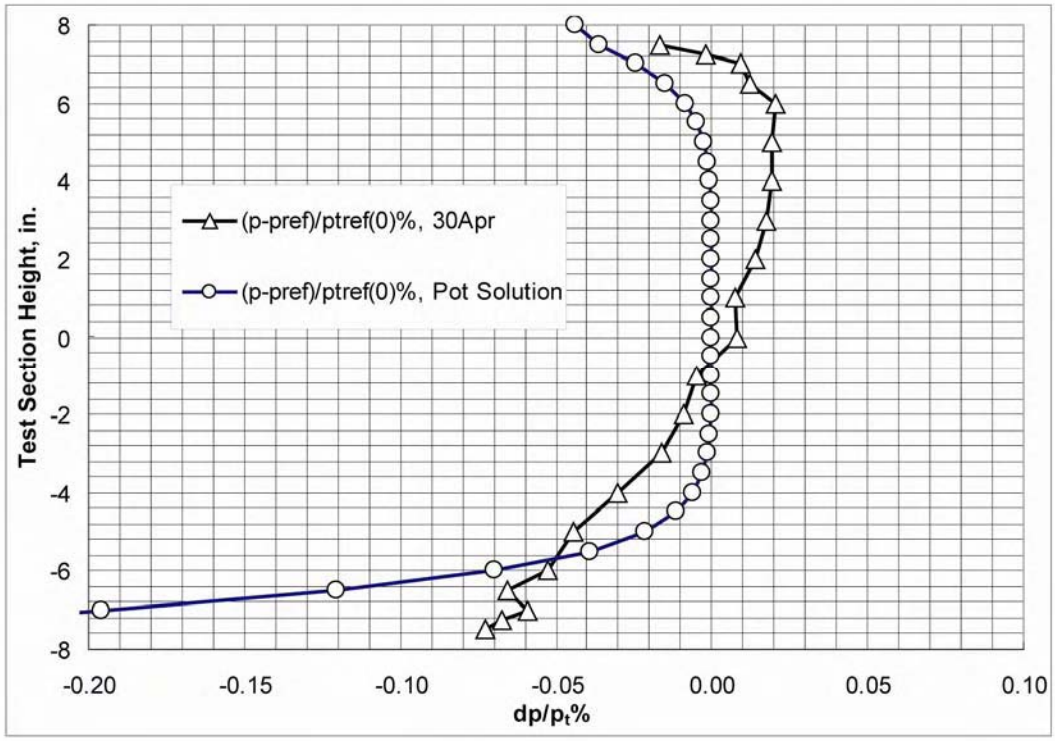

Figure 9. Static Pressure Profile with Potential Flow Solution

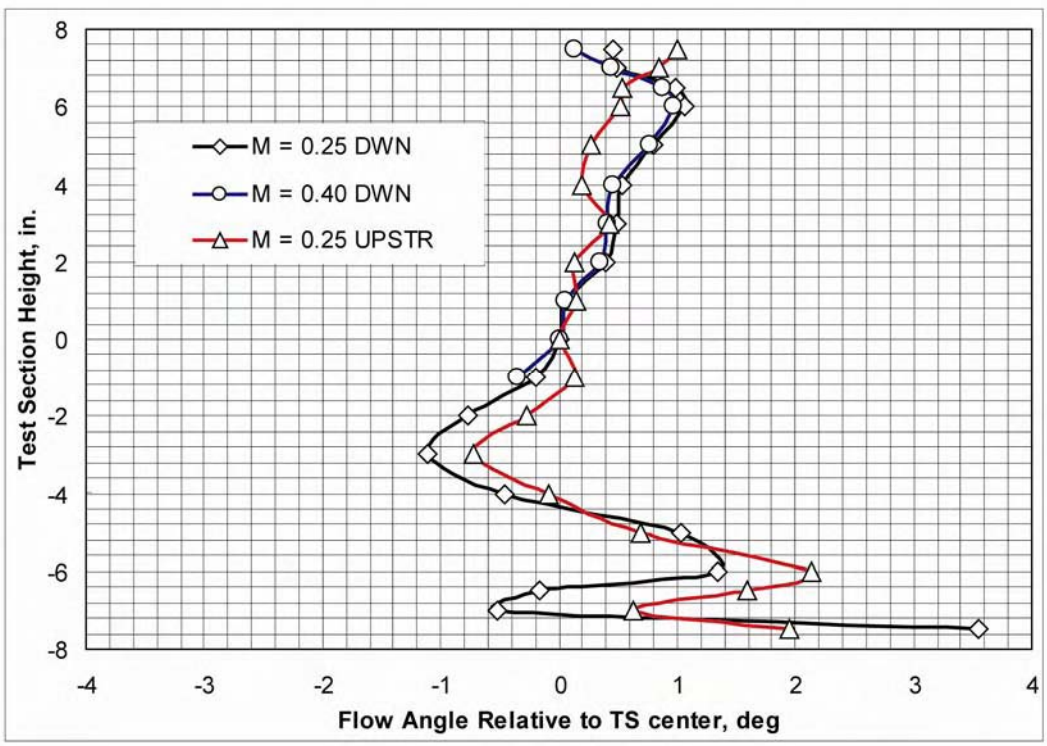

Figure 10. Pitch Angle on Tunnel Centerline with Rake Installed

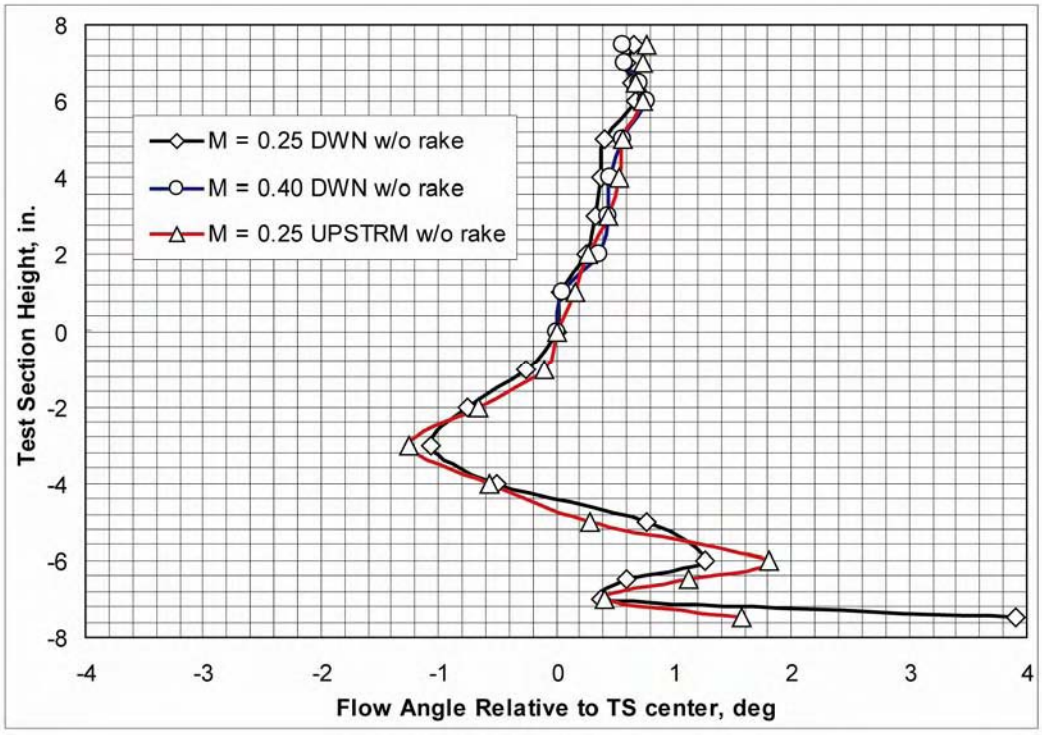

Figure 11. Pitch Angle on Tunnel Centerline with Rake Removed

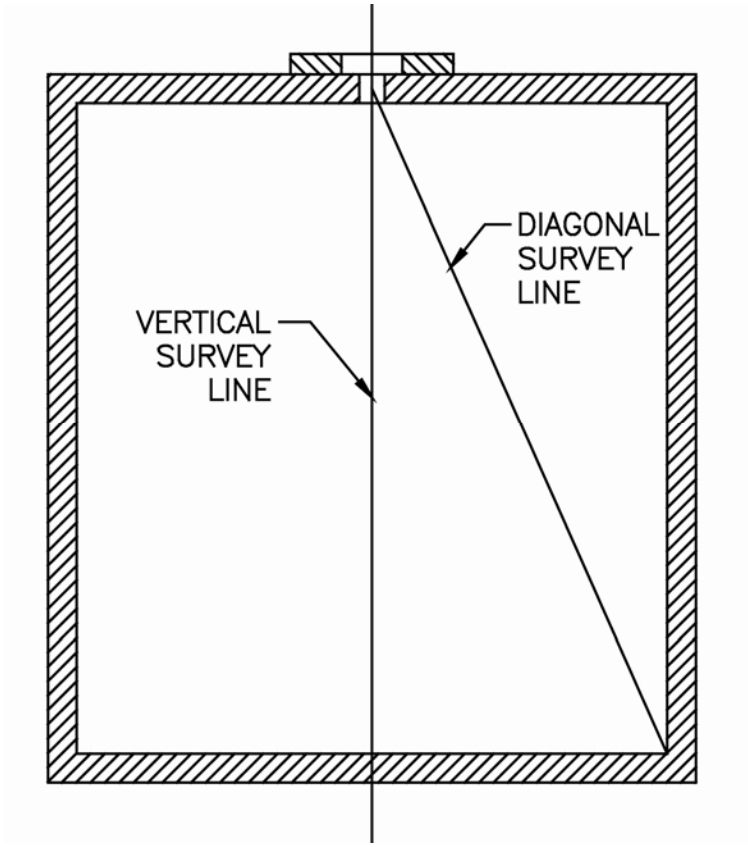

Figure 12. Sketch of Turbulence Survey Lines in Empty Test Section

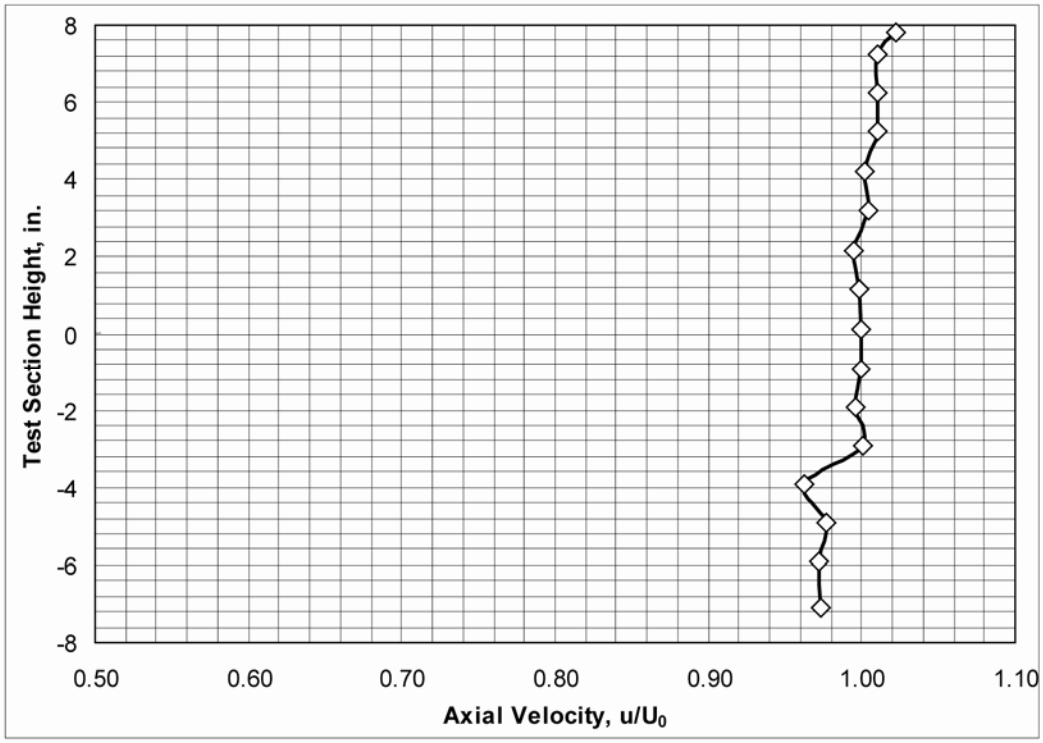

Figure 13. Axial-Velocity Profile on Tunnel Centerline

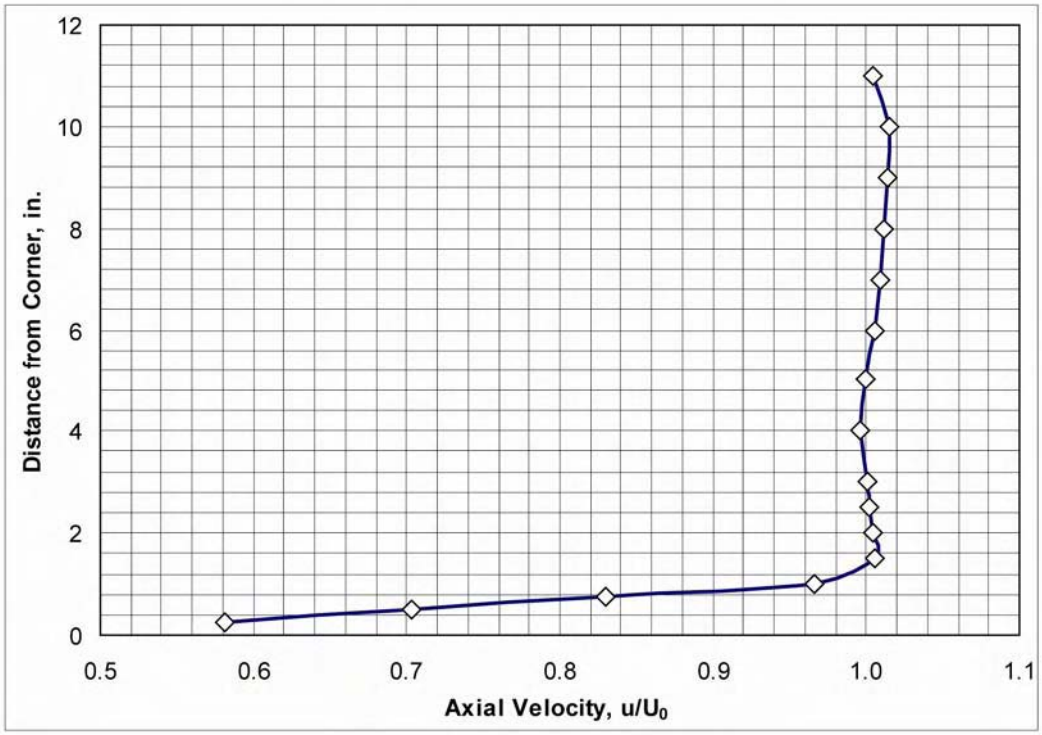

Figure 14. Axial-Velocity Profile on Tunnel Diagonal

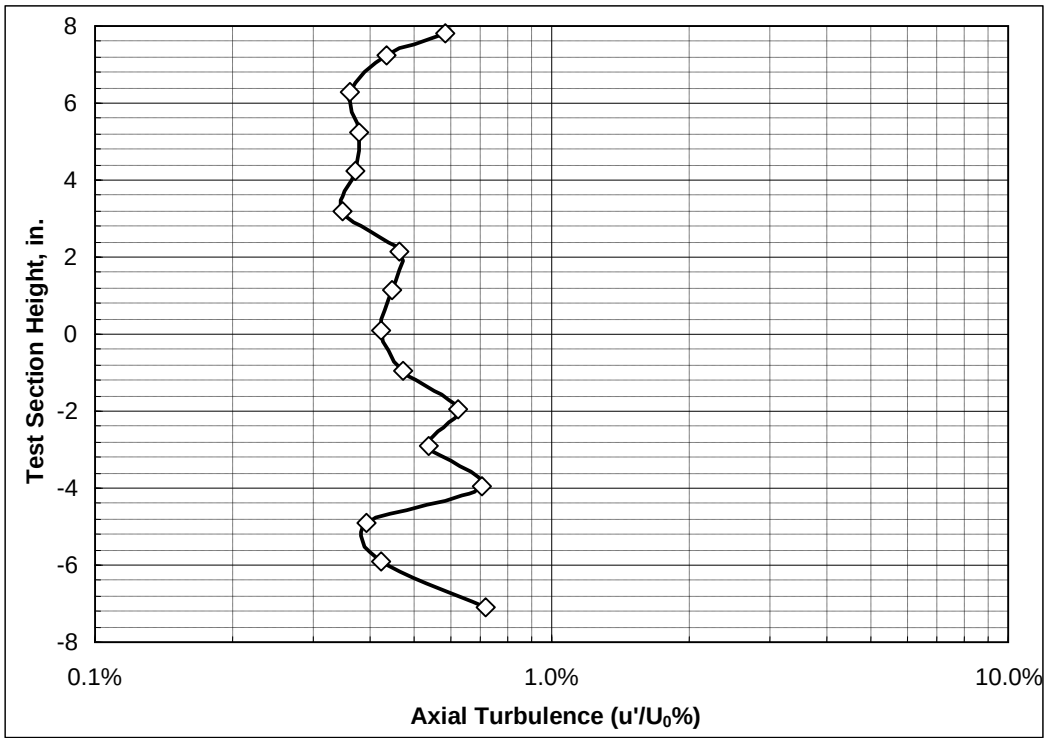

Figure 15. Axial Turbulence on Tunnel Vertical Centerline

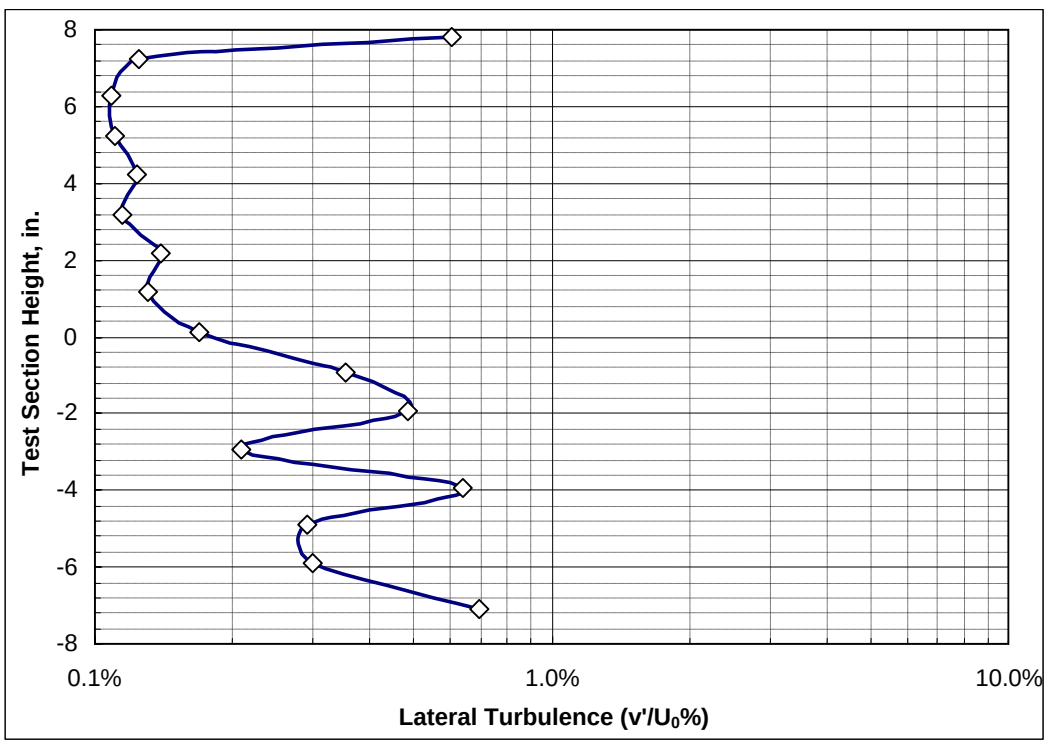

Figure 16. Lateral Turbulence on Tunnel Vertical Centerline

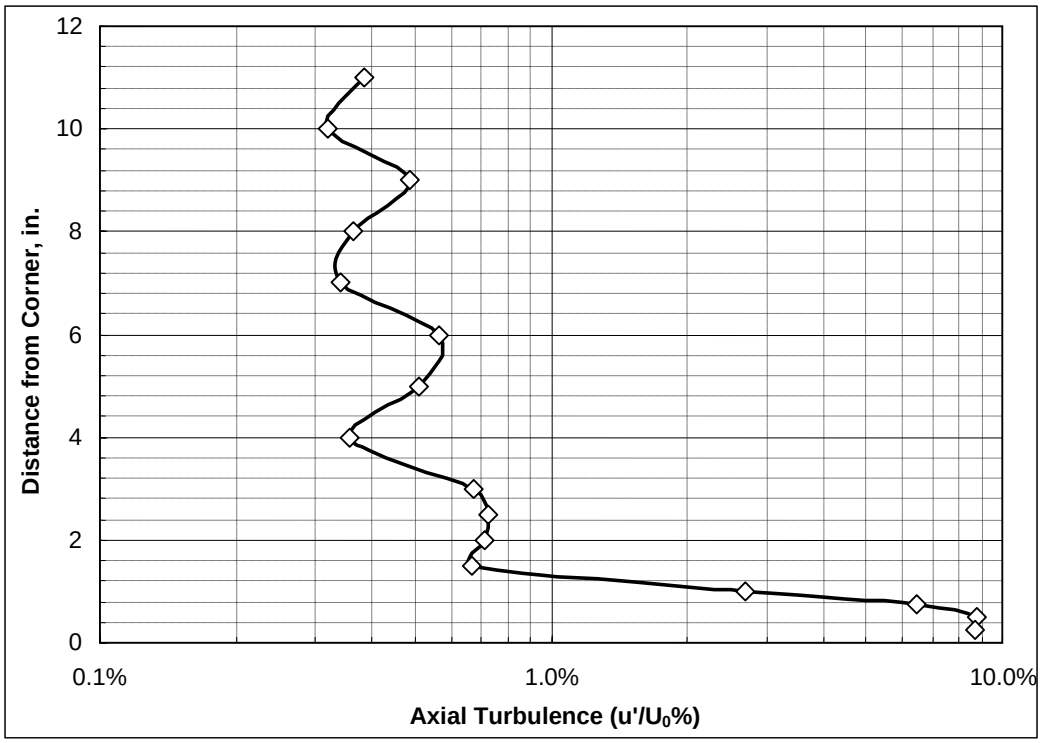

Figure 17. Axial Turbulence on Tunnel Diagonal

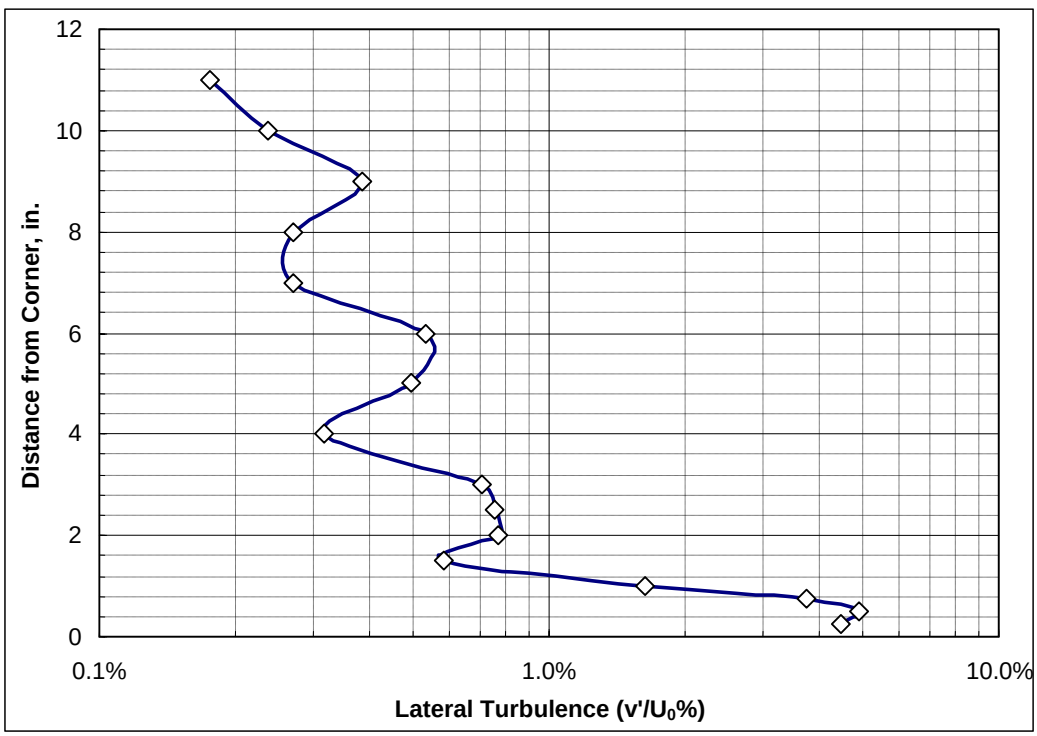

Figure 18. Lateral Turbulence on Tunnel Diagonal

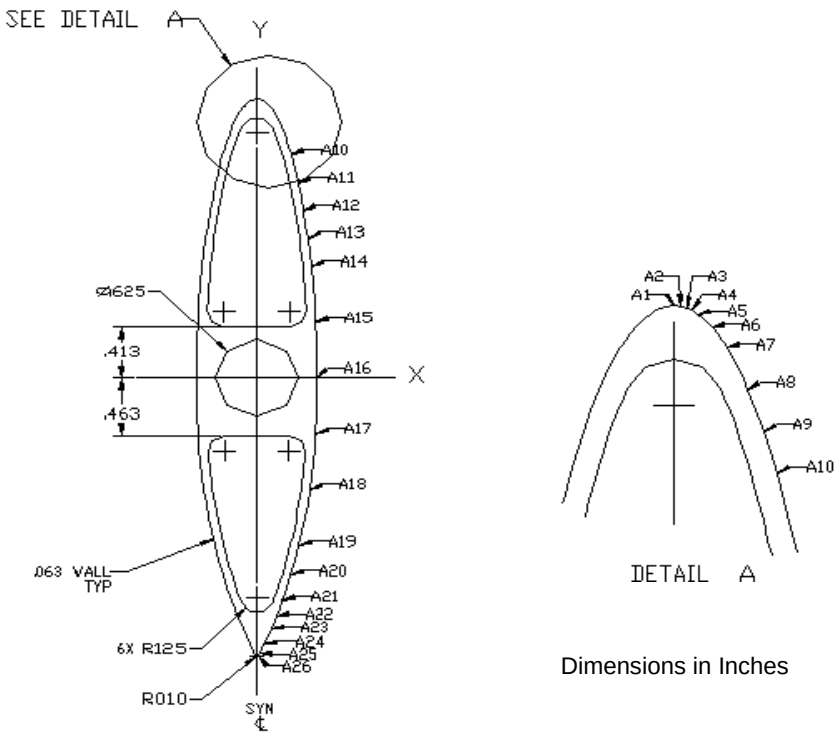

Point	X	Y	Point	X	Y	Point	X	Y
A1	0.000	2.250	A10	0.256	1.800	A19	0.315	-1.350
A2	0.016	2.248	A11	0.308	1.575	A20	0.253	-1.593
A3	0.032	2.244	A12	0.348	1.350	A21	0.189	-1.800
A4	0.046	2.237	A13	0.380	1.125	A22	0.146	-1.922
A5	0.060	2.228	A14	0.406	0.900	A23	0.106	-2.025
A6	0.094	2.194	A15	0.439	0.450	A24	0.053	-2.149
A7	0.132	2.138	A16	0.450	0.000	A25	0.020	-2.225
A8	0.184	2.025	A17	0.438	-0..450	A26	0.009	-2.250
A9	0.224	1.913	A18	0.395	-0.900			

Figure 19. Test Article Airfoil Cross Section

FSI Flexible air foil elastomer material properties tables - Simple Tension

Elastic Storage Modulus - psi

25% Constant strain

x freq Hz	y1 static	y2 4Hz	y3 25Hz	
xtemp	0	4	25	
30	*	81.3	91.3	
73	62.5	#	88.3	^^81
100	*	73.1	84.9	

73F Constant temperature vs variable strain rate

x freq Hz	y1 static	y2 4Hz	y3 25Hz	
xpcstrn	0	4	25	
10	78.5	91.5	94.8	
25	62.5	#	88.3	^^81
50	49.3	60.1	67.5	

73F Constant temperature vs variable frequency

x pc strain	y1 10%	y2 25%	y3 50%
x freq Hz	10	25	50
0	78.5	62.5	49.3
4	91.5	#	60.1
25	94.8	88.3	67.5
		^^81	

Loss Modulus - psi

25% Constant strain

x freq Hz	y1 static	y2 4Hz	y3 25Hz	
xtemp	0	4	25	
30	0	25.4	17.45	
73	0	#	8.3	^^12.8
100	0	8.1	8	

73F Constant temperature vs variable strain rate

x freq Hz	y1 static	y2 4Hz	y3 25Hz	
xpcstrn	0	4	25	
10	0	16.5	16.6	
25	0	#	8.3	^^12.8
50	0	12.9	7.5	

73F Constant temperature vs variable frequency

x pc strain	y1 10%	y2 25%	y3 50%
x freq Hz	10	25	50
0	0	0	0
4	16.5	#	12.9
25	16.6	8.3	7.5
		^^12.8	

Bad data
* Not Requested
^^ 25Hz 25%strn at 23C - cured longer

Figure 20. Airfoil Elastomer Properties

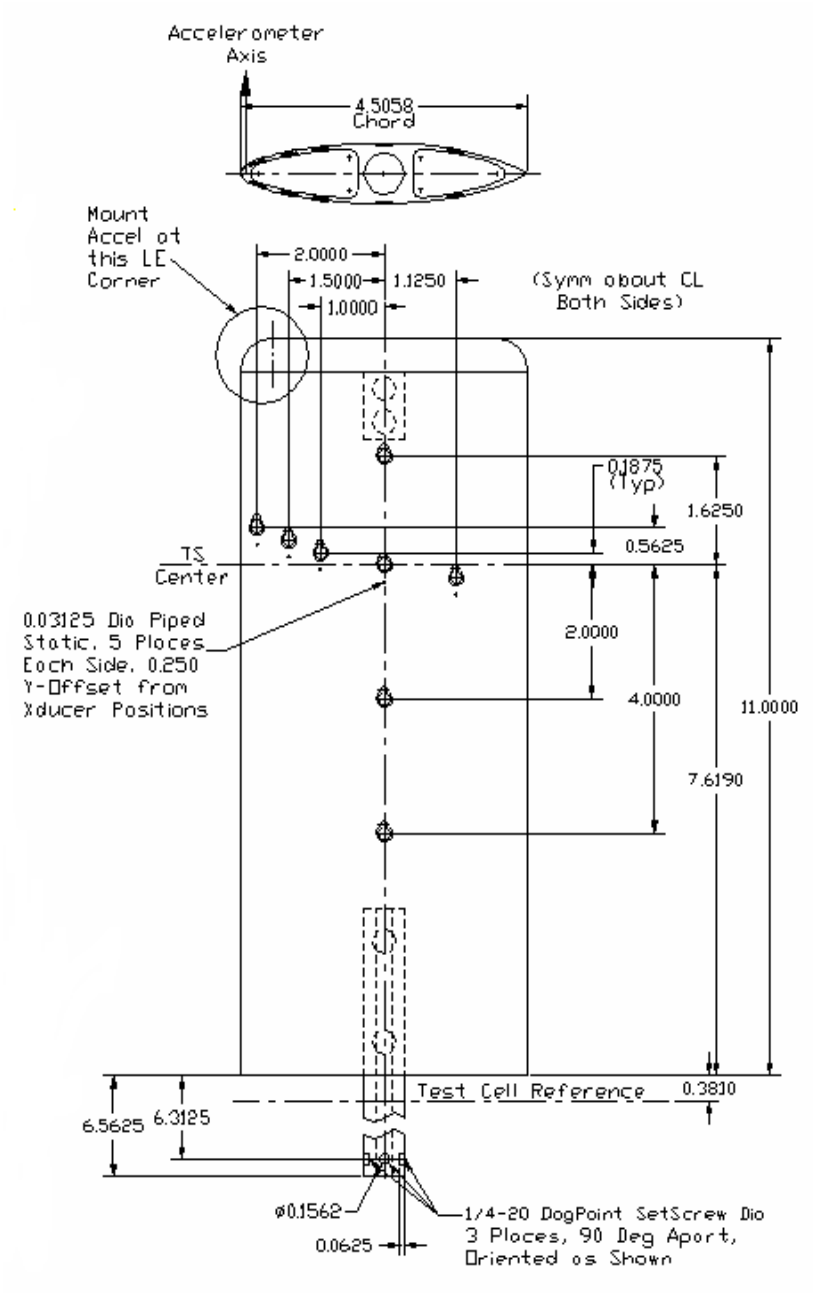

Figure 21. Basic Test Article Dimensions

Critical Velocity based upon Y.C. Fung (Assumes STRAIGHT wing with constant span-wise stiffness):

$R_{air} := 53.29$ (Ft-LBf)/(LBm-^{o}R)

$Mach := 0.2$

$Ps_{Tul} := 14.22$ PSIA

$Ts_{Tul} := 70 + 459.67$ ^{o}R

$\rho_{air.Tul} := \frac{Ps_{Tul} \cdot 144}{R_{air} \cdot Ts_{Tul}}$ LBm/Ft^3

$a_{Tul} := \sqrt{g_c \cdot \gamma_a \cdot R_{air} \cdot Ts_{Tul}}$

$a_{Tul} = 1127.566$ Ft/Sec

$V_{nom} := Mach \cdot a_{Tul}$

$V_{nom} = 225.513$ Ft/Sec

$q_{div} = \frac{\pi^2 \cdot G \cdot J}{4 \cdot a \cdot e \cdot c^2 \cdot s^2}$ Fung Eqn 3.3-17

$Chord := \frac{4.5}{12}$ Feet

$e := .25$ Eccentricity, in % chord (Elastic Axis to Aerodynamic Axis)

$\eta := 0.9$ Airfoil Efficiency Factor

$a_o := 2 \cdot \pi \cdot \eta$ Lift Curve Slope (Theoretical)

$Span := \frac{11}{12}$ Feet

$Ratio_{aspect} := \frac{Span^2}{Chord \cdot Span}$

$a_{fs} := \frac{a_o}{1 + \left(\frac{a_o}{\pi \cdot Ratio_{aspect}} \right)}$ Corrected Lift Curve for Finite Span

$q_{div} := \frac{1}{2} \cdot \rho_{air.Tul} \cdot V_{nom}^2 \cdot \frac{1}{g_c \cdot 144}$

$q_{div} = 0.398$ PSI

$q_{div} \cdot 27.707591 = 11.03$ In-H2O

$GJ := q_{div} \cdot 144 \cdot \frac{4 \cdot a_{fs} \cdot e \cdot Chord^2 \cdot Span^2}{\pi^2}$

$GJ = 2.236$ LBf-Ft^2

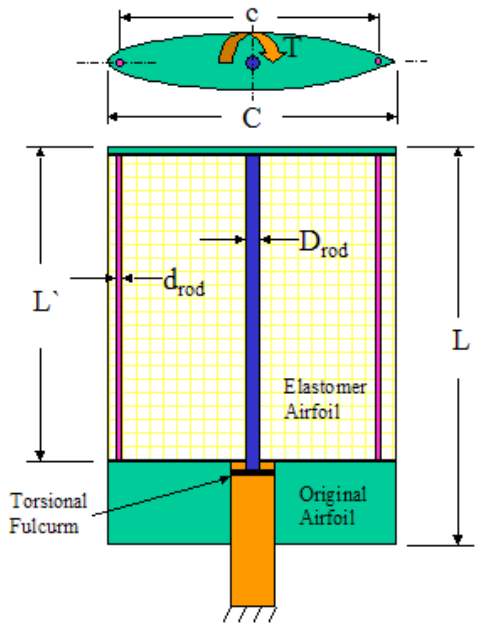

Assume a rod of given length and diameter connected by thin plates top and bottom with bottom plate fixed and top plate with an induced torque coincident with rod axis:

$D_{rod} := 0.171875$ Inches

$G_{rod} := 3.8 \cdot 10^6$ PSI (6061-T6)

$E_{rod} := 9.9 \cdot 10^6$

Assuming small rotations:

$\theta' := 10 \cdot \frac{\pi}{180}$

$J_{rod} := \frac{\pi}{32} \cdot D_{rod}^4$ IN^4

$G_{rod} \cdot J_{rod} \cdot \frac{1}{144} = 2.261$ LBf-Ft^2

$T_{rod} := \frac{\theta' \cdot G_{rod} \cdot J_{rod}}{Span \cdot 12}$

$T_{rod} = 5.166$ In-LBf

Now assume that use two small rods, one near TE, one near LE, then rods bend and twist (same θ) as the airfoil twists:

$d_{rod} := 0.1365$ Inches

$J'_{rod} := \frac{2 \cdot \pi}{32} \cdot d_{rod}^4$ IN^4

$I'_{rod} := \frac{2 \cdot \pi}{64} \cdot d_{rod}^4$ IN^4

$\frac{G_{rod} \cdot J'_{rod} + E_{rod} \cdot I'_{rod} \cdot \frac{Chord}{2 \cdot Span}}{144} = 2.278$ LBf-Ft^2

$T'_{rod} := \frac{\theta' \cdot \left(G_{rod} \cdot J'_{rod} + E_{rod} \cdot I'_{rod} \cdot \frac{Chord}{2 \cdot Span} \right)}{Span \cdot 12}$

$T'_{rod} = 5.205$ In-LBf

Figure 22. MathCAD Worksheet for Cylindrical-Rod-Based Flex-Wing Design

Now assume that use two thin flat strips in steel (like steel strapping) to increase fatigue capability, one near TE, one near LE, then strips bend and twist (same θ) as the airfoil twists:

$w_{strip} := 0.500$ Inches $\quad t_{strip} := 0.040$ Inches $\quad G_{strip} := 12 \cdot 10^6$ PSI $\quad E_{strip} := 30 \cdot 10^6$ PSI

$AR_{strip} := \frac{w_{strip}}{t_{strip}}$ $\quad AR_{strip} = 12.5$ $\quad bh2 := w_{strip} \cdot t_{strip}^2$ $\quad bh3 := w_{strip} \cdot t_{strip}^3$

$I_{xc.strip} := \frac{1}{12} \cdot w_{strip} \cdot t_{strip}^3$ $\quad I_{xc.strip} = 2.667 \times 10^{-6}$ IN^4

per Blake, *Practical Stress Analysis in Engineering Design*, pg 26

$$Blake\_Table_{2.4} := \begin{pmatrix} 1.0 & 1.2 & 1.5 & 2.0 & 2.5 & 3.0 & 4.0 & 5.0 & 10.0 \\ 0.141 & 0.166 & 0.196 & 0.229 & 0.249 & 0.263 & 0.281 & 0.291 & 0.312 \\ 0.208 & 0.219 & 0.231 & 0.246 & 0.258 & 0.267 & 0.282 & 0.291 & 0.312 \end{pmatrix}^T$$

$b\_ovr\_h := Blake\_Table_{2.4}^{\langle 0 \rangle}$ $\quad K_{ovr\_bh3} := Blake\_Table_{2.4}^{\langle 1 \rangle}$ $\quad K_{s\_ovr\_bh2} := Blake\_Table_{2.4}^{\langle 2 \rangle}$

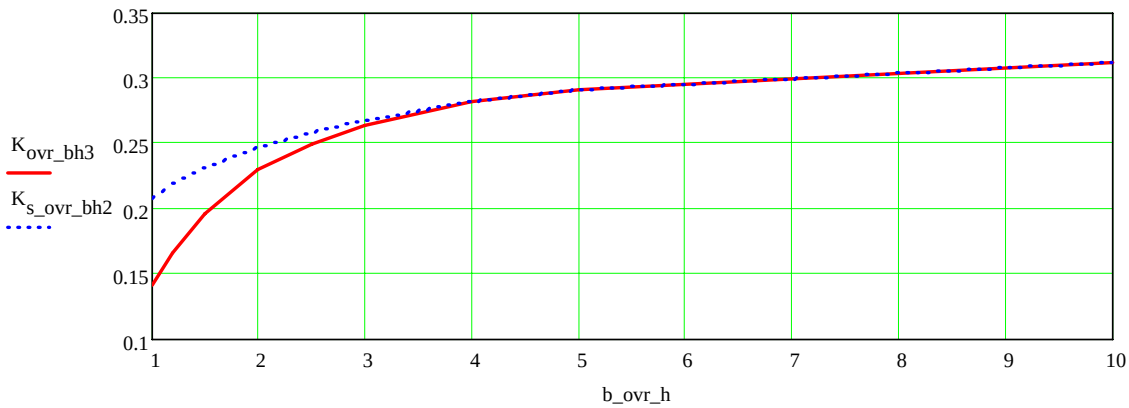

$$K_{strip} := \left| \begin{array}{l} \text{for } kk \in 0..\text{rows}(Blake\_Table_{2.4}) - 1 \\ \quad \left| \begin{array}{l} \text{if } b\_ovr\_h_{kk} > AR_{strip} \\ \quad \left| \begin{array}{l} Kstrip \leftarrow K_{ovr\_bh3_{kk}} \cdot bh3 \\ \text{break} \end{array} \right. \\ Kstrip \leftarrow \max\left(K_{ovr\_bh3_{kk}}\right) bh3 \quad \text{otherwise} \end{array} \right. \\ Kstrip \end{array} \right.$$

$\frac{K_{strip}}{bh3} = 0.312$

$$\frac{\left(G_{strip} \cdot K_{strip} + E_{rod} \cdot I_{xc.strip} \cdot \frac{Chord}{2 \cdot Span}\right) \cdot 2}{144} = 1.739 \quad \text{LBf-Ft}^2$$

$$T'_{strip} := \frac{\theta' \cdot \left(G_{strip} \cdot K_{strip} + E_{rod} \cdot I_{xc.strip} \cdot \frac{Chord}{2 \cdot Span}\right) \cdot 2}{Span \cdot 12}$$

$T'_{strip} = 3.973$ In-LBf

Figure 23. MathCAD Worksheet for Strap-Based Flex-Wing Design

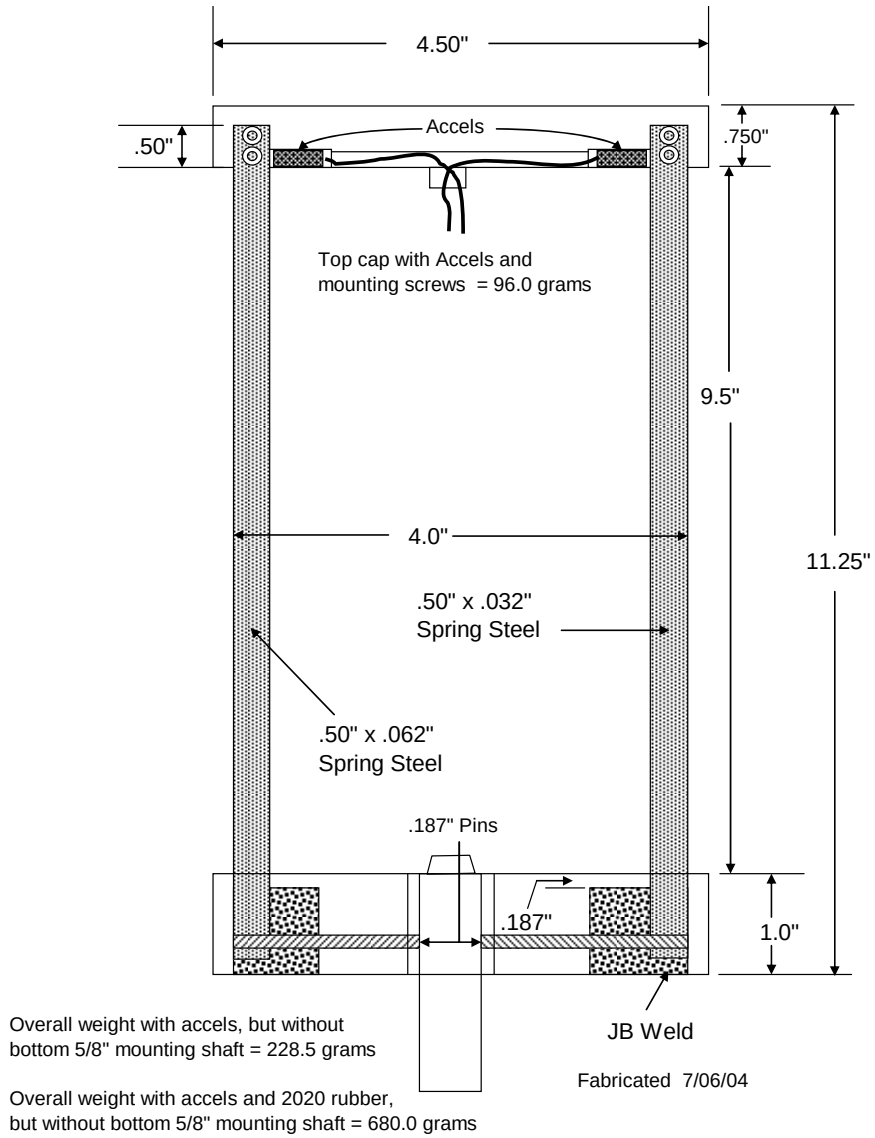

Figure 24. Typical Flex-Wing Skeleton

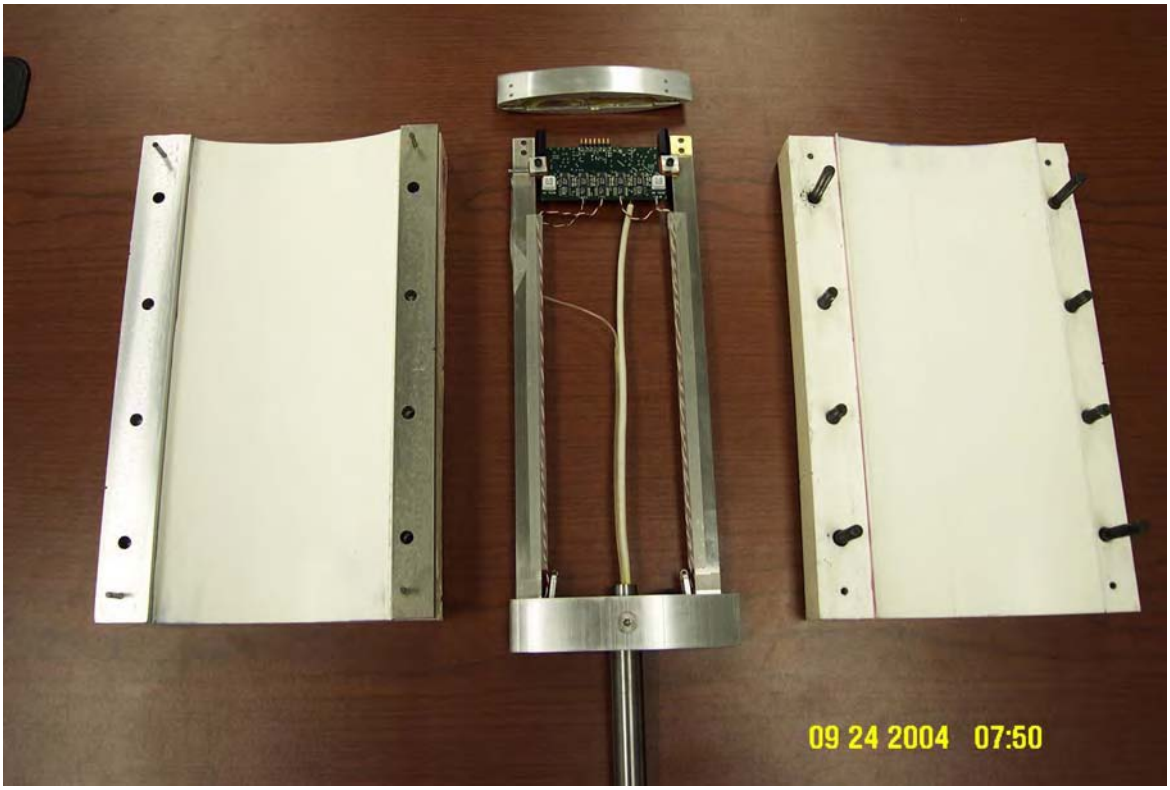

Figure 25. Elastomer Casting Molds

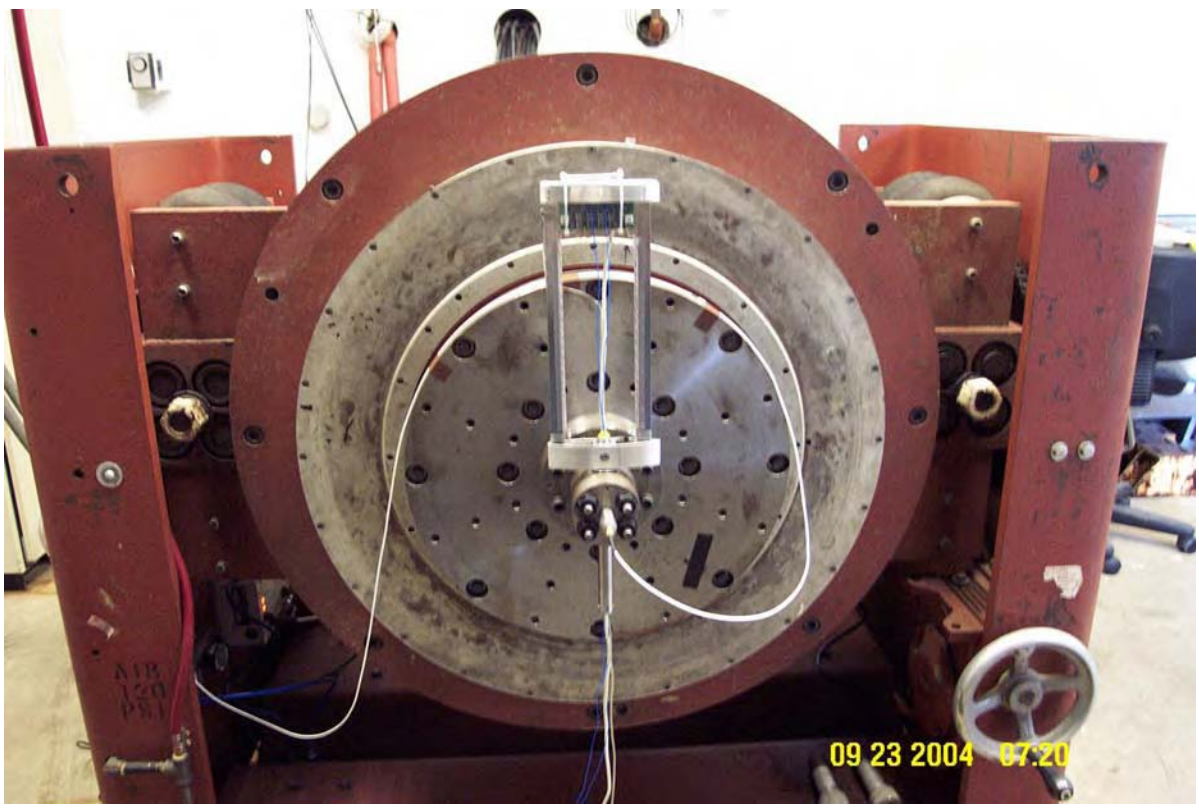

Figure 26. Flex-Wing Skeleton on Shaker Table

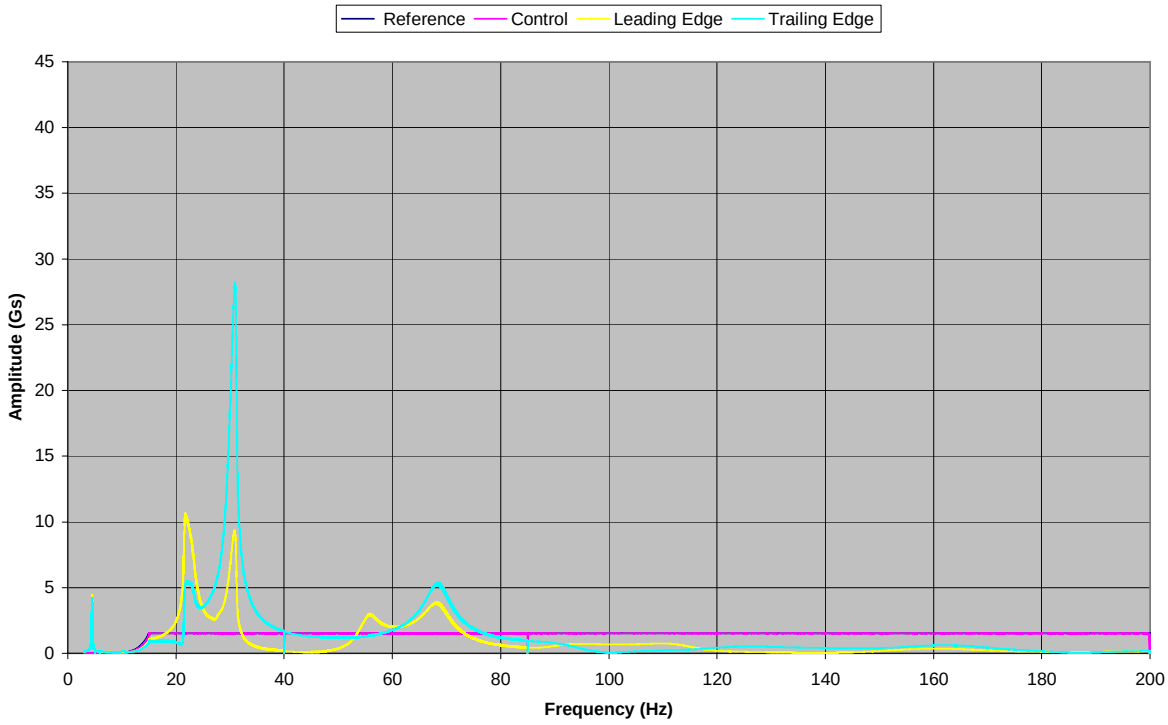

a. FW08 with Elastomer

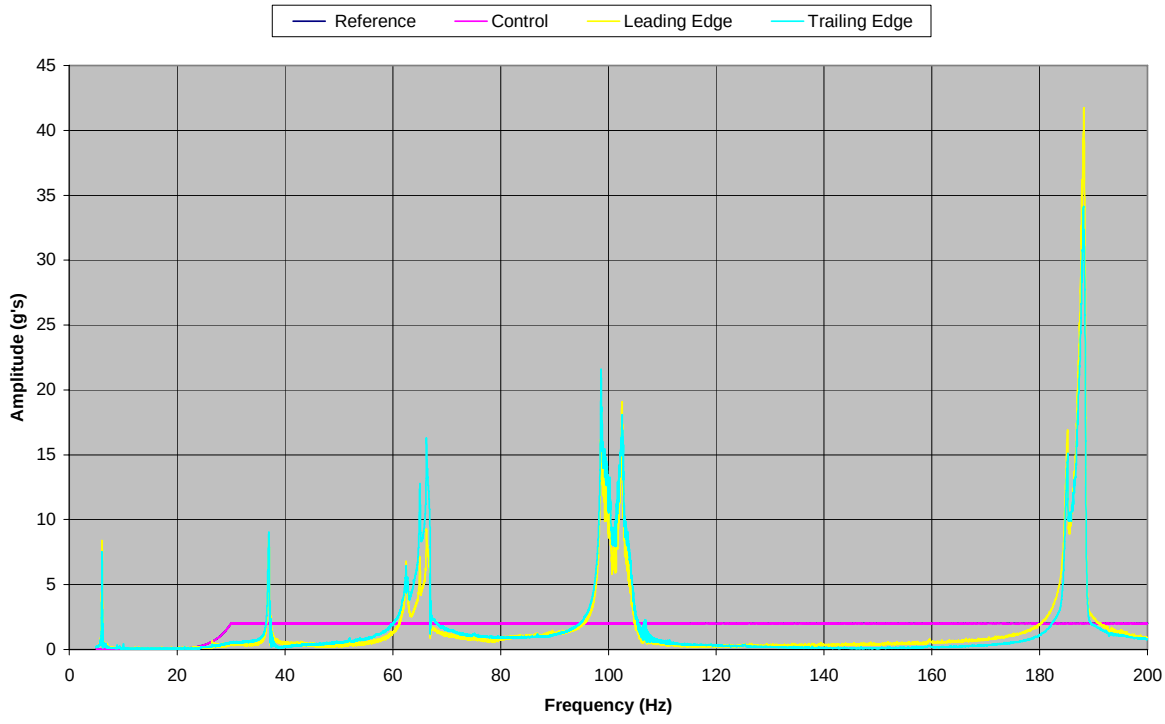

b. FW08 with No Elastomer

Figure 27. Flex-Wing Shaker Spectra

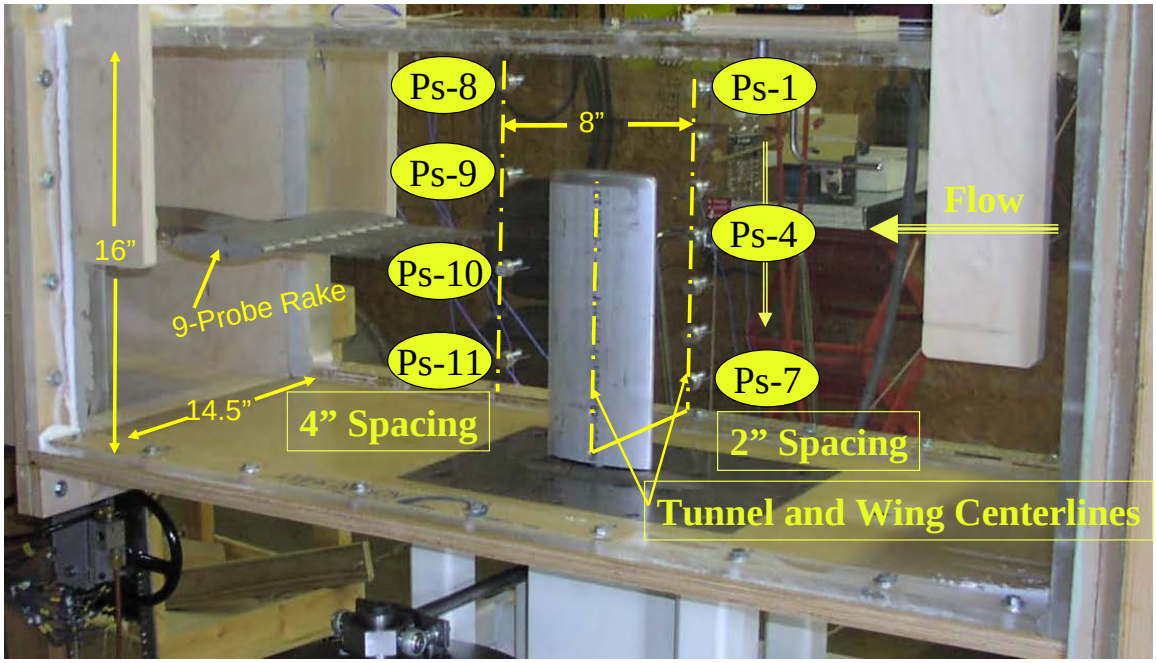

Figure 28. Test Section Instrumentation

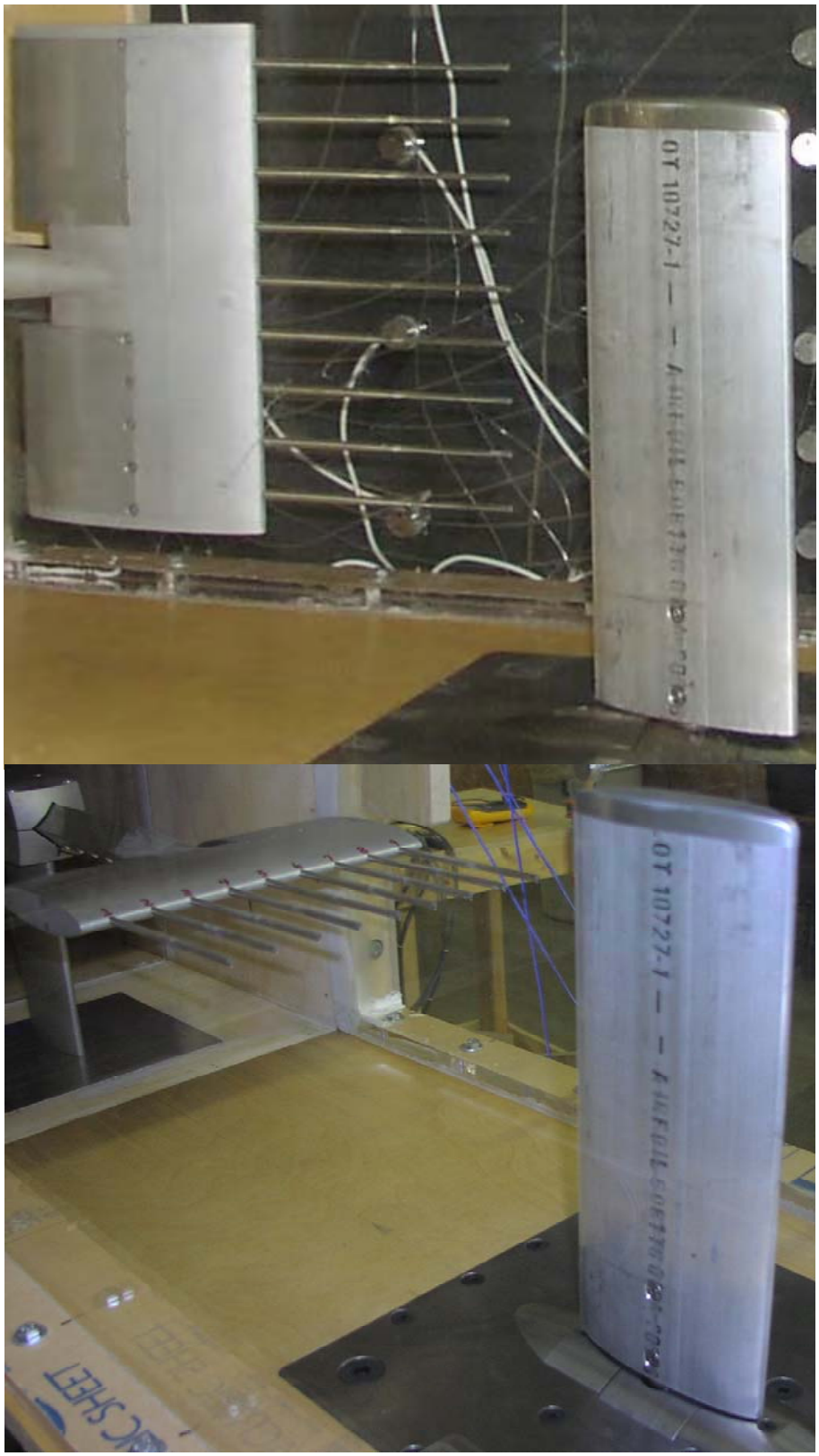

Figure 29. Nine-Probe Wake Survey Rake Configurations

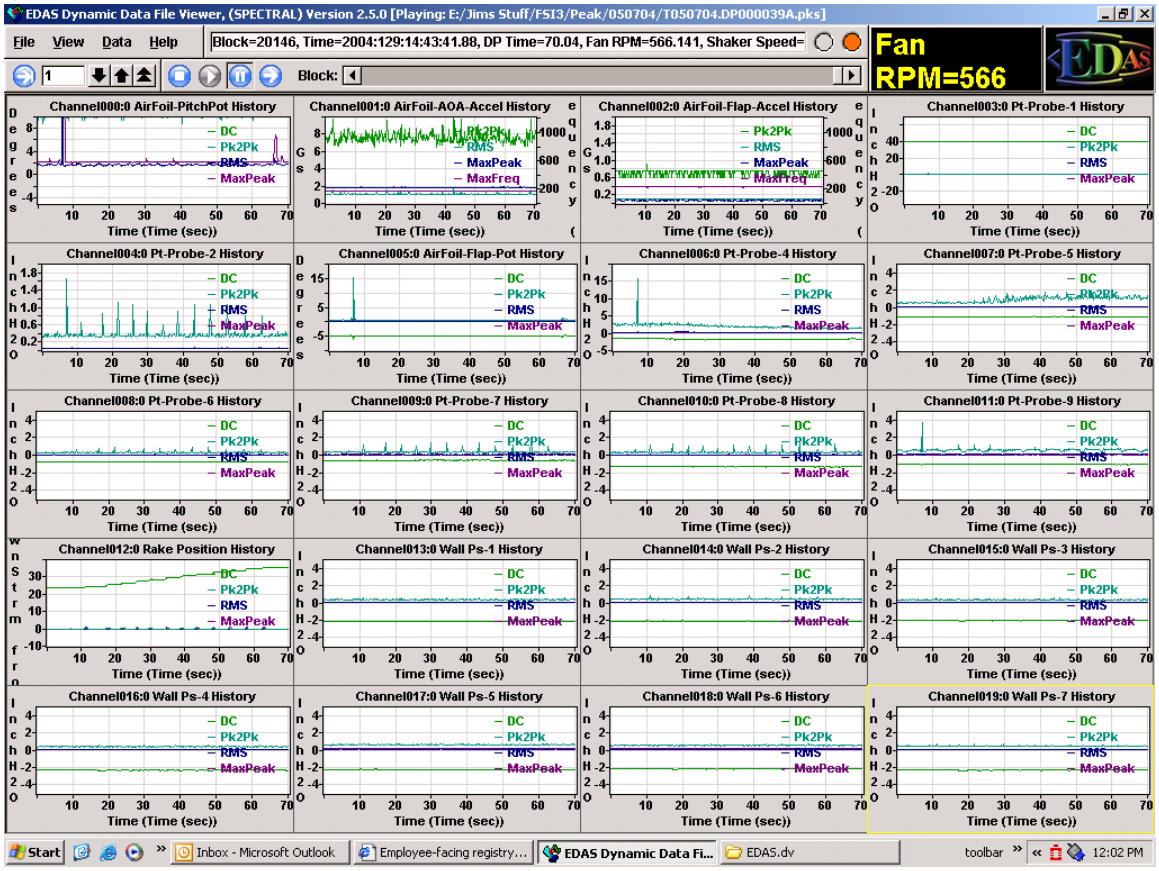

Figure 30. Typical CADDMAS Online Real-Time Display

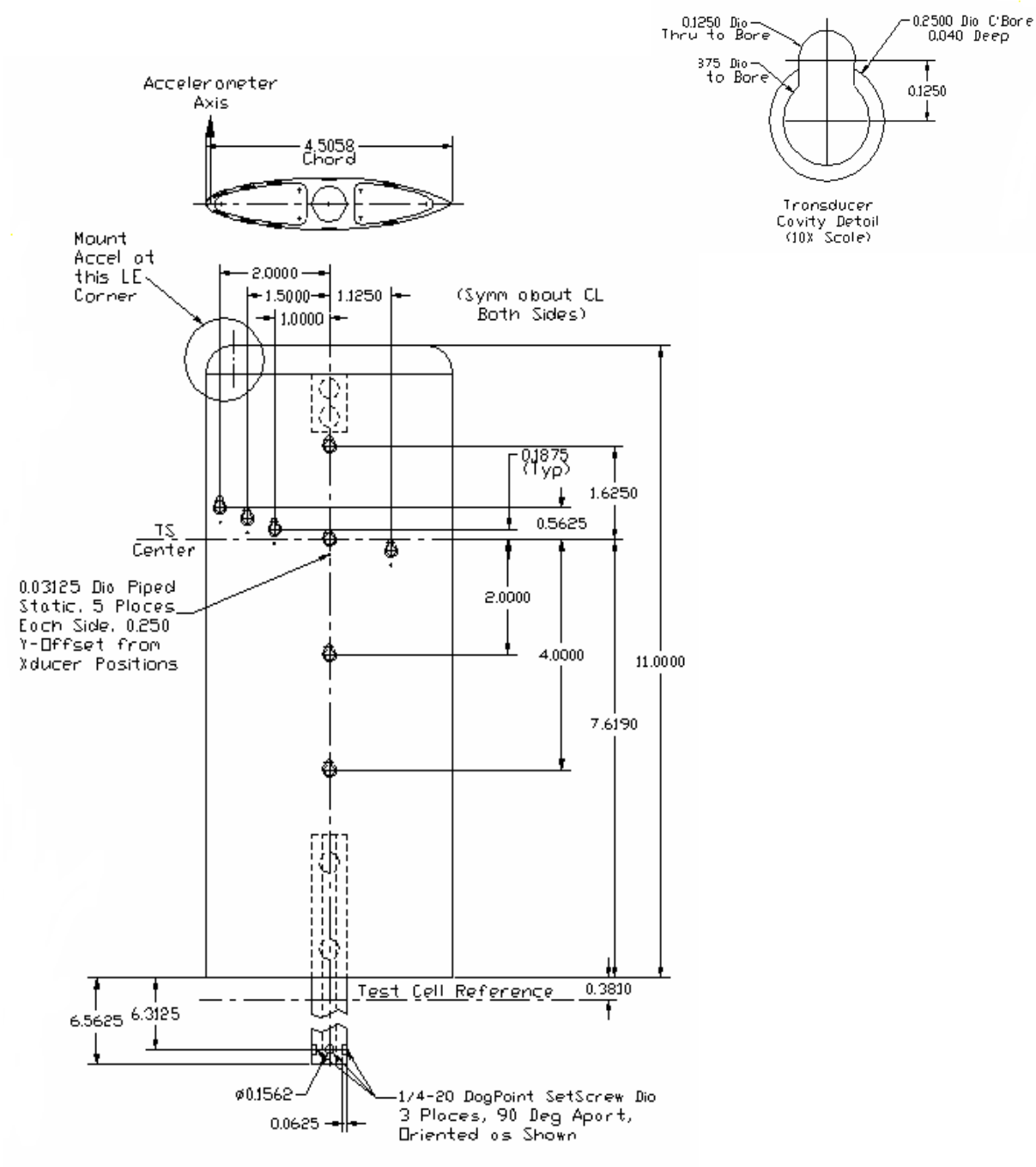

Figure 31. Rigid-Wing Instrumentation Drawing

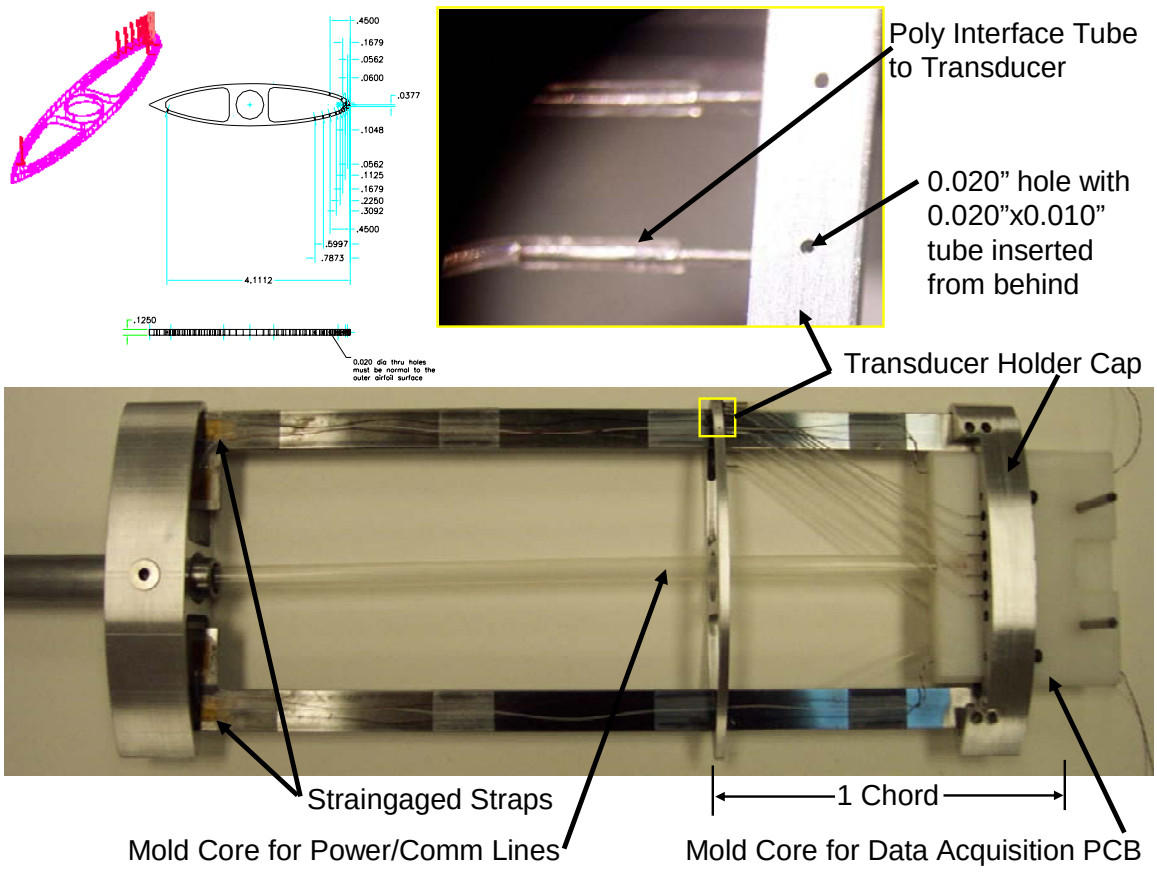

Figure 32. Flexible-Wing Instrumentation Drawing

Figure 33. Vibrometer Setup

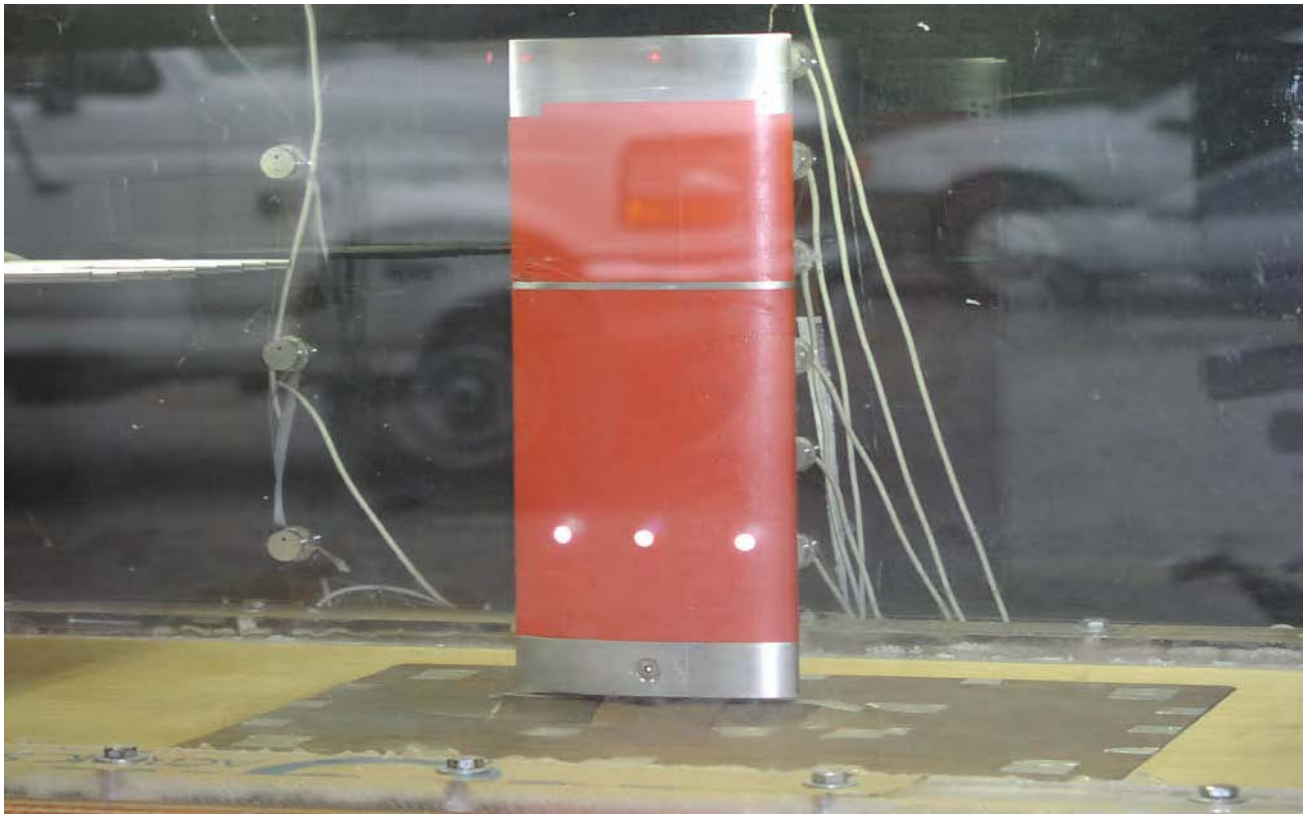

Figure 34. Flex-Wing Vibrometer Measurement Pattern (with Reflective "Dots")

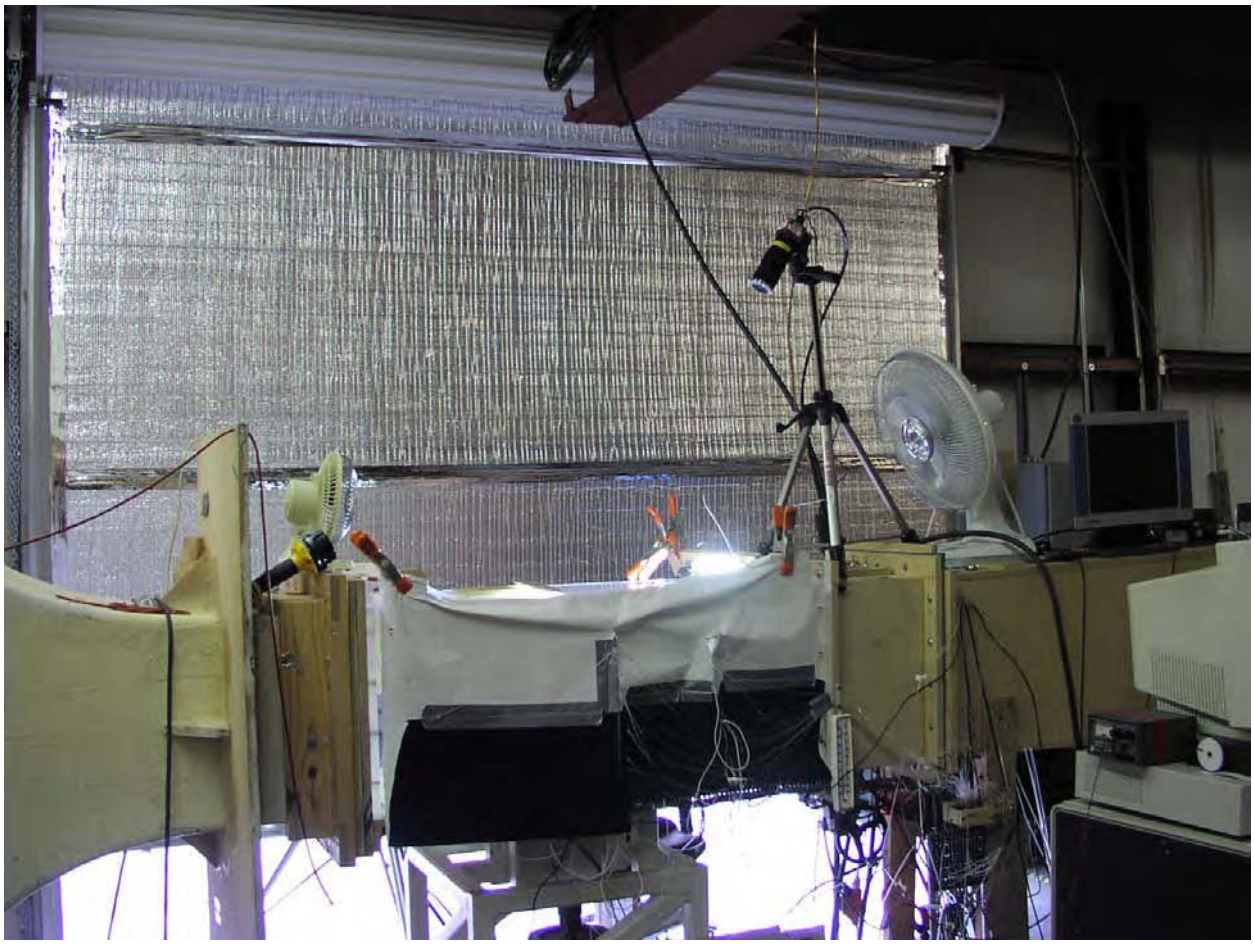

Figure 35. Displacement Camera Installation

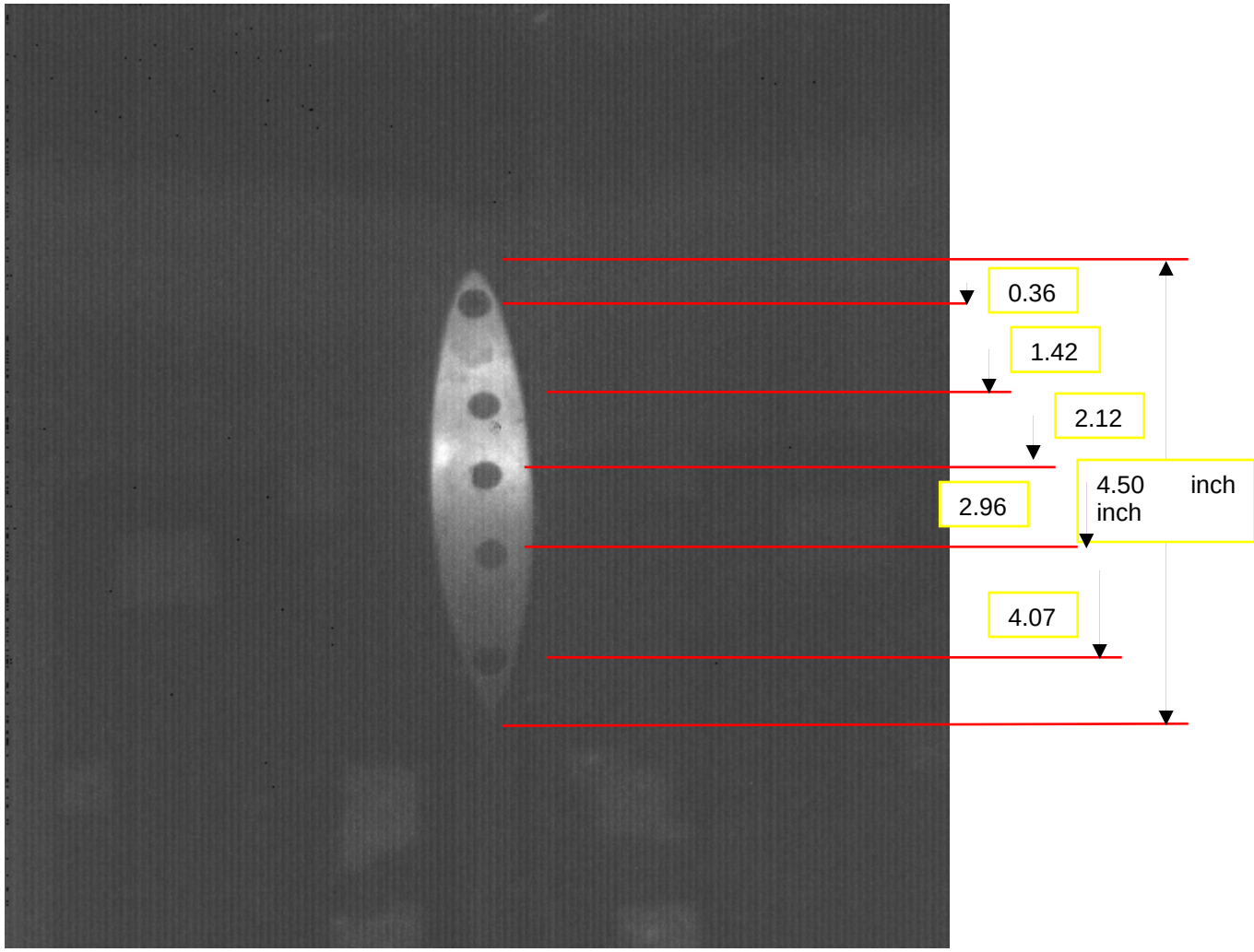

Figure 36. Displacement Camera Data Extraction Spots

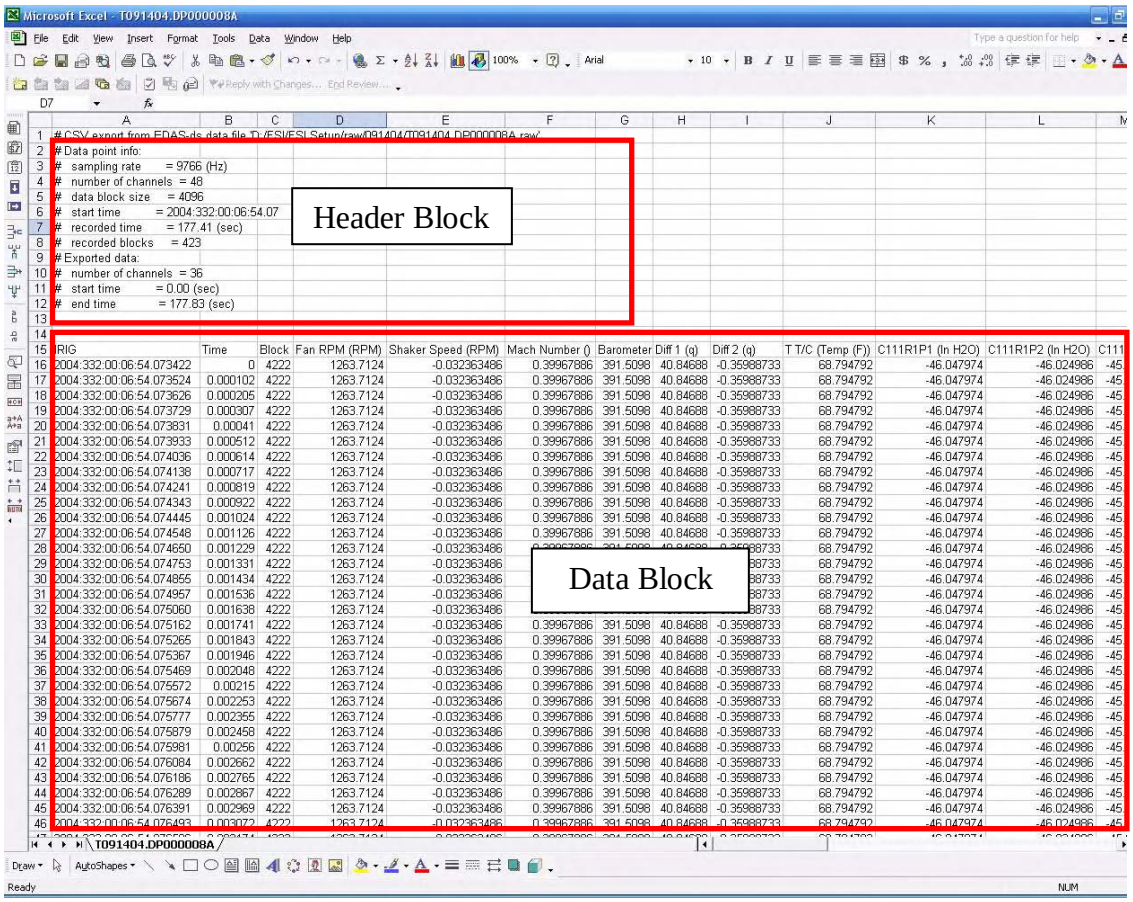

Figure 37. Example of a Recorded Data File Showing the Header and Data Blocks

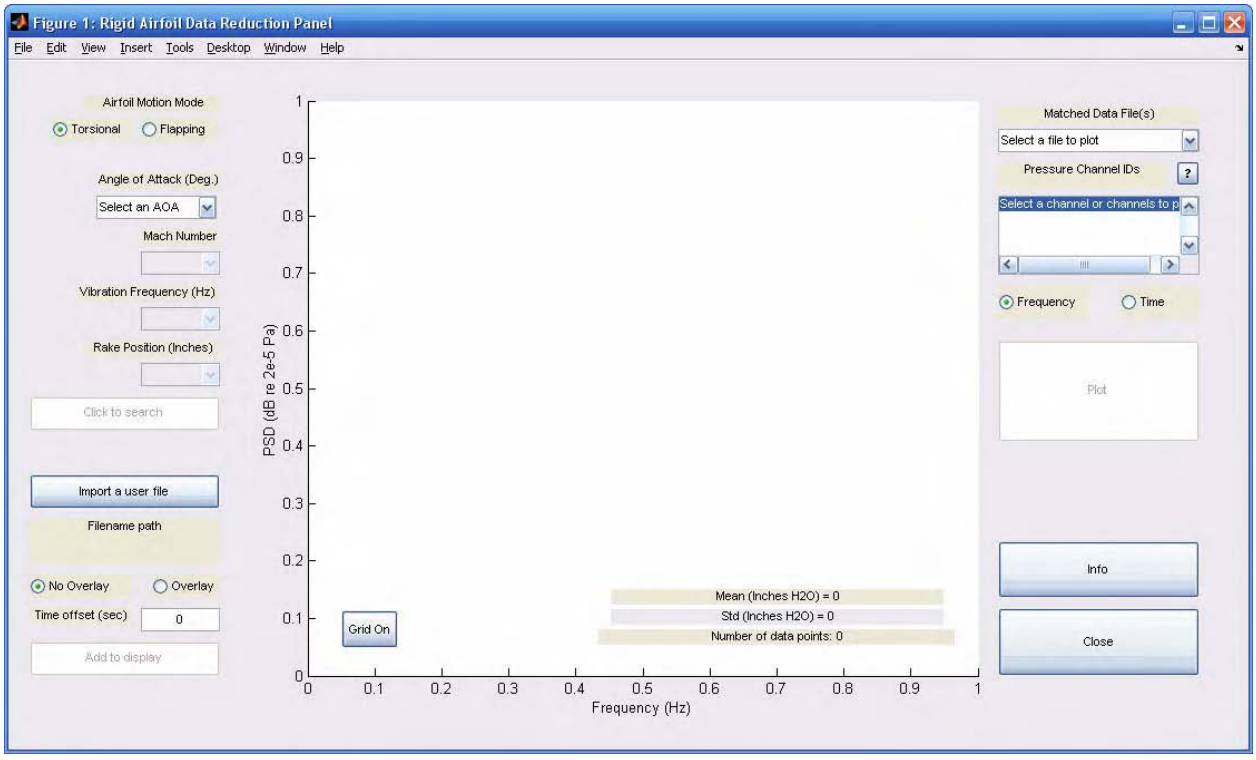

Figure 38. Startup GUI Window for the Rigid Airfoil Study

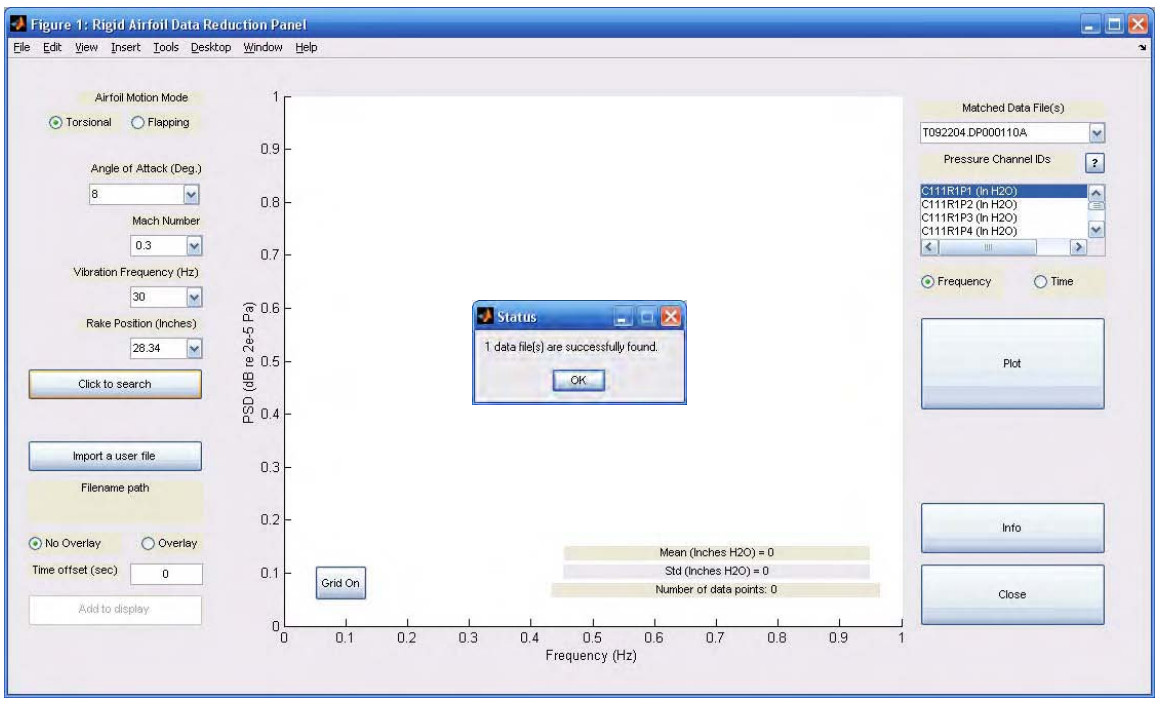

Figure 39. GUI Window Showing Example Input Parameters, Response, and Output Data File

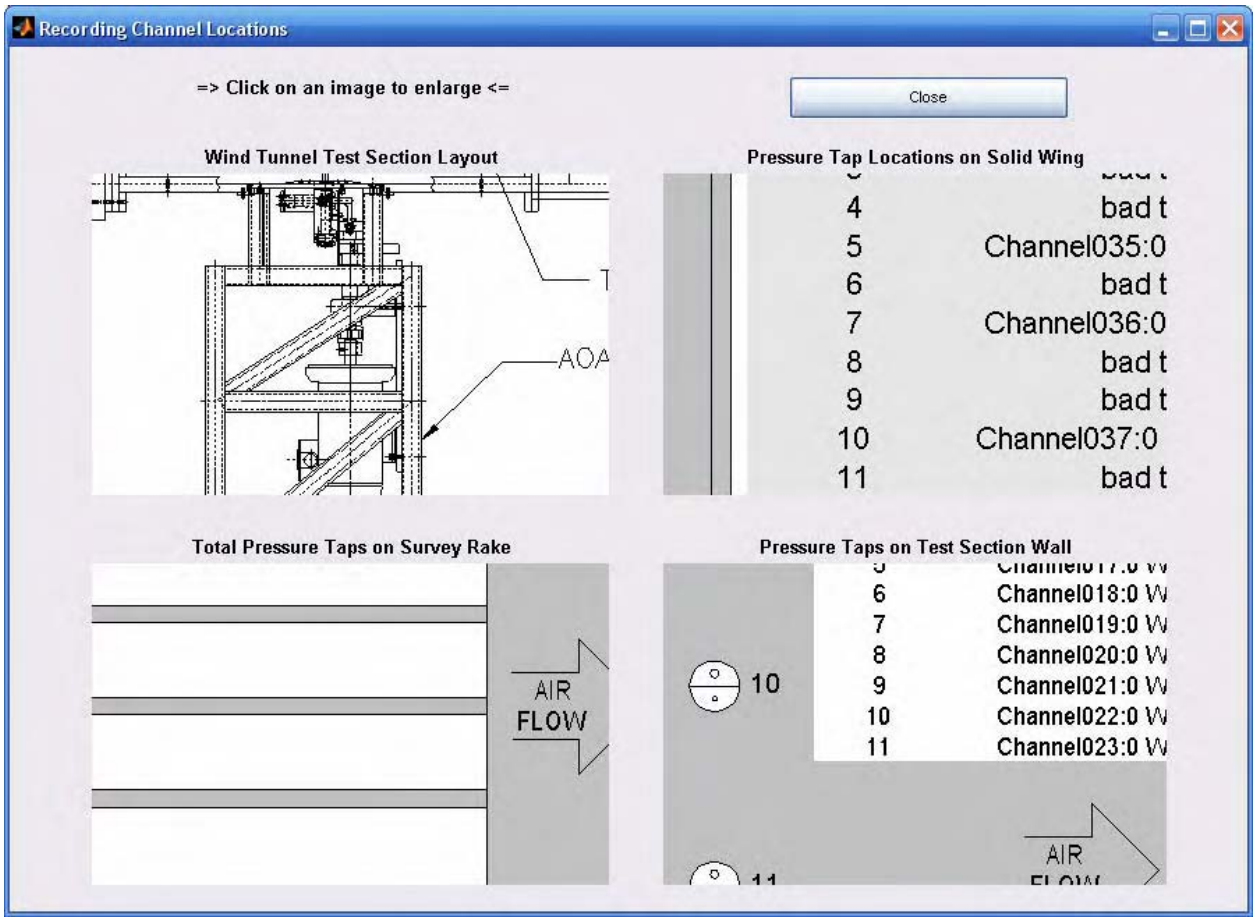

Figure 40. Sketches Showing the Data Recording Channels to the Locations of Measurement

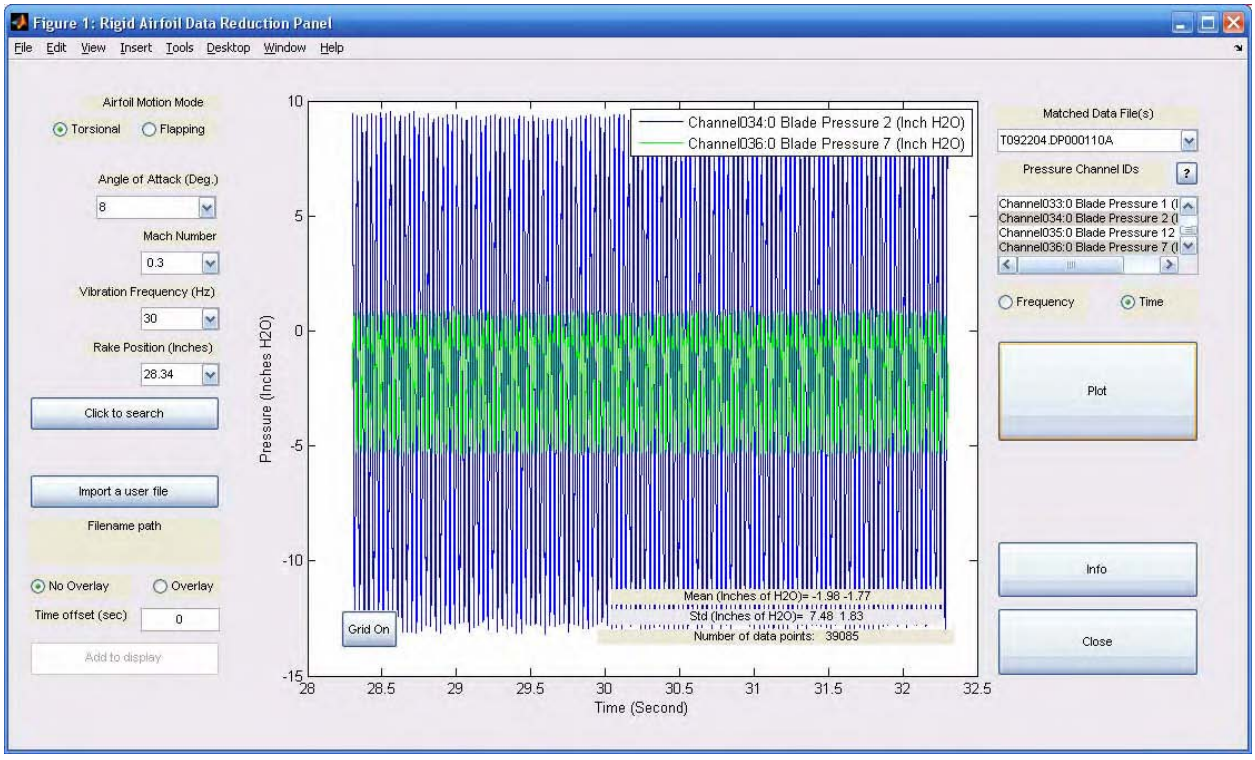

Figure 41. GUI Window Showing Example Data in Time Trace with Two Data Channels Displayed

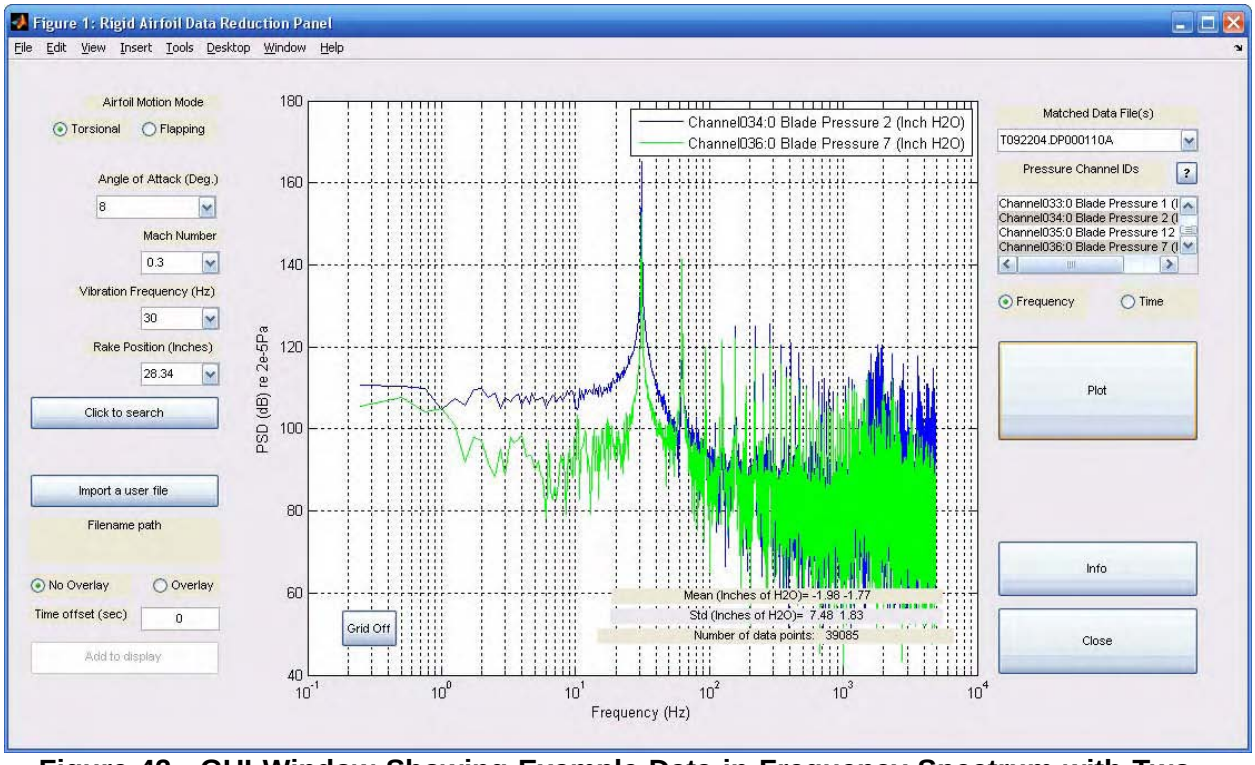

Figure 42. GUI Window Showing Example Data in Frequency Spectrum with Two Data Channels Displayed

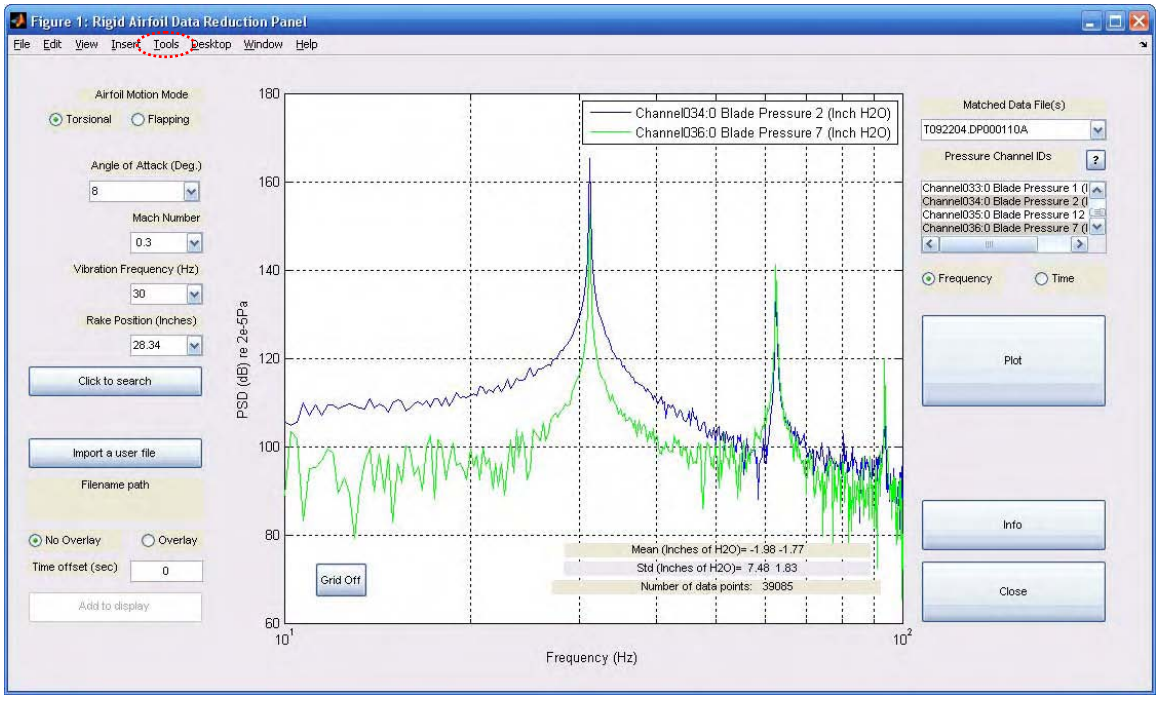

Figure 43. GUI Window Showing Blowup Frequency Range Using the Display Control on Axes Properties by "Tools" Menu (Circled)

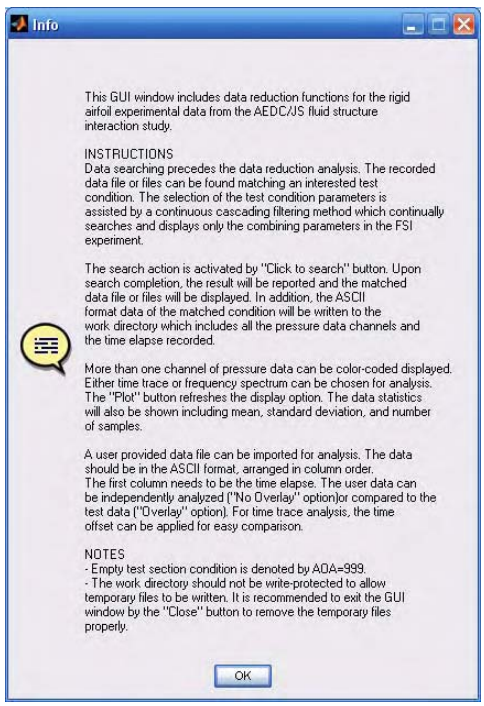

Figure 44. Text Window Showing Instructions for the GUI Functions

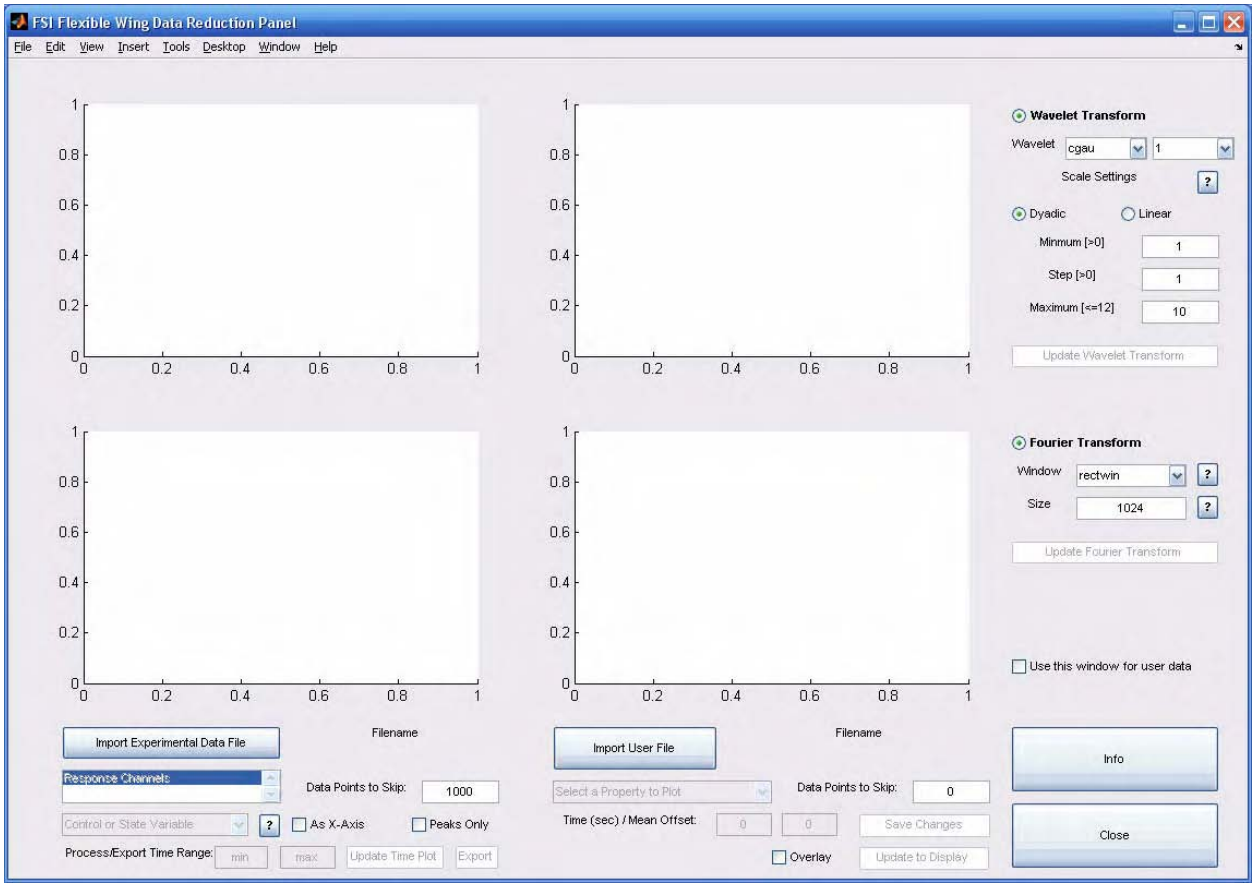

Figure 45. Startup GUI Window for Flexible Airfoil Data Reduction

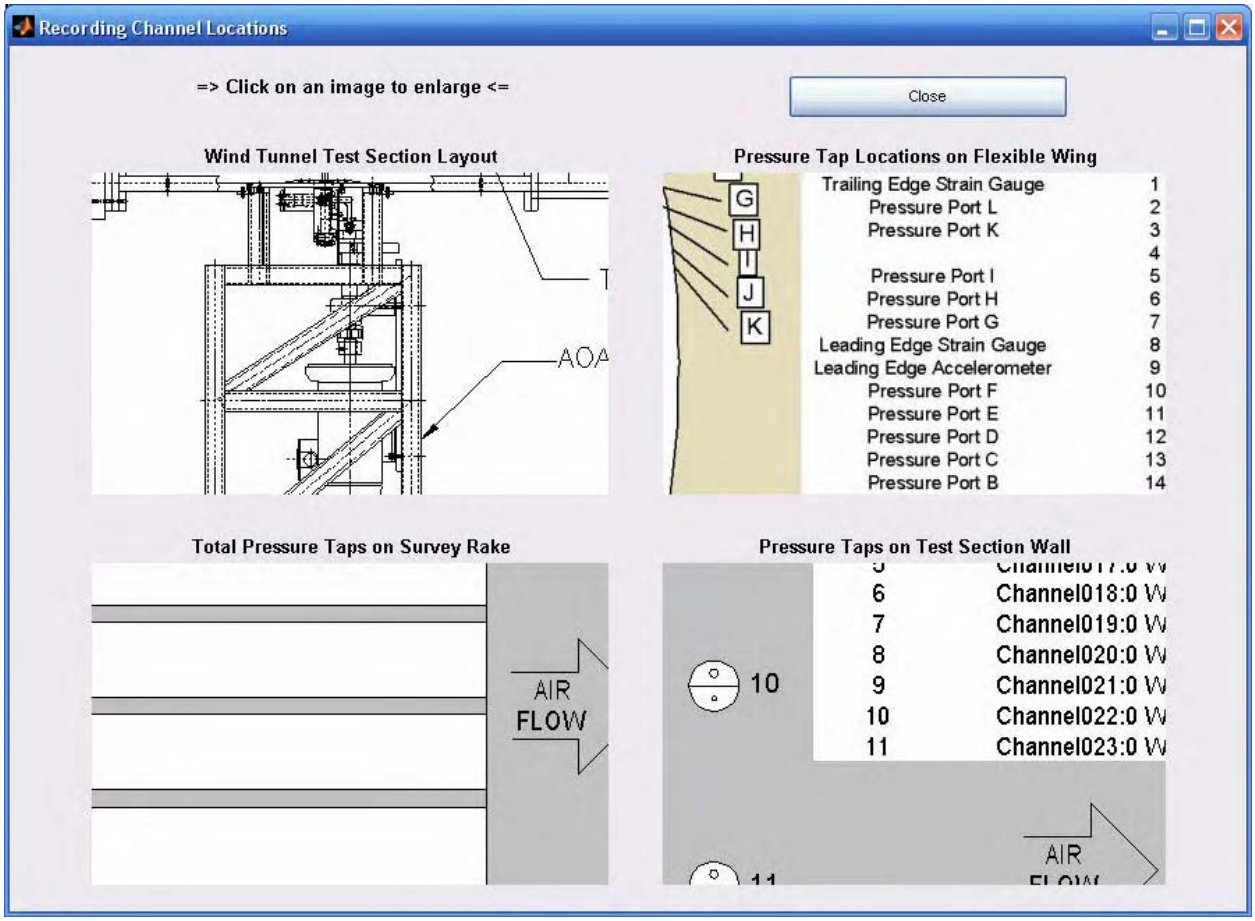

Figure 46. Sketches Showing the Correspondence of the Recording Channels to the Measurement Locations

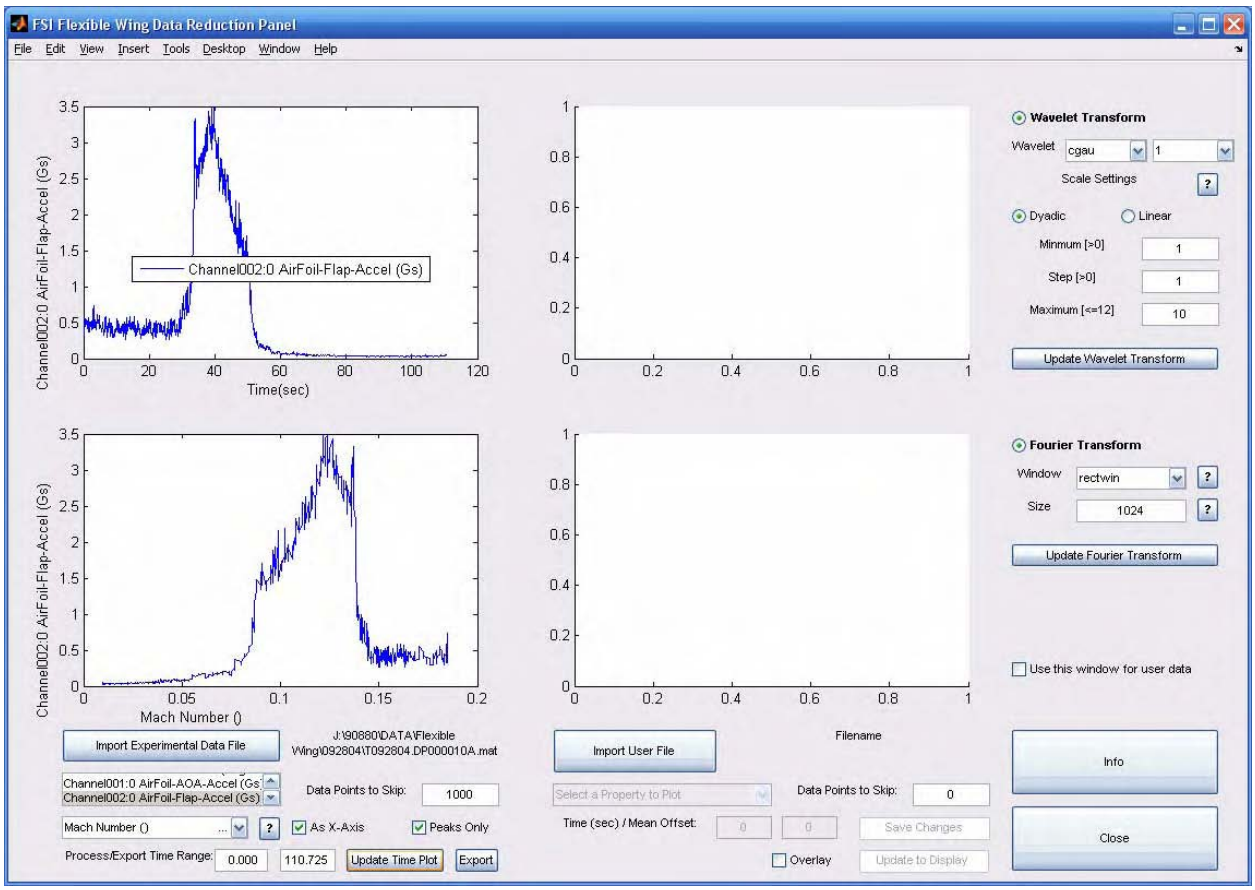

Figure 47. Sample Data Import Showing the Time Traces of Control (Bottom) and Response Parameters

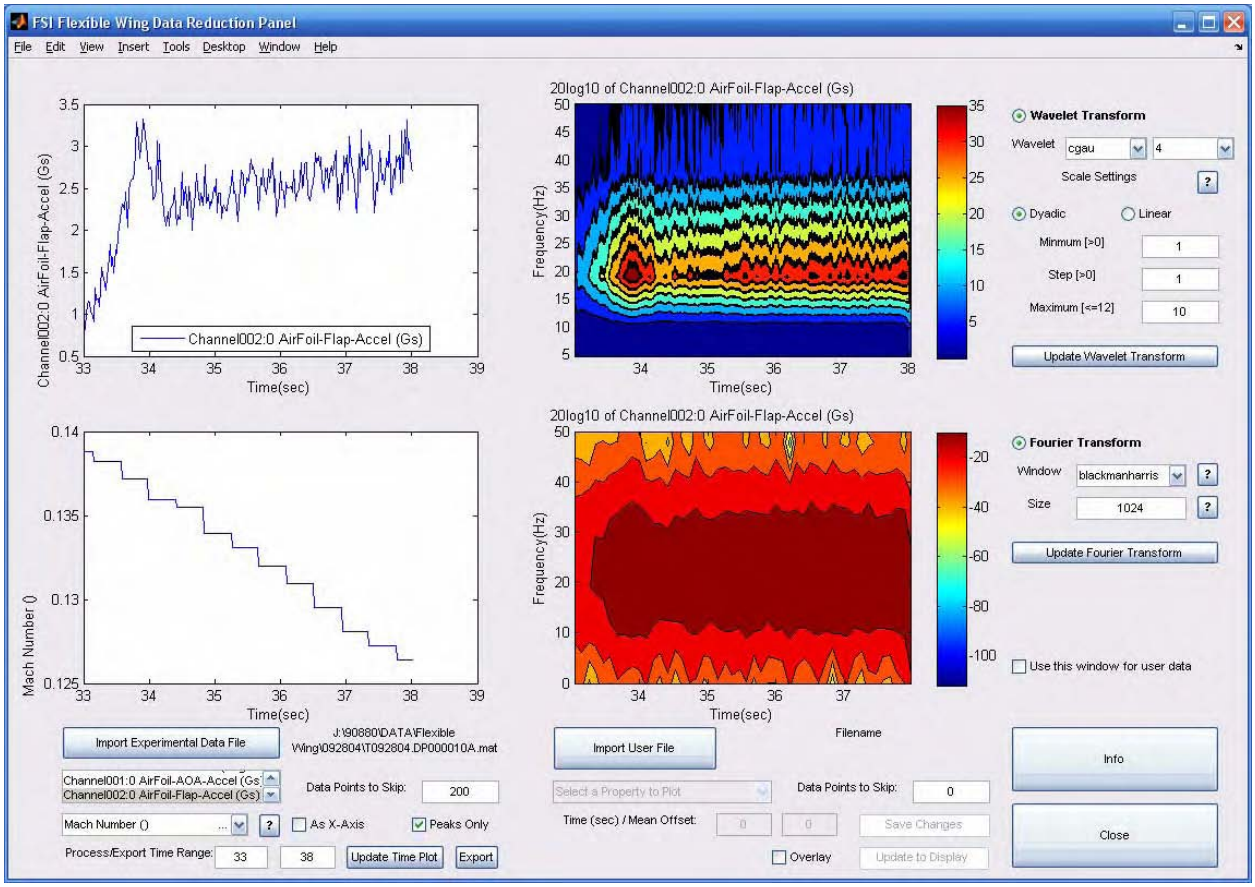

Figure 48. Sample Data Analysis Showing the Results of Wavelet and Fourier Transforms

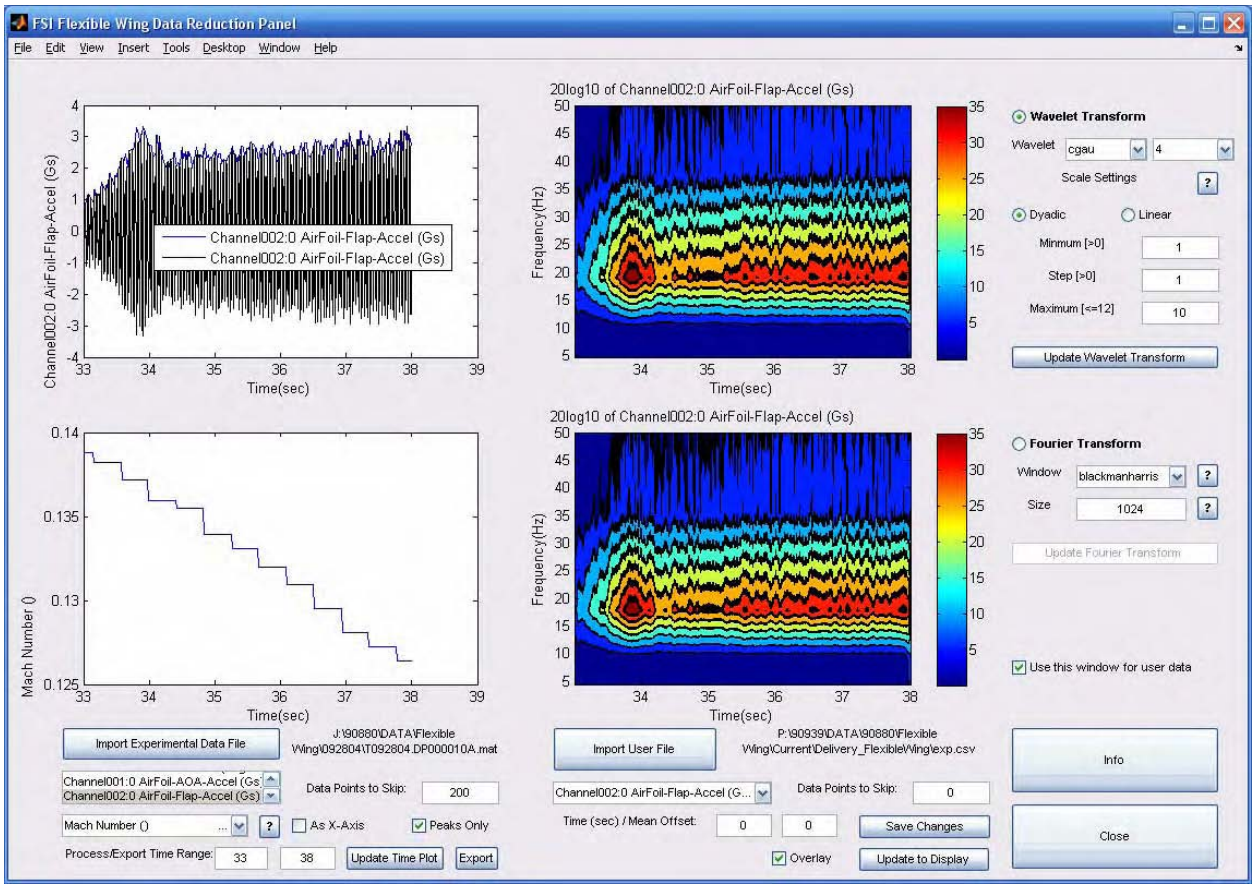

Note that this figure includes the time trace comparison; user data are shown in black by default.

Figure 49. Frequency Analysis of Sample Experiment and Sample User (Bottom Right) Data Using Wavelet Transform

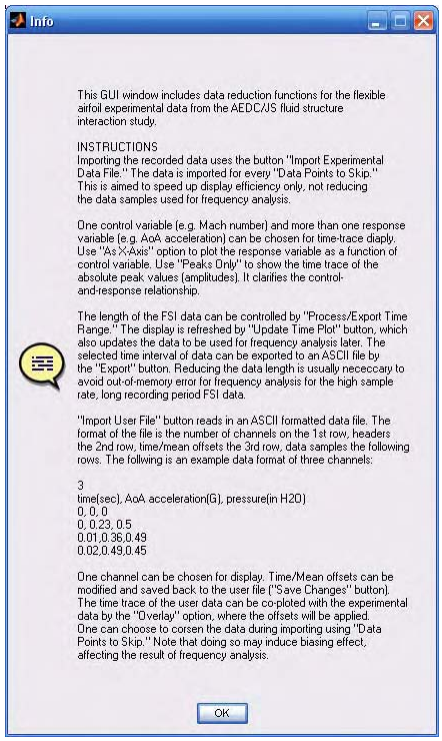

Figure 50. Software Instructions Available from the GUI Window

Figure 51. Typical Towed Device

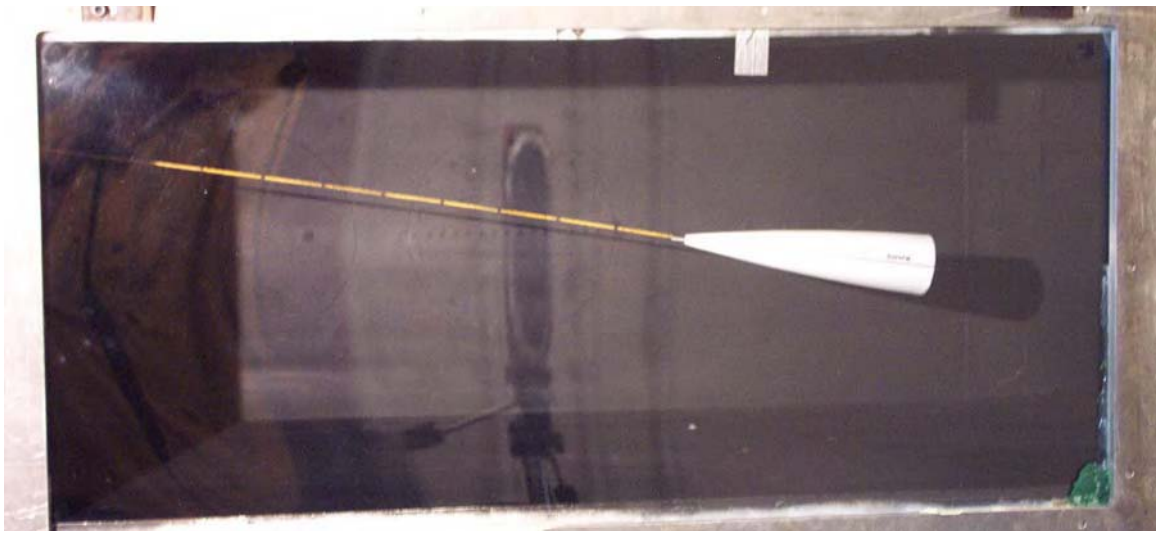

Figure 52. Tethered-Mass Model in UTSI Low-Speed Wind Tunnel

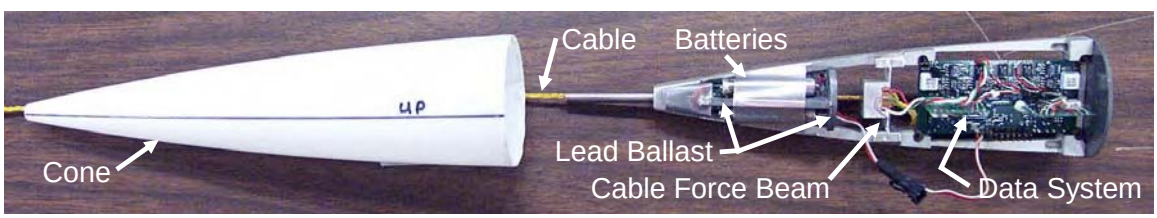

Figure 53. Tethered-Mass Assembly

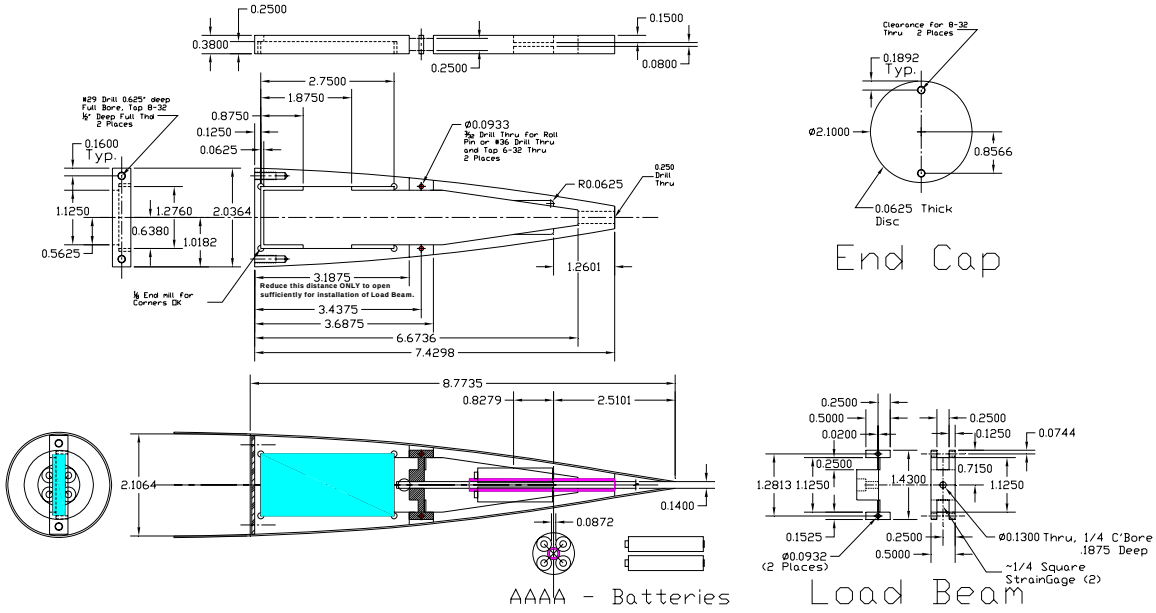

Figure 54. Tethered-Mass Cone and Skeleton Details

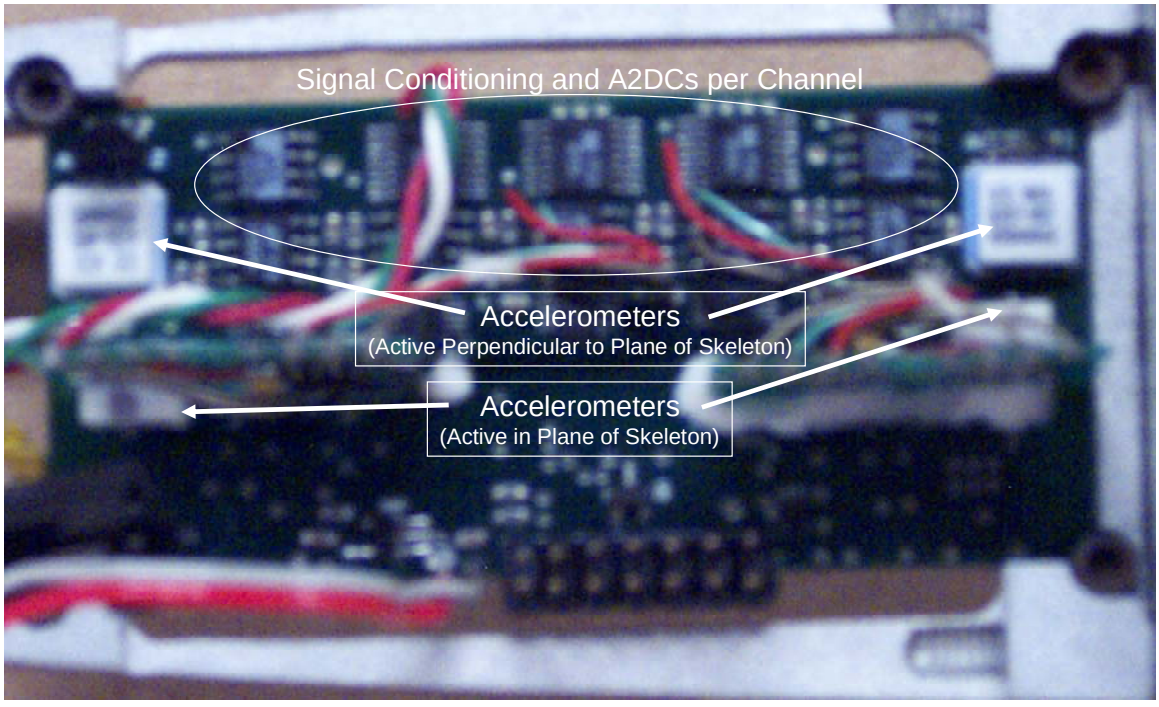

Figure 55. Six-Channel Data Acquisition System with Accelerometers

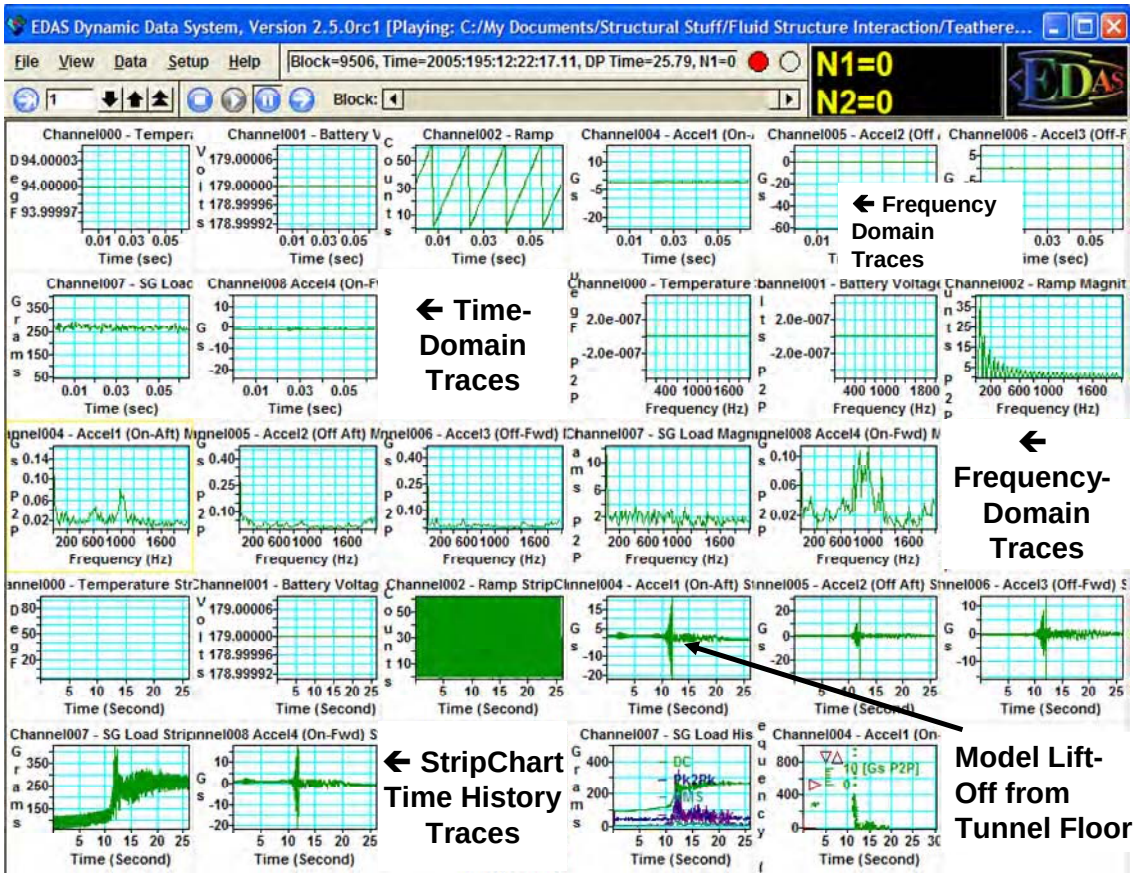

Figure 56. EDAS-dv Data Viewer Plots for 07/14/05 DP009 @ UTSI

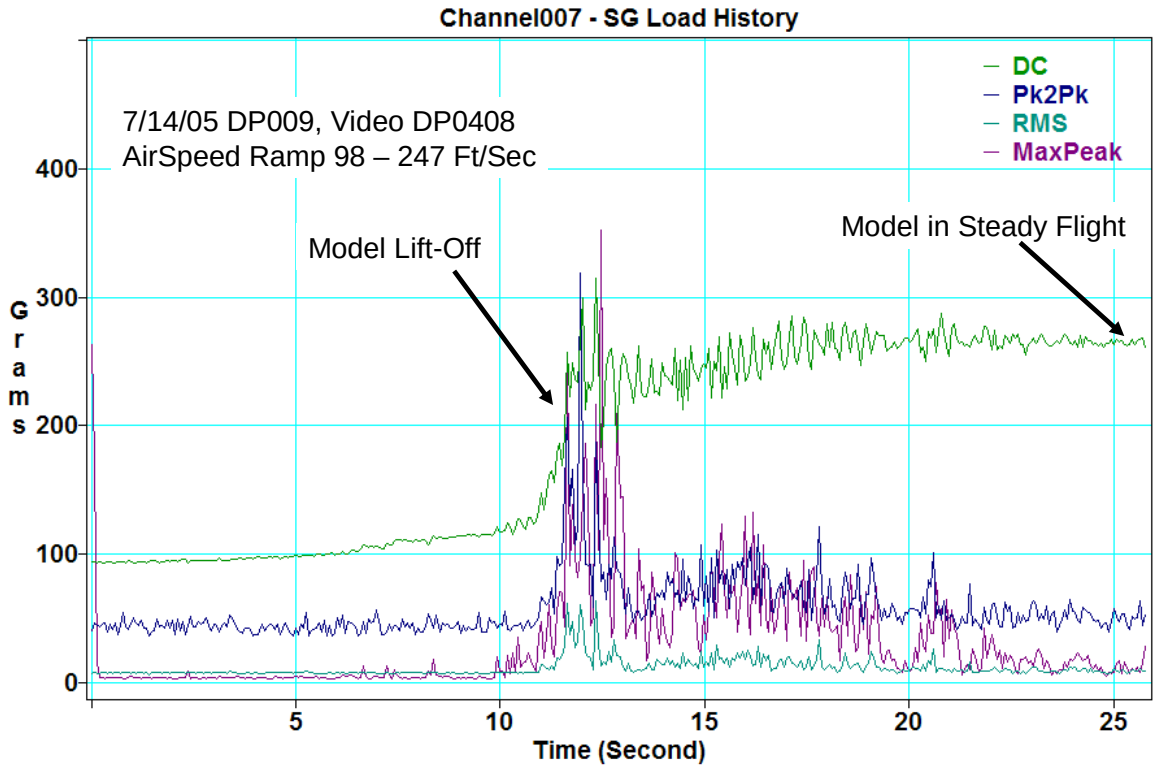

Figure 57. Cable Tension During Lift-Off for 07/14/05 DP009 @ UTSI

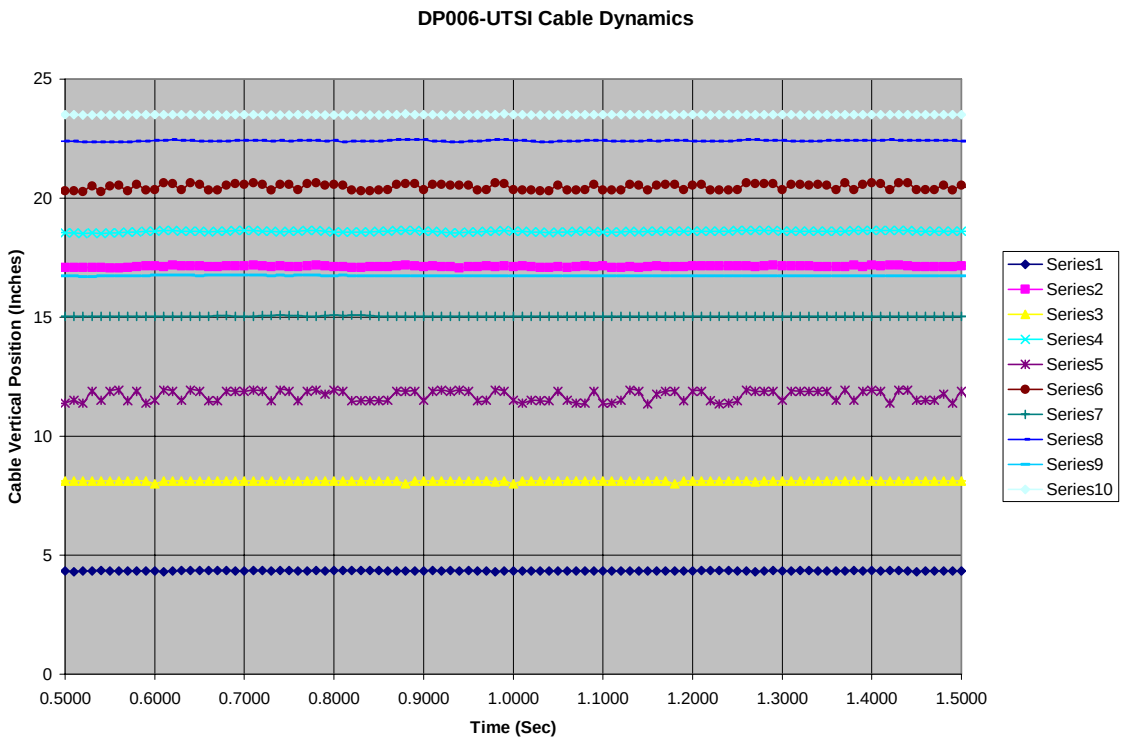

Figure 58. 07/14/05 DP009-UTSI Cable Dynamics Plot Generated from Video Data

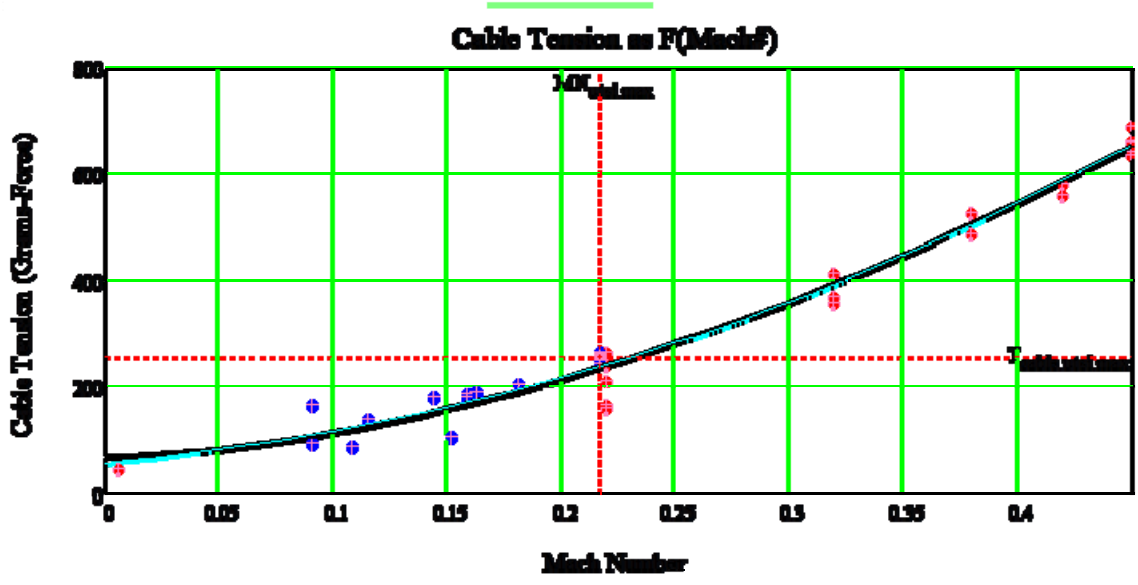

Figure 59. Cable Mean Tension vs. Mach Number

APPENDIX A. CFD SIMULATION OF THE JACOBS TECHNOLOGY INC. WIND TUNNEL

The Jacobs Technology Inc. (JTI) wind tunnel was simulated using the NXAIR flow solver. NXAIR is a finite-difference, density-based flow solver capable of handling perfect gas flows from very low Mach numbers to hypersonic Mach numbers. The geometry included in the tunnel model is shown in Fig. A-1, which also shows streamlines of the computed flow field.

The bellmouth, nozzle, test section, diffuser, and part of the exit leg were included in the simulation. The tunnel walls were treated as adiabatic and viscous, while the walls of the room at the tunnel inlet were treated as inviscid. The drive unit and the 90-deg turn leading into the drive unit at the exit of the tunnel were not modeled. The exit leg was extended downstream to place the location of the numerical boundary far from the expected unsteady flow in the diffuser. Since one of the main purposes of the simulation was to see what effect the unsteadiness in the diffuser could have on the test section flow, this was deemed to be an acceptable approximation to the geometry.

A second purpose in performing this simulation was to see what effect the asymmetric enclosure around the bellmouth inlet would have on the test section flow. Turbulence in the flow was modeled using the Shear Stress Transport (SST) multiscale model within NXAIR. Initial attempts to create a boundary condition to represent the honeycombs and screens in the inlet section were not successful, so the simulation was run without the screens and honeycombs. Thus, the results shown here represent a worst-case scenario of flow irregularities propagating downstream.

Flow was initiated by setting the exit-plane pressure and allowing the flow to accelerate from quiescent flow to reach the test section Mach number. Figures A-2 and A-3 are Mach number distributions on cut planes taken down the tunnel centerline.

It can be seen that the test section appears to be quite uniform, and the diffuser flow is highly dynamic. Although these are simply snapshots in time, the test section Mach number remains quite uniform during the course of the simulation, and no appreciable effect from the diffuser can be observed. Figure A-4 shows a plot of the sound pressure level at two locations in the tunnel – one in the test section wall, and one on the diffuser wall.

These plots were constructed using a total of 7500 points of sampled data and five windows of 1024 samples each. The plots represent the averages of the windows. All the data were collected after starting transients had died down. A comparison of the two curves indicates that the test section does not seem to be strongly affected by the unsteadiness in the diffuser, as evidenced by the lack of any real correlation between the responses beyond the behavior approaching zero Hertz. The dynamic behavior in the diffuser appears to be captured by the peak around 35 Hz and does not appear to feed back into the test section. The test section does show a small peak near 50 Hz, but the amplitude is significantly smaller than the level of dynamics in the diffuser, being roughly 10 db lower in amplitude than the diffuser peak.

Figure A-5 is a plot of centerline Mach number in the test section. Although the Mach number is slightly higher than the nominal experimental value of 0.28, the conclusions that have been drawn are still valid. The behavior of the Mach number is consistent with

APPENDIX A. CONCLUDED

a solid-wall tunnel. Thickening of the boundary layer down the tunnel walls results in a slight acceleration of the flow down the length of the test section. With this caveat (and this is common to solid-wall tunnels), the flow appears to be of good quality.

Figure A-6 shows the Mach contours within the inlet region and the test section. As can be seen, the inlet region possesses a definite asymmetry in the flow. This asymmetry is caused by the close presence of the walls of the room. As seen, the nonuniformity is not present in the test section. Since this run was made without the honeycombs and screens of the real tunnel, and since such devices should serve to minimize such nonuniformities, it is safe to assume that this simulation represents a worst-case scenario. Thus, the presence of the confining walls and the resultant nonuniformity in inlet behavior should have no significant impact on the flow quality in the test section.

In summary, the test section of the Jacobs Technology Inc. tunnel provides good uniform flow that should be adequate for the dynamic testing desired in the MASTER effort. The level of unsteadiness in the test section is very low and does not appear to be driven by the diffuser. The presence of screens and honeycombs in the inlet section will serve to further diminish the unsteadiness that the simulation indicates. For the purpose of further simulations, it would appear that the entire tunnel does not need to be modeled. It should be sufficient to model only the test section, including a portion of the inlet section and nozzle to provide some separation of the test section from the upstream boundary condition. Downstream of the test section, a good, nonreflective boundary condition should be used to propagate out the unsteady flow arising from the motion of the test article. Barring that, a section of the diffuser and straight run can be included in the model to allow the unsteadiness to dissipate ahead of the numerical boundary. The location of the numerical boundary can be estimated from Fig. A-2 or A-3 as roughly one diffuser length past the end of the diffuser.

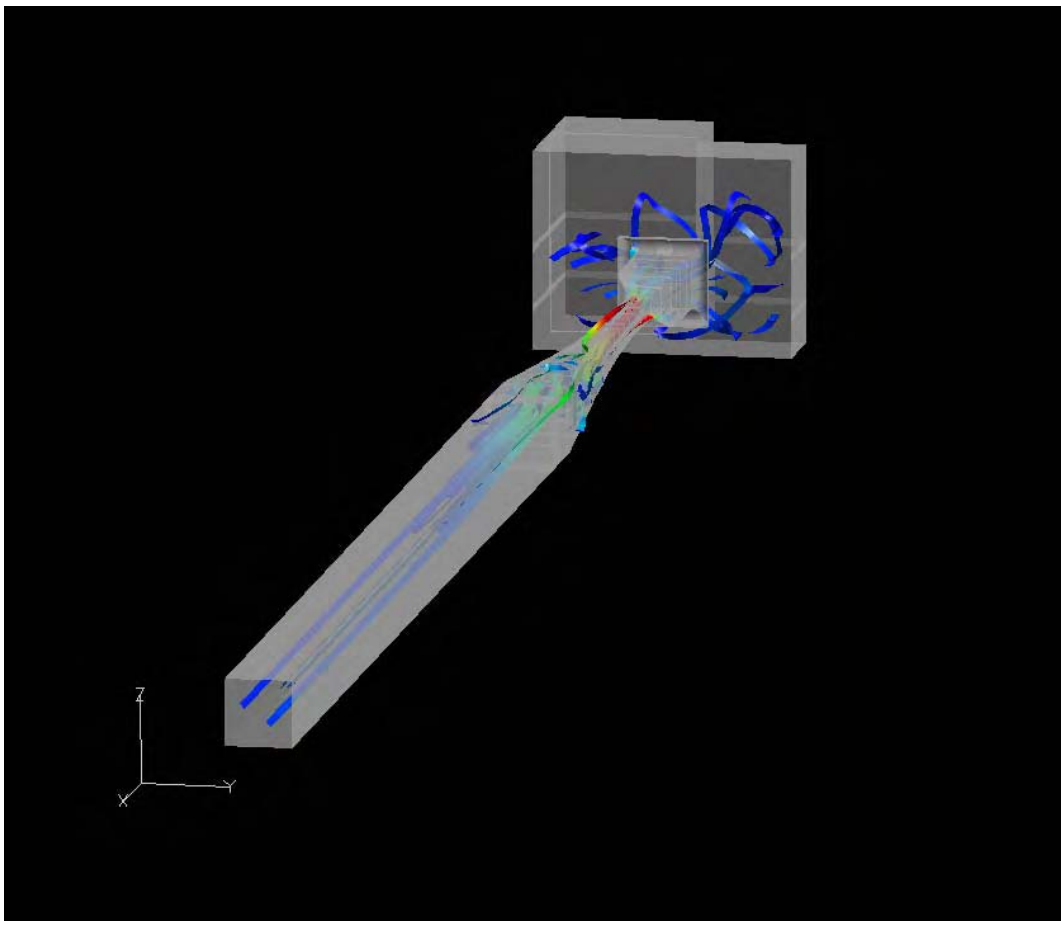

Figure A-1. Tunnel Geometry and Streamlines of Simulated Flow

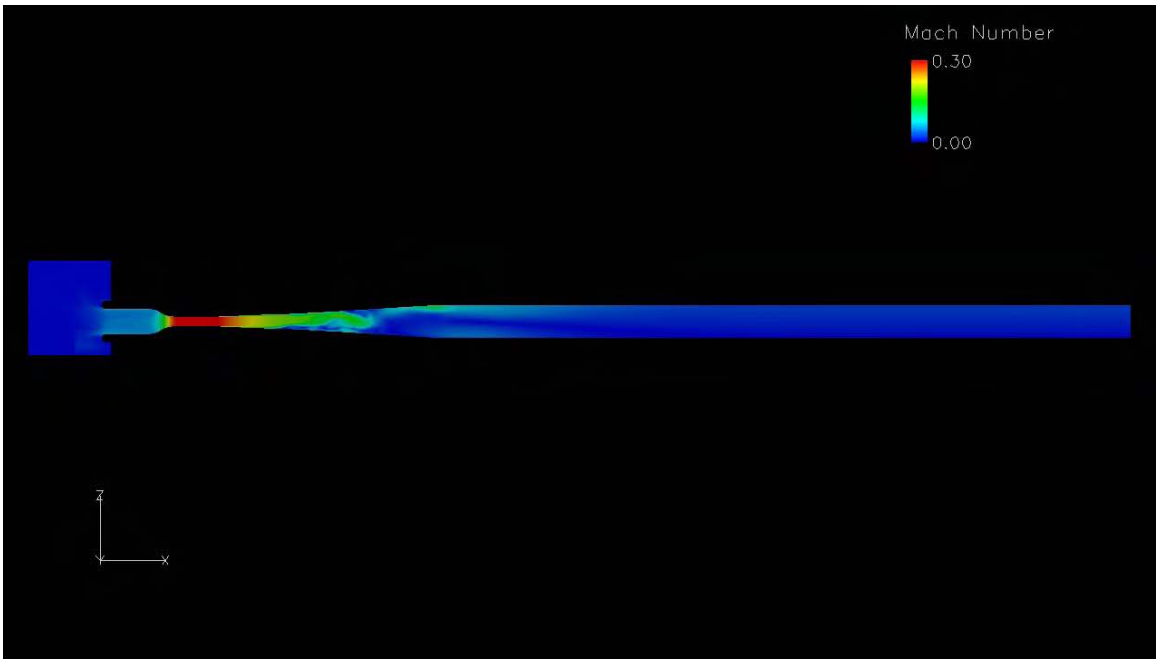

Figure A-2. Mach Number on Tunnel Center Plane, y = constant

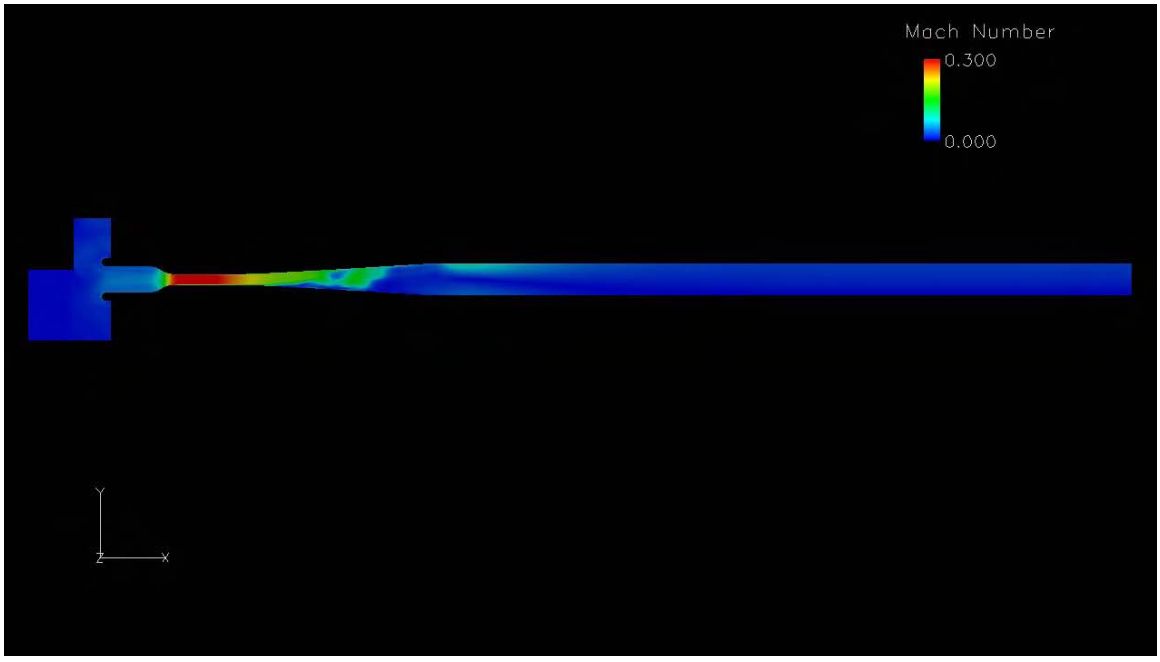

Figure A-3. Mach Number on Tunnel Center Plane, z = constant

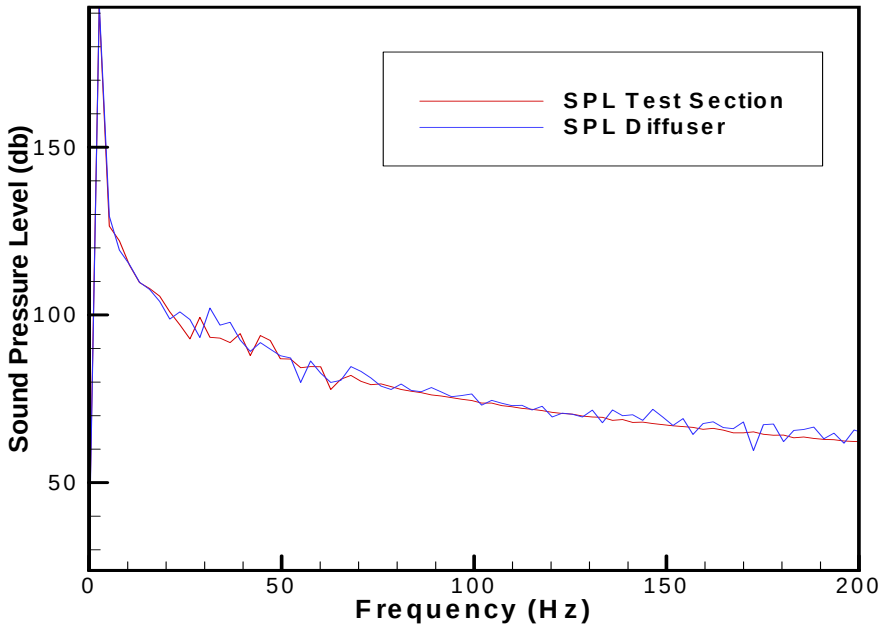

Figure A-4. Sound Pressure Levels in the Wind Tunnel at Two Locations

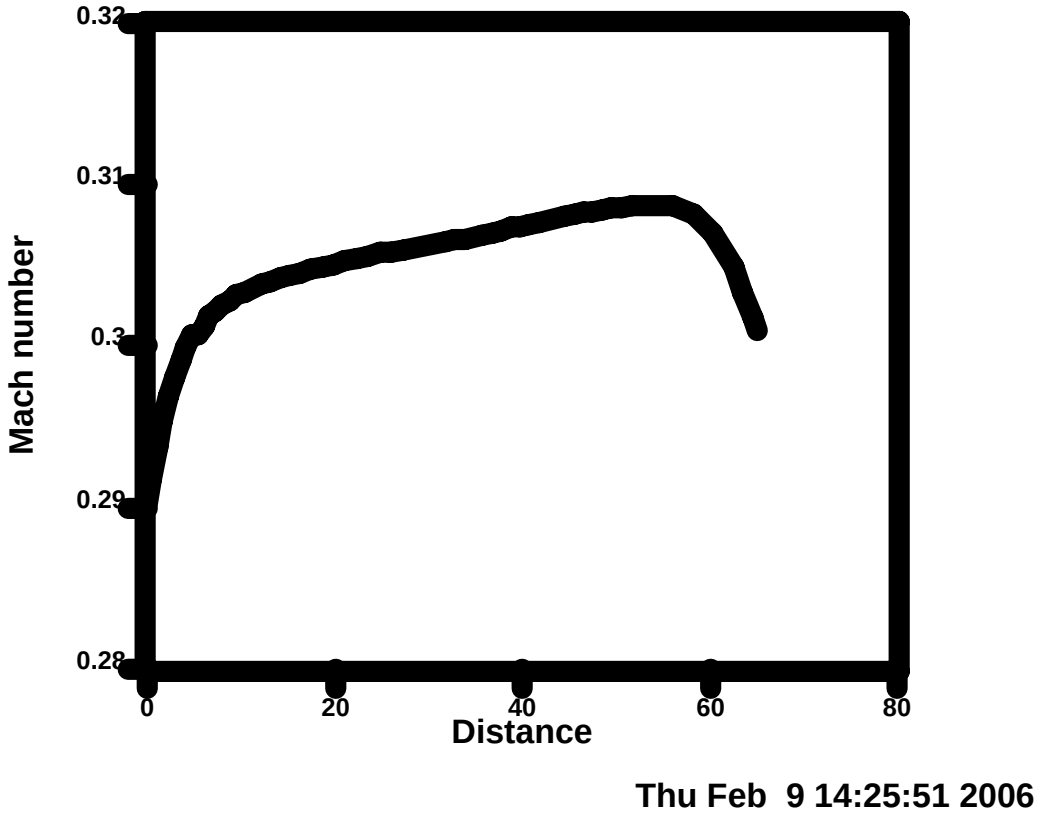

Figure A-5. Centerline Mach Number Distribution

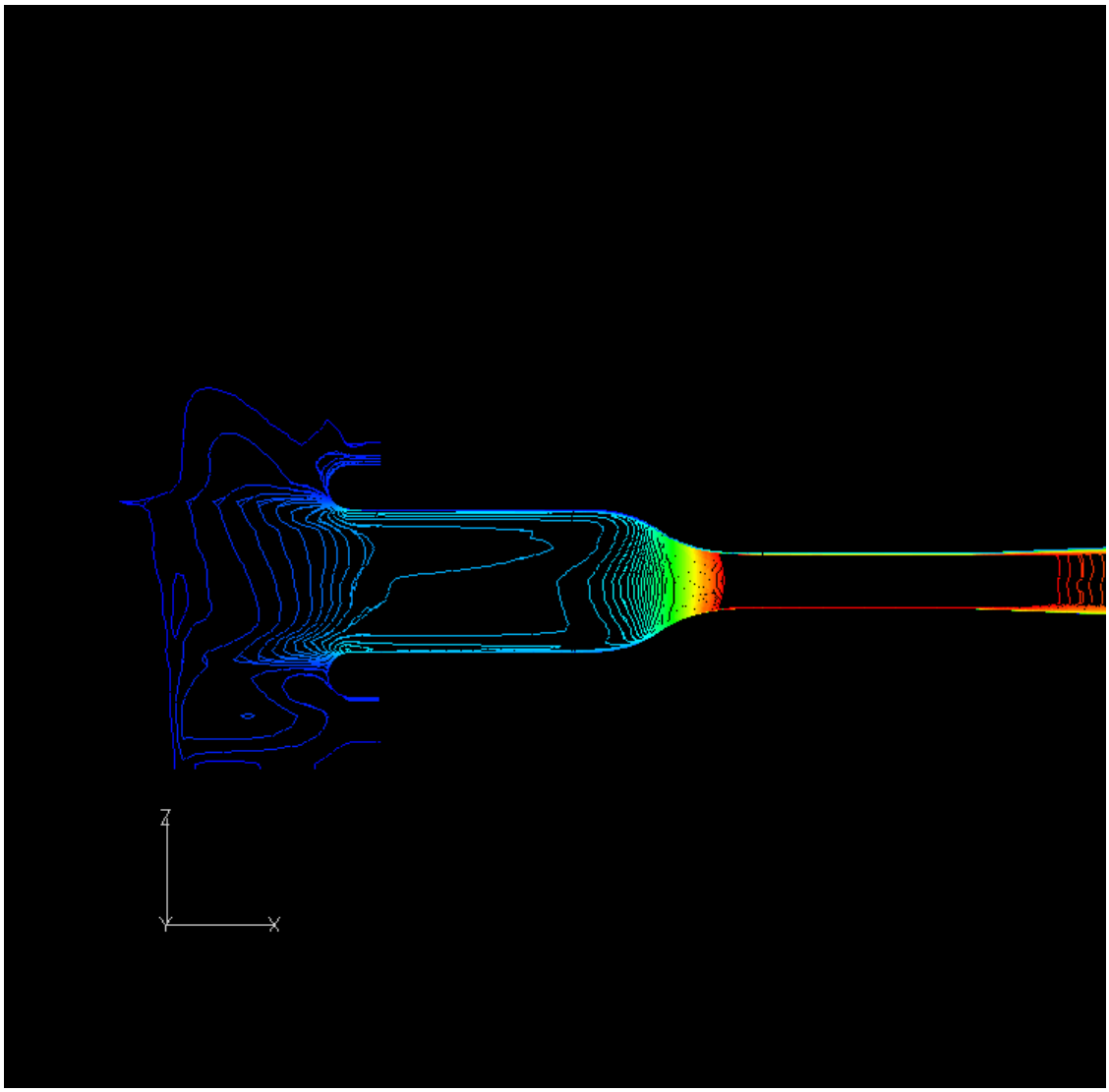

Figure A-6. Mach Contours Within the Inlet Region

APPENDIX B. FLEXIBLE AIRFOIL ELASTOMER MATERIAL PROPERTIES REPORT

The elastomer material testing for the flexible airfoil was accomplished at Axel Products, Inc. (http://www.axelproducts.com) in Ann Arbor, MI. The testing consisted of those conditions shown in Table B-1. These tests were chosen to help evaluate how the material stiffness properties varied with strain level, frequency, and temperature since it has been well established that elastomeric material properties are significantly affected by changes in these conditions. (Refer to the Axel Products web site under technical downloads for documents listed below (Refs. B-1 and B-2) describing the test processes employed for these tests.) At each condition, three individual tests were done for consistency and averaging. For most of the conditions, the three sets of data were evaluated with consistent results. Plots of the results for the static data were received from Axel Products and are shown in Figs. B-2, B-3, and B-4. Dynamic data were received in text file format in the time domain. A sample of dynamic data is plotted in Fig. B-1.

The method used to calculate the complex modulus of this elastomer material is described below. Percent strain level referred to in Table B-2 is conventional engineering strain, i.e., the amount of elongation divided by the original length of a specimen.

The dynamic modulus E_d is calculated from peak stress and strain values from data such as that in Fig. B-1 using Eq. (B-1). The storage and loss modulus, E_s and E_l, respectively, which make up the complex stiffness components in Table B-3 are calculated as shown in Eqs. B-2 (Refs. B-3 and B-4). Equation (B-3) is the complex modulus E* of the material where η is the loss factor. The angle δ in equations 2 is the phase angle between the stress and strain curves in Fig. B-1. This angle reflects the loss or damping properties in the material at the test conditions. The angle was computed from the test data using algorithms developed in Matlab (Ref. B-5). Table B-3 contains the calculated storage and loss modulus at the conditions specified in Table B-2. Figures B-2, B-3, and B-4 show plots of the static elastic (storage) modulus for 10-, 25-, and 50-percent strain levels at 73°F (23°C). The static tests included additional specimen types to evaluate the elastic modulus in shear and compressive strain states, also as described in Refs. B-1, B-2, and B-4, to aid in developing a material model for finite element analysis. However, these data are not applicable to any of the dynamic tests, and, on hindsight, it may have been more effective to have additional tests done at another distinct dynamic frequency instead of doing static tests.

$$E_d = \sigma_{pk}/\varepsilon_{pk} \tag{B-1}$$

$$E_s = E_d^* \cos\delta \qquad E_l = Ed^* \sin\delta \tag{B-2}$$

$$E^* = E_s\left(1+\frac{iE_l}{E_s}\right) = E_s(1+\eta) \tag{B-3}$$

FLEXIBLE AIRFOIL MODAL ANALYSIS

Several modal solutions of the flexible airfoil were accomplished in ANSYS (Ref. B-6) using the material properties from Table B-3 to get an idea of the impact that modal frequency variations in the elastomer material properties may have. Modal frequencies

APPENDIX B. CONCLUDED

are presented in Table B-4 for the first four modes. Damping was included in four cases using various values from Table B-3 of both the storage and loss modulus to get an idea of how damping affects the response results.

The material property variations exhibited in the elastomer material for the conditions tested showed little impact on the modal frequencies, as seen in Table B-4. Therefore, it is most likely, from a frequency identification standpoint, that variations in the elastomer material caused by changes in environmental conditions, strain, and frequency have negligible effects on airfoil modal frequencies. With regard to mode shapes, an examination of shape variations was not performed; instead, it was thought that accomplishing a harmonic analysis and doing amplitude comparisons would produce a good initial assessment to evaluate whether mode changes caused by the elastomer material variations were significant. The initial clue that amplitude changes were significant was the mode complex eigenvalues (real part indicates decay or growth). For the higher damped case, the real part was negative and an order of magnitude higher than the other damped cases, indicating that the higher damping increased the rate of amplitude decay. As discussed below, amplitude changes in the harmonic analysis were found to be significant.

As reported in Table B-4, harmonic solutions were run for two cases using a high- and low-loss modulus (E_l = 25.4 and E_l = 8, respectively) with a correlating storage modulus. It should be noted that when doing damping calculations the material damping coefficient β should be calculated for the frequency of interest. Otherwise, other modes, especially higher ones, will be overdamped with no oscillation. Table B-5 lists the material data for the harmonic solutions run with corresponding maximum amplitude at a specified location.

Separate analyses were done for mode 1 and mode 2 resonant frequencies. As seen in the table, the amplitude at the specified node increased markedly when β was reduced to correspond to the material properties at lesser damping. The increase is 64 percent and 200 percent, respectively, for mode 1 and mode 2. Figures B-5 and B-6 show plots of the displacement frequency response at the nodes specified for mode 2. The plot shows both a higher amplitude and a more sharply peaked response for the lightly damped case, which is typical.

CONCLUSION

Based on these results, the following recommendation is made for the fluid-structure modeling and code validation: Elastomer material properties should be carefully chosen from the test data results in Table B-3 to have potential for the predicted structural response of the airfoil to be reasonably accurate.

REFERENCES

B-1. Miller, K., “Testing Elastomers for Hyperelastic Models,” Axel Products, Ann Arbor, MI.

B-2. Miller, K., “Measuring Dynamic Properties,” Axel Products, Ann Arbor, MI.

B-3. Nashif, A.D., Jones, D.I.G. and Henderson, J.P. 1985 Vibration Damping, John Wiley and Sons, New York.

B-4. Miller, K., “Measuring Material Properties to Build Material Models in FEA,” Axel Products, Physical Testing Services White Paper, http://www.axelproducts.com .

B-5. Matlab, *Matlab User’s Manual*, Version 7.1.2005, The MathWorks, Inc., Natick, MA.

B-6. ANSYS, *ANSYS User’s Manual for Revision 10*, 2005, Swanson Analysis Systems, Inc., Houston, PA.

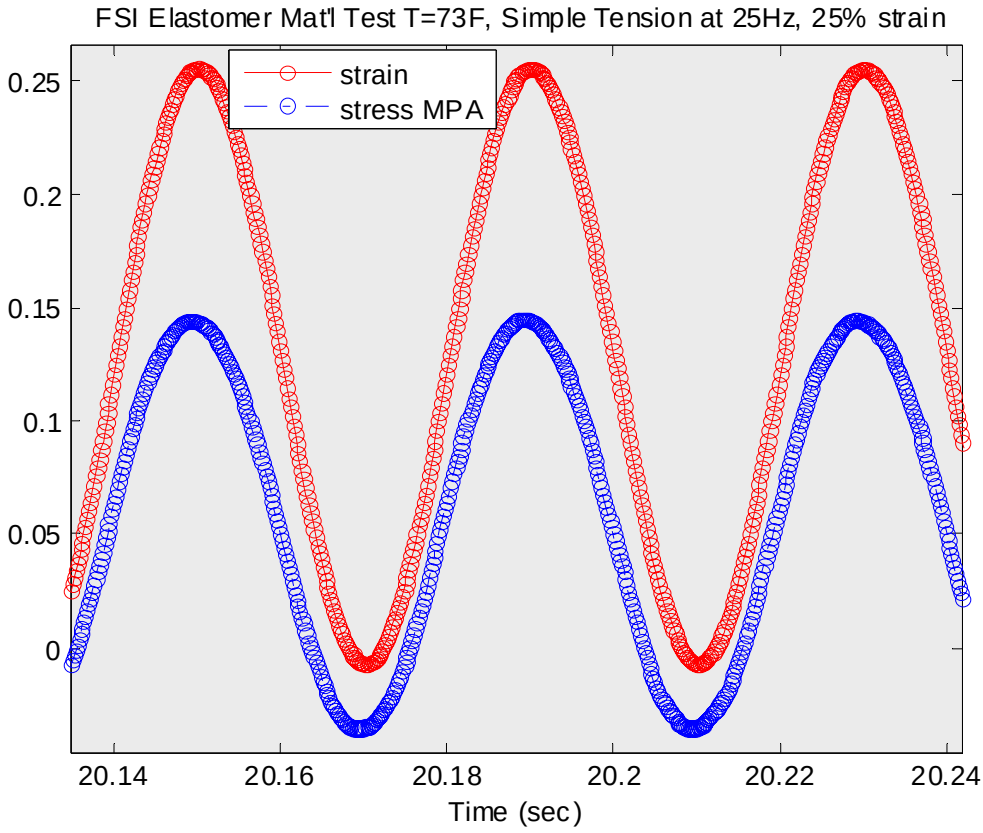

Figure B-1. Elastomer Stress Strain Test Data vs. Time

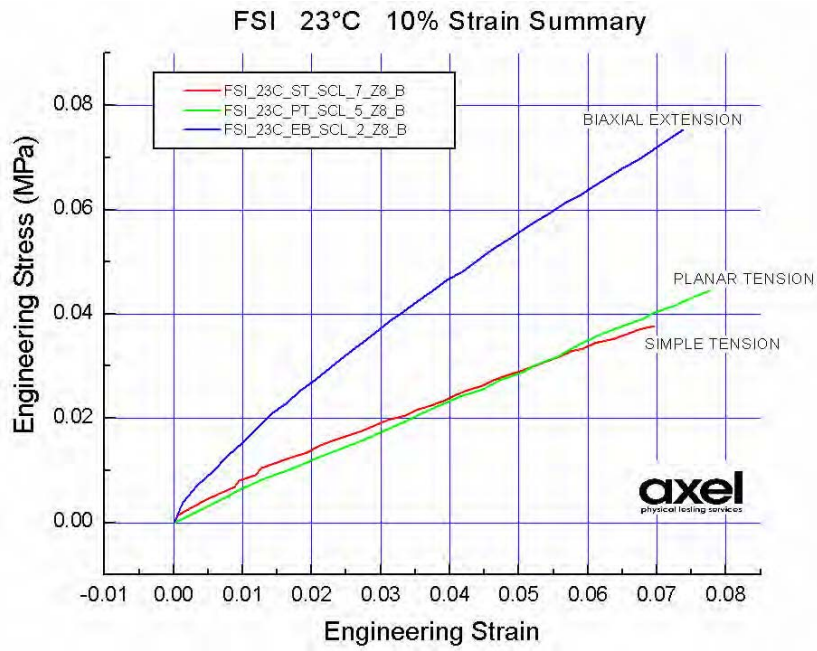

Figure B-2. Static Stress Strain Curves at 10-percent Strain

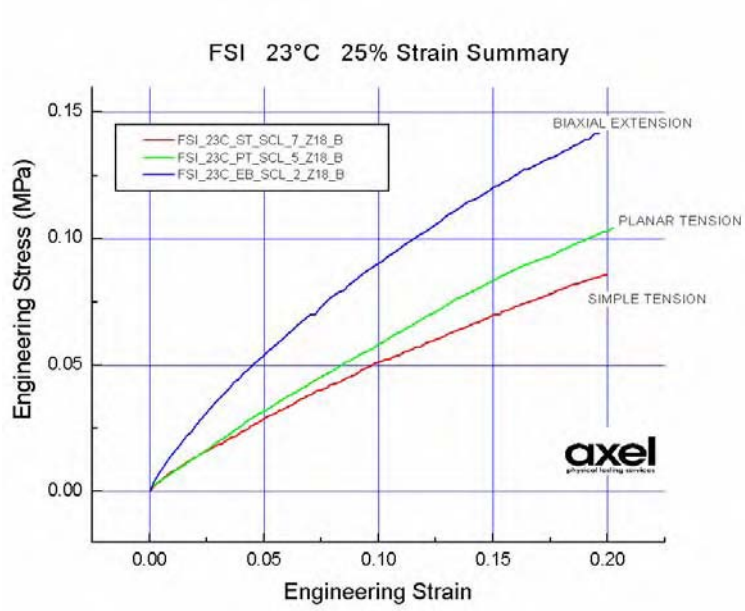

Figure B-3. Static Stress Strain Curves at 25-percent Strain

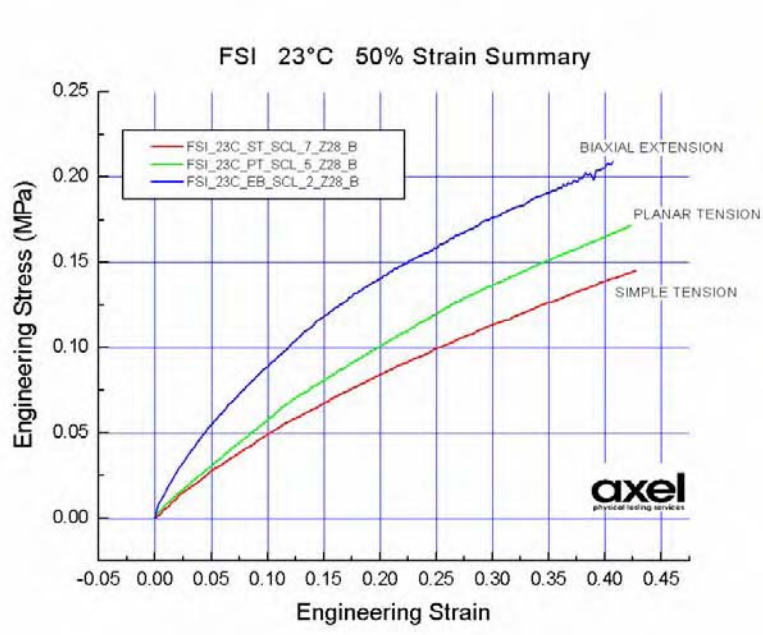

Figure B-4. Static Stress Strain Curves at 50-percent Strain

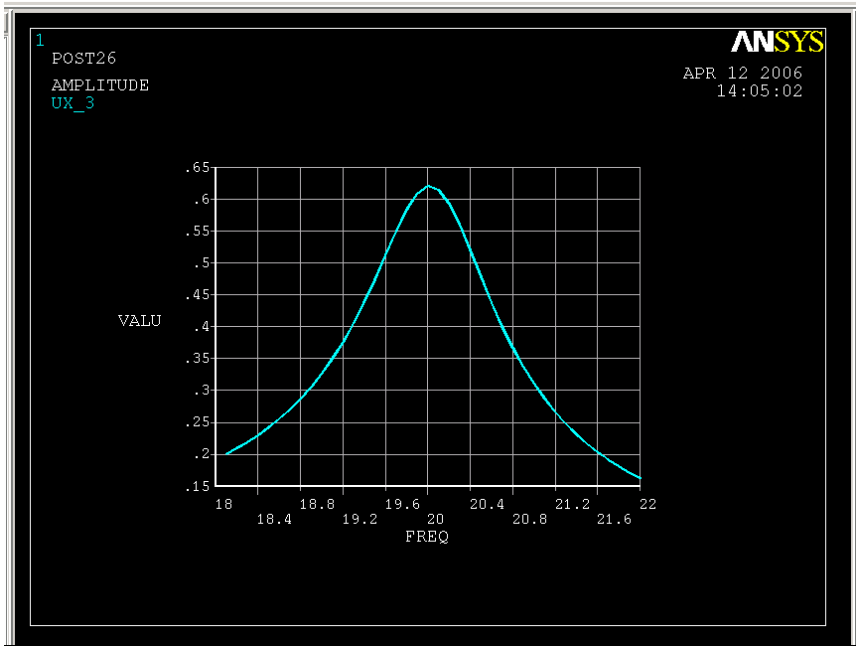

Figure B-5. Displacement vs. Frequency for Mode 2; β = 0.0024

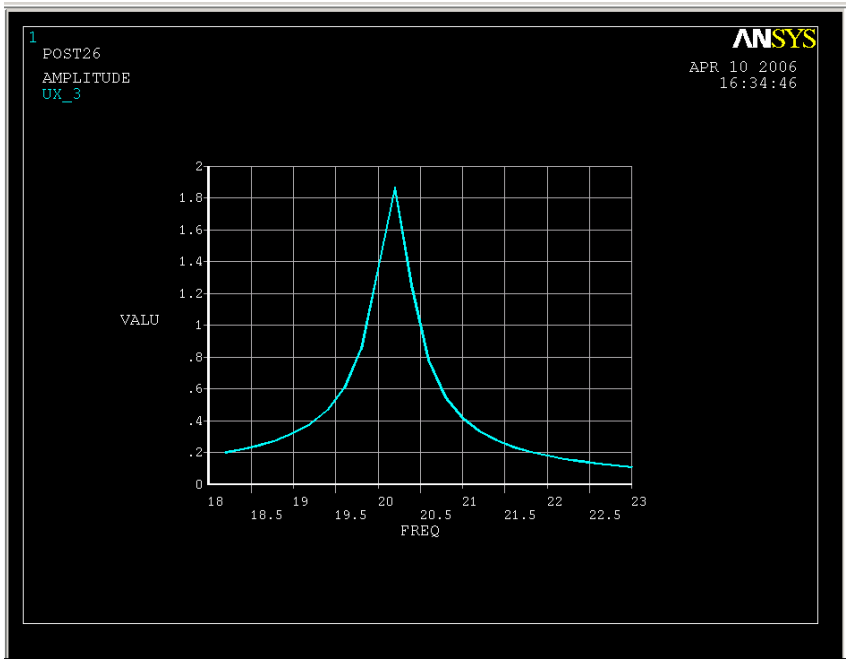

Figure B-6. Displacement vs. Frequency for Mode 2; β = 0.00075

Table B-1. Contraction Coordinates (x = 0 Inlet)

			Height		Width	Height/2	Width/2
X=	0	HEIGHT=	40	WIDTH=	38	20	19
X=	1	HEIGHT=	39.99909	WIDTH=	37.99911	19.999545	18.999555
X=	2	HEIGHT=	39.99272	WIDTH=	37.99287	19.99636	18.996435
X=	3	HEIGHT=	39.97544	WIDTH=	37.97595	19.98772	18.987975
X=	4	HEIGHT=	39.94178	WIDTH=	37.943	19.97089	18.9715
X=	5	HEIGHT=	39.8863	WIDTH=	37.88867	19.94315	18.944335
X=	6	HEIGHT=	39.80353	WIDTH=	37.80762	19.901765	18.90381
X=	7	HEIGHT=	39.68801	WIDTH=	37.69451	19.844005	18.847255
X=	8	HEIGHT=	39.53429	WIDTH=	37.54399	19.767145	18.771995
X=	9	HEIGHT=	39.3369	WIDTH=	37.35072	19.66845	18.67536
X=	10	HEIGHT=	39.0904	WIDTH=	37.10935	19.5452	18.554675
X=	11	HEIGHT=	38.78933	WIDTH=	36.81455	19.394665	18.407275
X=	12	HEIGHT=	38.42822	WIDTH=	36.46096	19.21411	18.23048
X=	13	HEIGHT=	38.00162	WIDTH=	36.04325	19.00081	18.021625
X=	14	HEIGHT=	37.50407	WIDTH=	35.55606	18.752035	17.77803
X=	15	HEIGHT=	36.93011	WIDTH=	34.99407	18.465055	17.497035
X=	16	HEIGHT=	36.27429	WIDTH=	34.35191	18.137145	17.175955
X=	17	HEIGHT=	35.53115	WIDTH=	33.62425	17.765575	16.812125
X=	18	HEIGHT=	34.69523	WIDTH=	32.80575	17.347615	16.402875
X=	19	HEIGHT=	33.76108	WIDTH=	31.89105	16.88054	15.945525
X=	20	HEIGHT=	32.72323	WIDTH=	30.87483	16.361615	15.437415
X=	21	HEIGHT=	31.57623	WIDTH=	29.75172	15.788115	14.87586
X=	22	HEIGHT=	30.31462	WIDTH=	28.51639	15.15731	14.258195
X=	23	HEIGHT=	28.93604	WIDTH=	27.16654	14.46802	13.58327
X=	24	HEIGHT=	27.58036	WIDTH=	25.83911	13.79018	12.919555
X=	25	HEIGHT=	26.32287	WIDTH=	24.60781	13.161435	12.303905
X=	26	HEIGHT=	25.15988	WIDTH=	23.46905	12.57994	11.734525
X=	27	HEIGHT=	24.08769	WIDTH=	22.4192	12.043845	11.2096
X=	28	HEIGHT=	23.10262	WIDTH=	21.45465	11.55131	10.727325
X=	29	HEIGHT=	22.20096	WIDTH=	20.57178	11.10048	10.28589
X=	30	HEIGHT=	21.37904	WIDTH=	19.76698	10.68952	9.88349
X=	31	HEIGHT=	20.63316	WIDTH=	19.03663	10.31658	9.518315
X=	32	HEIGHT=	19.95963	WIDTH=	18.37713	9.979815	9.188565
X=	33	HEIGHT=	19.35476	WIDTH=	17.78486	9.67738	8.89243
X=	34	HEIGHT=	18.81485	WIDTH=	17.25621	9.407425	8.628105
X=	35	HEIGHT=	18.33622	WIDTH=	16.78755	9.16811	8.393775
X=	36	HEIGHT=	17.91518	WIDTH=	16.37528	8.95759	8.18764

Table B-1. Concluded

			Height		Width	Height/2	Width/2
X=	37	HEIGHT=	17.54803	WIDTH=	16.01578	8.774015	8.00789
X=	38	HEIGHT=	17.23108	WIDTH=	15.70544	8.61554	7.85272
X=	39	HEIGHT=	16.96065	WIDTH=	15.44064	8.480325	7.72032
X=	40	HEIGHT=	16.73304	WIDTH=	15.21777	8.36652	7.608885
X=	41	HEIGHT=	16.54456	WIDTH=	15.03322	8.27228	7.51661
X=	42	HEIGHT=	16.39153	WIDTH=	14.88337	8.195765	7.441685
X=	43	HEIGHT=	16.27024	WIDTH=	14.7646	8.13512	7.3823
X=	44	HEIGHT=	16.177	WIDTH=	14.67332	8.0885	7.33666
X=	45	HEIGHT=	16.10814	WIDTH=	14.60588	8.05407	7.30294
X=	46	HEIGHT=	16.05995	WIDTH=	14.5587	8.029975	7.27935
X=	47	HEIGHT=	16.02874	WIDTH=	14.52815	8.01437	7.264075
X=	48	HEIGHT=	16.01084	WIDTH=	14.51061	8.00542	7.255305
X=	49	HEIGHT=	16.00253	WIDTH=	14.50248	8.001265	7.25124
X=	50	HEIGHT=	16.00013	WIDTH=	14.50013	8.000065	7.250065
X=	51	HEIGHT=	16	WIDTH=	14.5	8	7.25

Table B-2. Elastomer Material Test Matrix

Fluid Structure Elastomer Test Matrix				
Testing for Young's Mod vs. Strain Level at Freq , T = 73F				
Strain Lev % -->	10	25	50	
Frequency, Hz				
Static	X	X	X	ST PT EB
4	X	X	X	ST
25	X	X*	X	ST
Testing for Cyclic E vs Temperature, @strain level 25%				
Temperature, F	30	73	100	
Frequency, Hz				
4	X	X	X	ST
25	X	X	X	ST
Testing for Bulk Modulus vs. Temperature				
Temperature F	30	73	100	Vol Compr Exper

* One additional data point for extended cure time at this condition
ST = simple tension, PT = planar tension, EB = equal biaxial

Table B-3. Storage and Loss Modulus of Complex Stiffness E*

FSI Flexible air foil elastomer material properties tables - Simple Tension

Elastic Storage Modulus - psi

25% Constant strain

x freq Hz	y1 static	y2 4Hz	y3 25Hz	
xtemp	0	4	25	
30	*	81.3	91.3	
73	62.5	#	88.3	^^81
100	*	73.1	84.9	

73F Constant temperature vs variable strain rate

x freq Hz	y1 static	y2 4Hz	y3 25Hz	
xpcstrn	0	4	25	
10	78.5	91.5	94.8	
25	62.5	#	88.3	^^81
50	49.3	60.1	67.5	

73F Constant temperature vs variable frequency

x pc strain	y1 10%	y 25%	y3 50%
x freq Hz	10	25	50
0	78.5	62.5	49.3
4	91.5	#	60.1
25	94.8	88.3	67.5
		^^81	

Loss Modulus - psi

25% Constant strain

x freq Hz	y1 static	y2 4Hz	y3 25Hz	
xtemp	0	4	25	
30	0	25.4	17.45	
73	0	#	8.3	^^12.8
100	0	8.1	8	

73F Constant temperature vs variable strain rate

x freq Hz	y1 static	y2 4Hz	y3 25Hz	
xpcstrn	0	4	25	
10	0	16.5	16.6	
25	0	#	8.3	^^12.8
50	0	12.9	7.5	

73F Constant temperature vs variable frequency

x pc strain	y1 10%	y 25%	y3 50%
x freq Hz	10	25	50
0	0	0	0
4	16.5	#	12.9
25	16.6	8.3	7.5
		^^12.8	

Bad data
* Not Requested
^^ 25Hz 25%strn at 23C - cured longer

Table B-4. Flex Airfoil Modal Frequencies (Hz) vs. Elastomer Modulus (PSI)

• Undamped	• Damped - 1	• 2	• 3	• 4
• Es = 88 El = 0	• Es = 88 El = 8.3	• Es = 95 El = 16.6	• Es = 68 El = 7.5	• Es = 81 El = 25.4
• **4.3655**	• **4.3655**	• **4.3747**	• **4.3353**	• **4.3353**
• **20.144**	• **20.148**	• **20.301**	• **19.608**	• **19.608**
• **27.982**	• **27.994**	• **28.164**	• **27.406**	• **27.406**
• **45.271**	• **45.418**	• **46.415**	• **42.009**	• **42.009**

Table B-5. Amplitude Results from Harmonic Analysis

• E_s- psi	• E_l - psi	• Damp: β at 4.3 Hz	• Mode 1 MaxAmpl nd 5690
• 81.3	• 25.4	• .011	• 4.93 in.
• 85	• 8	• .0035	• 8.09 in.
• E_s - psi	• E_l - psi	• Damp: β at 20.2 Hz	• Mode 2 MaxAmpl nd 5706
• 81.3	• 25.4	• .0026	• .62 in.
• 85	• 8	• .00075	• 1.86 in.

APPENDIX C. TEST DATES

		Fluid/Structure Experiment																																					
Blade/Date	7/14/2003	7/25/2003	7/28/2003	7/29/2003	9/18/2003	9/29/2003	9/30/2003	4/12/2004	4/20/2004	4/21/2004	5/5/2004	5/6/2004	5/7/2004	5/10/2004	5/14/2004	7/19/2004	9/14/2004	9/16/2004	9/22/2004	9/23/2004	9/24/2004	9/28/2004	9/29/2004	9/30/2004	12/14/2004	12/16/2004	12/17/2004	11/30/2005	12/9/2005	12/14/2005	12/15/2005	1/6/2006	9/14/2006							
Empty Tunnel						X								X			X	X																					
Solid	X	X	X		X				X	X	X	X	X																										
Prototype Flexible (1st ver)				X																																		
Red Flexible							X																																
New Stiffer Flex. Wing								X																															
Brown Flex Wing															X																							
Maroon Flex Wing																X																						
Blue Flex Wing																X																						
Red Flex Wing																						X	X															
Instrumented Airfoil																			X	X	X																	
Green Wing w/ telemetry																								X														
Hot Wire Anemometry																									X	X	X											
Orange Flex Wing-Shaker Table																												X										
Orange Flex Wing w/ Instrumentation-FSI Tunnel																													X	X	X	X	X					
		Tethered Mass																																					
	7/12/2005	7/13/2005	7/14/2005	7/22/2005	7/25/2005	7/27/2005	8/2/2005	8/5/2005																															
Tethered Mass Cal	X	X																																				
Tethered Mass @ UTSI			X																																			
Tethered Mass @ SvT/Tull				X	X	X	X	X																															

APPENDIX D. TEST RUN LOG

Date	Time	Data Point Number	Angle of Attack, α, deg.	Mach Number	Frequency, Hz	Mode	HWA Probe Position, inches	Velocity, m/sec	Comment
7/14/2003		0							File storage check,, Pt probe retracted near end of test section
7/14/2003		1							Move Pt probe to approx. mid position (check out only)
7/14/2003		2	+/- 14	0.2534	10	flap			Pt probe approx. 1 inch aft of airfoil
7/14/2003		3	+/- 14	0.2534	10	flap			Pt probe approx. 2 inch aft of airfoil
7/14/2003		4	+/- 14	0.2534	10	flap			Pt probe approx. 3 inch aft of airfoil
7/14/2003		5	+/- 14	0.2534	10	flap			Pt probe approx. 4 inch aft of airfoil
7/14/2003		6	+/- 14	0.2534	10	flap			Pt probe approx. 5 inch aft of airfoil
7/14/2003		7	+/- 14	0.2534	10	flap			Pt probe approx. 6 inch aft of airfoil
7/14/2003		8	+/- 14	0.2534	10	flap			Pt probe approx. 7 inch aft of airfoil
7/14/2003		9	+/- 14	0.2534	10	flap			Pt probe approx. 8 inch aft of airfoil
7/14/2003		10	+/- 14	0.2534	10	flap			Pt probe approx. 9 inch aft of airfoil
7/14/2003		11	+/- 14	0.2534	10	flap			Pt probe approx. 10 inch aft of airfoil
7/14/2003		12	+/- 14	0.2534	10	flap			Pt probe approx. 11 inch aft of airfoil
7/14/2003		13	+/- 14	0.2534	10	flap			Pt probe approx. 12 inch aft of airfoil, full aft.
7/14/2003		14	+/- 14	0.2534	10	flap			Pt probe sweep from full aft to 1 inch from wing to full aft
7/14/2003		15	+/- 14	0.2534	10	pitch			Pt probe @ full aft (12 inches)
7/14/2003		16	+/- 14	0.2534	10	pitch			Pt probe approx. 11 inch aft of airfoil
7/14/2003		17	+/- 14	0.2534	10	pitch			Pt probe approx. 10 inch aft of airfoil
7/14/2003		18	+/- 14	0.2534	10	pitch			Pt probe approx. 9 inch aft of airfoil
7/14/2003		19	+/- 14	0.2534	10	pitch			Pt probe approx. 8 inch aft of airfoil
7/14/2003		20	+/- 14	0.2534	10	pitch			Pt probe approx. 7 inch aft of airfoil
7/14/2003		21	+/- 14	0.2534	10	pitch			Pt probe approx. 6 inch aft of airfoil
7/14/2003		22	+/- 14	0.2534	10	pitch			Pt probe approx. 5 inch aft of airfoil
7/14/2003		23	+/- 14	0.2534	10	pitch			Pt probe approx. 4 inch aft of airfoil
7/14/2003		24	+/- 14	0.2534	10	pitch			Pt probe approx. 3 inch aft of airfoil
7/14/2003		25	+/- 14	0.2534	10	pitch			Pt probe approx. 2 inch aft of airfoil
7/14/2003		26	+/- 14	0.2534	10	pitch			Pt probe approx. 1 inch aft of airfoil
7/14/2003		27	+/- 14	0.2534	10	pitch			Pt probe sweep, 1 inch increments from full aft to 1 inch from wing to full aft
7/14/2003		28	+/- 14	0.2534	30	pitch			Pt probe sweep, 1 inch increments
7/14/2003		29							skipped
7/14/2003		30	+/- 14	0.2534	50	pitch			Pt probe sweep, 1 inch increments; NOTE: was standing on Ref. Hose for part of sweep
7/14/2003		31	+/- 14	0.295	50	pitch			Pt probe sweep, 1 inch increments

APPENDIX D. CONTINUED

Date	Time	Data Point Number	Angle of Attack, α, deg.	Mach Number	Frequency, Hz	Mode	HWA Probe Position, inches	Velocity, m/sec	Comment
7/25/2003		0							Checkout run
7/25/2003		1	0	0.15					Pt probe sweep, 1 inch increments
7/25/2003		2	0	0.25					Pt probe sweep, 1 inch increments
7/25/2003		3	4	0.25					Pt probe sweep, 1 inch increments
7/28/2003									Pitch pot is crazy, using position via mechanical cal.; accels in mv not g's.
									Wind tunnel fan kicks off due to humidity
7/28/2003		1	4	0.15					angle of attach set with TE toward Ps taps; Pt probe sweep, 1 inch increments.
7/28/2003		2	4	0.25					angle of attach set with TE toward Ps taps; Pt probe sweep, 1 inch increments.
7/28/2003		3	8	0.25					angle of attach set with TE toward Ps taps; Pt probe sweep, 1 inch increments.
7/28/2003		4	8	0.15					angle of attack set with TE toward Ps taps; Pt probe sweep, 1 inch increments.
7/28/2003		5	12	0.15					angle of attack set with TE toward Ps taps; Pt probe sweep, 1 inch increments.
7/28/2003		6	12	0.25					angle of attack set with TE toward Ps taps; Pt probe sweep, 1 inch increments.
7/28/2003		7	16	0.25					angle of attack set with TE toward Ps taps; Pt probe sweep, 1 inch increments.
7/28/2003		8	16	0.15					angle of attack set with TE toward Ps taps; Pt probe sweep, 1 inch increments.
7/28/2003		9	20	0.15					angle of attack set with TE toward Ps taps; Pt probe sweep, 1 inch increments.
7/28/2003		10	20	0.25					angle of attack set with TE toward Ps taps; Pt probe sweep, 1 inch increments.
7/28/2003									NOTE: saw some radical (non-input) tunnel tone changes--ground vortex ? Something in unstable, dirt of floor--vortex
7/28/2003		11	20	0.25					angle of attack set with TE toward Ps taps; Pt probe sweep, 1 inch increments. Notes: Small personnel door was closed. Sweep started out with couple of positions forward, then went to full aft, swept, then to midpoint with no steps; then back to aft in steps; saw lots of instability
7/28/2003		12	20	0.15					angle of attack set with TE toward Ps taps; Pt probe sweep, 1 inch increments; small personnel door was closed.
7/28/2003		13	+/- 20	0.15	10	pitch			angle of attack set with TE toward Ps taps; Pt probe sweep, 1 inch increments. Reopened small personnel door.
7/28/2003		14	+/- 20	0.15	25	pitch			angle of attack set with TE toward Ps taps; Pt probe sweep, 1 inch increments.
7/28/2003		15	+/- 20	0.15	50	pitch			angle of attack set with TE toward Ps taps; Pt probe sweep, 1 inch increments.
7/28/2003		16	+/- 20	0.25	10	pitch			angle of attack set with TE toward Ps taps; Pt probe sweep, 1 inch increments.
7/28/2003		17	+/- 20	0.25	25	pitch			angle of attack set with TE toward Ps taps; Pt probe sweep, 1 inch increments.
7/28/2003									Note: @ this frequency & Mach number, Pt probe rake oscillates significantly (sideways) when within last 4 stops closest to airfoil.
7/28/2003		18	+/- 20	0.25	50	pitch			angle of attack set with TE toward Ps taps; Pt probe sweep, 1 inch increments.
7/28/2003		19	+/- 20	0.15	1 to 50 to 1	pitch			Pt probe full forward

APPENDIX D. CONTINUED

Date	Time	Data Point Number	Angle of Attack, α, deg.	Mach Number	Frequency, Hz	Mode	HWA Probe Position, inches	Velocity, m/sec	Comment
7/28/2003		20	+/- 20	0.25 to 0.15 to 0.25	1	pitch			Pt probe full aft
7/28/2003		21	+/- 20	0.25	1 to 50 to 1	pitch			Pt probe full aft
7/28/2003		22	+/- 20	0.25 to 0.15 to 0.25	25	pitch			Pt probe full aft
									NOTE: Steady state data is invalid, brick was in CAL position all the time. N2 gone. Dynamic pressures are OK, ref to tunnel floor static=barom-diff1, but CADDMAS wasn't recording it. Will have to get from tunnel data.
									Added barometer, since can get static from Pt and M. Diff1=Pt-Ps.
7/28/2003		23	+/- 20	0.15 to 0.25 to 0.15 to0.25 to 0.15	25	pitch			Pt probe full aft; faster Mach number ramp than previously; at end of data point, changed pitch rate to 1 Hz.
									Performed CAL check, Pt-2 looks like a large DC off-set??--didn't recal due to time and can compare zeros with PSI system later.
7/28/2003		24	+/- 14	0.15	1	Flap			Pt sweep
7/28/2003		25	+/- 14	0.15	5	Flap			Pt sweep
7/28/2003		26	+/- 14	0.15	10	Flap			Pt sweep
7/28/2003		27	+/- 14	0.25	10	Flap			Pt sweep
7/28/2003		28	+/- 14	0.25	5	Flap			Pt sweep
7/28/2003		29	+/- 14	0.25	1	Flap			Pt sweep
7/28/2003		30							skipped
7/28/2003		31							Zero cal, doors closed, fan exhaust capped. NOTE: Pt-5 very high offset, and Pt-1, -3, & -4 also high offset.
7/29/2003									Installed flexible wing--first version, prototype only; test for flutter--no instrumentation used.
7/29/2003									Saw flapping (1st bend mode) @ M=0.07; probably due to tunnel @ such low flow coupled with super low 1st bend frequency.
7/29/2003									Not sure of effects of 3/4 inch long 1/8 inch diameter rods sticking out top of wing (vortex shedding causing flapping?)
7/29/2003									Need to check vortex shedding frequency.
7/29/2003									Very slight bend oscillation @ M=0.10; may be due to tunnel instability
7/29/2003									at M=0.12 torsional flutter; definitely oscillation about approx. 1/4 chord. LE rod not moving, TE rod flapping--Torsion.

APPENDIX D. CONTINUED

Date	Time	Data Point Number	Angle of Attack, α, deg.	Mach Number	Frequency, Hz	Mode	HWA Probe Position, inches	Velocity, m/sec	Comment
7/29/2003									Slight non-uniformity in extrusion--asymmetry in airfoil--lift. That's why we are getting torsional flutter @ AOA=0.
7/29/2003									Top of airfoil not in centerline by approx. 1/4 inch top to side opposite Ps taps
7/29/2003									at M=0.13, shift laterally increased to approx. 0.05 inch, flutter approx. the same.
7/29/2003									Tried to find aerodynamic zero AOA, increase flutter substantially and symmetry about #5 Pt probe
7/29/2003									Note: Pt probe moved to within 1/8 inch of TE (I didn't try to stop with fixed wing)
7/29/2003									Wing need more stiffness in LE to eliminate flap mode and bending due to lift while maintaining same torsional stiffness.
7/29/2003									Very sensitive to AOA--not very stable
9/18/2003									Installed solid blade--flap and pitch correlations to past test points since now have good wall statics (ref 7/28/2003). Note: Pt-3 is bad.
9/18/2003		1	+/-14	0.15	1	Flap			
9/18/2003		2	+/-14	0.15	5	Flap			
9/18/2003		3	+/-14	0.15	10	Flap			
9/18/2003		4	+/-14	0.25	10	Flap			
9/18/2003		5	+/-14	0.25	5	Flap			
9/18/2003		6	+/-14	0.25	1	Flap			
9/18/2003		7	+/-20	0.15	10	Pitch			Pt rake horizontal
9/18/2003		8	+/-20	0.15	25	Pitch			
9/18/2003		9	+/-20	0.15	50	Pitch			
9/18/2003		10	+/-20	0.25	10	Pitch			
9/18/2003		11	+/-20	0.25	25	Pitch			
9/18/2003		12	+/-20	0.25	50	Pitch			
9/18/2003		13	+/-20	0.15	10	Pitch			Pt rake vertical. NOTE: Pt-1 & -2 appear to be swapped in CADDMAS
9/18/2003		14	+/-20	0.15	25	Pitch			some Pt rake flutter @ 3-2 inches from airfoil TE.
9/18/2003		15	+/-20	0.15	50	Pitch			
9/18/2003		16	+/-20	0.25	50	Pitch			
9/18/2003		17	+/-20	0.25	25	Pitch			
9/18/2003		18	+/-20	0.25	10	Pitch			Pt rake motion @ tip follows blade with +/- 1/16 inch displacement
9/29/2003									Empty Tunnel Scope for FSI

APPENDIX D. CONTINUED

Date	Time	Data Point Number	Angle of Attack, α, deg.	Mach Number	Frequency, Hz	Mode	HWA Probe Position, inches	Velocity, m/sec	Comment
									Vibrometer @ center of side wall (looking downstream vibrometer in on left hand side of tunnel)
9/29/2003		1		0.1					Sweep Pt Probe
9/29/2003									Problem with Pt Probe not extending fully due to cable not rotated (couldn't reach with airfoil installed)--missing last 2 points.
9/29/2003									Full retracted is 35.5004 inches from tunnel LE; fully extended is 1.8181 inches from tunnel LE; last detent is 3.040 inches from tunnel LE
9/29/2003		2		0.1					Pt Probe sweep out; probe is vertical
9/29/2003		3		0.1					Pt probe sweep back, probe is vertical
9/29/2003		4		0.2					Pt Probe sweep out; probe is vertical
9/29/2003		5		0.2					Pt probe sweep back, probe is vertical
9/29/2003		6		0.3					Pt Probe sweep out; probe is vertical (1.818 inch)
9/29/2003		7		0.3					Pt probe sweep back, probe is vertical (35.5 inch)
9/29/2003		8		0.1					Pt Probe sweep out; probe is horizontal
9/29/2003		9		0.1					Pt probe sweep back, probe is horizontal
9/29/2003		10		0.2					Pt Probe sweep out; probe is horizontal
9/29/2003		11		0.2					Pt probe sweep back, probe is horizontal
9/29/2003		12		0.3					Pt Probe sweep out; probe is horizontal
									Had detent problems, recentered actuator & cycled--seems OK
9/29/2003		13		0.3					Pt Probe sweep out; probe is horizontal
9/29/2003		14		0.3					Pt probe sweep back, probe is horizontal
9/29/2003		15		0.3					Pt Probe horizontal at airfoil centerline (steady)
9/29/2003									New setup for EAFB demo
									Using red flexible wing with caps; zero AOA; trying to make it flutter @ M=0.1; flutter @ approx. 28 HZ
9/30/2003				0.1					Picture #4
9/30/2003				0.115					Picture #6
9/30/2003									Picture #7= Camera setup
9/30/2003									Failed flutter conditions on 9/29/2003 due to loosening of shaft set screws. Re-established flutter @ M=0.1 as previously done.
									Drove blade @ 6 Hz, approx. M=0.1, saw flapping mode--but eventually fatigued the torsion rods (LE) in wing

APPENDIX D. CONTINUED

Date	Time	Data Point Number	Angle of Attack, α, deg.	Mach Number	Frequency, Hz	Mode	HWA Probe Position, inches	Velocity, m/sec	Comment
									NOTE: on Pt-5, see 2x oscillation frequency due to 2x passing per cycle of AOA. Verified this with rigid blade.
4/12/2004									Running new stiffer flex wing @ aero AOA; M= 0.05 to 0.08, erratic oscillations probably tunnel turbulence; began to oscillate during climb to M=0.085; lowered back to 0.081--erratic, but every now and then can see LE oscillate. NOTE: Erratic means now periodic, typically larger & low frequency
4/12/2004				0.082					ion.
4/12/2004				0.083					LE oscillation approx. 2x displacement of TE; very steady & continuous peaks in FFT @ approx. 12, 24, @33 1/2 Hz; but "frequency hack" is not working
4/12/2004									pure 1st
4/12/2004				0.1					12 Hz is now more peaked @ similar in amplitude to others
4/12/2004									Repositioned vibrometer to LE only, frequency=22.9 Hz, nice peak, better amplitude
4/12/2004				0.115					Start to see some low frequency (approx. 7 Hz) come in & out with high amplitude using vibro-velocity. This look like a 1st bend mode creeping into otherwise
4/12/2004				0.13					Oscillation stopped @ approx. M=0.12, steady without oscillation @ M=0.13
									Saw nothing until approx. M=0.25, just starting to see TE oscillation. LE approx. fixed.
									Large oscillation @ >0.251 heading to 0.255
									Went back to M=0.25 & see large first bending with some TE torsion, TE approx. 2x LE displacement
4/12/2004				0.249					Can see 1st bend develop from 1st torsion on TE. @ M=0.249 & steady, TE= 1st torsion only @ approx. 12 Hz.
4/12/2004				0.25					TE getting large then erratic 1st bending mode starts
4/12/2004				0.255					Mostly 1st bending but TE still 2x LE displacement. Peak approx. 7 HZ.

NOTE: All data taken on 4/20 & 4/21 were taken WITHOUT adjusting balance weights on AOA device.
White cover for bottom of AOA was not installed, hence all dynamic wing pressures are referenced to barometric pressure and not to tunnel total pressure.

4/20/2004		1	0	0.05	0				Traverse Rake

APPENDIX D. CONTINUED

Date	Time	Data Point Number	Angle of Attack, α, deg.	Mach Number	Frequency, Hz	Mode	HWA Probe Position, inches	Velocity, m/sec	Comment
4/20/2004		2	0	0.1	0				
4/20/2004		3	0	0.15	0				
4/20/2004		4	0	0.2	0				
4/20/2004		5	0	0.25	0				
4/20/2004		6	4	0.25	0				potentiometer to set angle out of cal (came loose and turned). Using AOA device pin holes
4/20/2004		7	4	0.2	0				
4/20/2004		8	4	0.15	0				
4/20/2004		9	4	0.1	0				
4/20/2004		10	4	0.05	0				
4/20/2004		11	8	0.05	0				
4/20/2004		12	8	0.1	0				
4/20/2004		13	8	0.15	0				
4/20/2004		14	8	0.2	0				
4/20/2004		15	8	0.25	0				
4/20/2004		16	8	0.25	0				Computer failed, DP 16 not taken.
4/20/2004		17	20	0.25	0				
4/20/2004		18	20	0.2	0				
4/20/2004		19	20	0.15	0				
4/20/2004		20	20	0.1	0				
4/20/2004		21	20	0.05	0				
4/20/2004		22	0	0	0				Air off
4/21/2004		1	0	0	0				Air off; forgot to do data input start
4/21/2004		2	0	0	0				Air off
4/21/2004		3	4	0.05	10				data points 3-12: data file will say were flap mode by really were pitch oscillation
4/21/2004		4	4	0.1	10				
4/21/2004		5	4	0.15	10				
4/21/2004		6	4	0.2	10				
4/21/2004		7	4	0.25	10				
4/21/2004		8	4	0.25	20				
4/21/2004		9	4	0.2	20				
4/21/2004		10	4	0.15	20				
4/21/2004		11	4	0.1	20				
4/21/2004		12	4	0.05	20				

APPENDIX D. CONTINUED

Date	Time	Data Point Number	Angle of Attack, α, deg.	Mach Number	Frequency, Hz	Mode	HWA Probe Position, inches	Velocity, m/sec	Comment
									Changed vibrometer individual points to: x: -2.000 1.650 y: 4.70 4.70
4/21/2004		13	4	0.05	30				Vibration in rake turning handle noticeable. Board with electrical connectors has visible vibration on non-clamped edge.
4/21/2004		14	4	0.1	30				
4/21/2004		15	4	0.15	30				
4/21/2004		16	4	0.2	30				
4/21/2004		17	4	0.25	30				Rake pressure tubes vibrating in both forward & aft positions. Loose items on top of tunnel move around--bolts, nuts, etc.
4/21/2004		18	4	0.25	45				
4/21/2004		19	4	0.2	45				
4/21/2004		20	4	0.15	45				
4/21/2004		21	4	0.1	45				
4/21/2004		22	4	0.05	45				
4/21/2004		23	8	0.05	10				
4/21/2004		24	8	0.1	10				
4/21/2004		25	8	0.15	10				
4/21/2004		26	8	0.2	10				
4/21/2004		27	8	0.25	10				
4/21/2004		28	8	0.25	20				
4/21/2004		29	8	0.2	20				
4/21/2004		30	8	0.15	20				
4/21/2004		31	8	0.1	20				
4/21/2004		32	8	0.05	20				
4/21/2004		33	8	0.05	30				
4/21/2004		34	8	0.1	30				
4/21/2004		35	8	0.15	30				
4/21/2004		36	8	0.2	30				
4/21/2004		37	8	0.25	30				
4/21/2004		38	8	0.25	45				
4/21/2004		39	8	0.2	45				
4/21/2004		40	8	0.15	45				
4/21/2004		41	8	0.1	45				

APPENDIX D. CONTINUED

Date	Time	Data Point Number	Angle of Attack, α, deg.	Mach Number	Frequency, Hz	Mode	HWA Probe Position, inches	Velocity, m/sec	Comment
4/21/2004		42	8	0.05	45				Approx. 3-4 inches behind wing, rake has more vibration than closer or farther away.
4/21/2004		43	20	0.05	10				
4/21/2004		44	20	0.1	10				Tunnel sounds different. The sinusoidal shape has changed some. See hand written notes for sketch.
4/21/2004		45	20	0.15	10				Video of CADDMAS screen of wing surface pressure. Forgot to turn off data point after took video of CADDMAS screen. Rake all the way back & started increasing M from 0.15 to 0.2 when turned off data point.
4/21/2004		46	20	0.2	10				
4/21/2004		47	20	0.25	10				
4/21/2004			4	0.1	10				Sounds like before, sinusoidal pattern is back. Video to CADDMAS wing pressures. No data was taken.
4/21/2004		48	20	0.05	20				
4/21/2004		49	20	0.1	20				
4/21/2004		50	20	0.15	20				
4/21/2004		51	20	0.2	20				
4/21/2004		52	20	0.25	20				When put back of hand on tunnel wall at start of diffuser and relax hand, can see fingers vibrate.
4/21/2004		53	20	0.25	30				Lot of tunnel vibration, video of underneath of the tunnel.
									Terminated testing because of vibration.
									See Note at start of run log.
5/5/2004		1	0	0.2	0				Setup Check
5/5/2004		2	20	0.05	10				
5/5/2004		3	20	0.1	10				Wing pressures 1,2, 10 pattern looks similar to data taken on 4/21. Pressures 5,7,13 appear to have noise that was not there on 4/21. During setup there were several parameters that appeared to by "noisy".
5/5/2004		4	20	0.15	10				
5/5/2004		5	20	0.2	10				
5/5/2004		6	20	0.25	10				
5/5/2004		7	20	0.25	20				
5/5/2004		8	20	0.2	20				
5/5/2004		9	20	0.15	20				
5/5/2004		10	20	0.1	20				

APPENDIX D. CONTINUED

Date	Time	Data Point Number	Angle of Attack, α, deg.	Mach Number	Frequency, Hz	Mode	HWA Probe Position, inches	Velocity, m/sec	Comment
5/5/2004		11	20	0.05	20				feel wind coming thru garage door, can this wind thru normal door get into the inlet & cause asymmetric flow in the tunnel?
5/5/2004		12	20	0.05	30				
5/5/2004		13	20	0.1	30				
5/5/2004		14	20	0.15	30				
5/5/2004		15	20	0.2	30				
5/5/2004		16	20	0.25	30				rake wing quiet.
5/5/2004		17	20	0.25	45				
5/5/2004		18	20	0.2	45				
5/5/2004		19	20	0.15	45				
5/5/2004		20	20	0.1	45				
5/5/2004		21	20	0.05	45				
5/5/2004		22	8	0.05	10				
5/5/2004		23	8	0.1	10				
5/5/2004		24	8	0.15	10				
5/5/2004		25	8	0.2	10				
5/5/2004		26	8	0.25	10				
5/5/2004		27	8	0.25	20				
5/5/2004		28	8	0.2	20				
5/5/2004		29	8	0.15	20				
5/5/2004		30	8	0.1	20				
5/5/2004		31	8	0.05	20				
5/5/2004		32	8	0.05	30				
5/5/2004		33	8	0.1	30				
5/5/2004		34	8	0.15	30				
5/5/2004		35	8	0.2	30				
5/5/2004		36	8	0.25	30				
5/5/2004		37	8	0.25	45				
5/5/2004		38	8	0.2	45				
5/5/2004		39	8	0.15	45				
5/5/2004		40	8	0.1	45				
5/5/2004		41	8	0.05	45				
5/5/2004		42	4	0.05	10				
5/5/2004		43	4	0.1	10				
5/5/2004		44	4	0.15	10				

APPENDIX D. CONTINUED

Date	Time	Data Point Number	Angle of Attack, α, deg.	Mach Number	Frequency, Hz	Mode	HWA Probe Position, inches	Velocity, m/sec	Comment
5/5/2004		45	4	0.2	10				
5/5/2004		46	4	0.25	10				
5/5/2004		47	4	0.25	20				
5/5/2004		48	4	0.2	20				
5/5/2004		49	4	0.15	20				
5/5/2004		50	4	0.1	20				
5/5/2004		51	4	0.05	20				
5/5/2004		52	4	0.05	30				
5/5/2004		53	4	0.1	30				
5/5/2004		54	4	0.15	30				
5/5/2004		55	4	0.2	30				
5/5/2004		56	4	0.25	30				
5/5/2004		57	4	0.25	45				
5/5/2004		58	4	0.2	45				
5/5/2004		59	4	0.15	45				
5/5/2004		60	4	0.1	45				
5/5/2004		61	4	0.05	45				
5/5/2004		62	4	0	0				Air Off Data Points 40-62 in pitch mode are not recorded on disk because data disk got full. Will rerun these data points. Change AOA configuration to flap mode Vibrometer: x = +/-1.75; y = 4.25 Re-aligned cap at top of instrumented wing.
5/6/2004		1	0	0	0				Air Off
5/6/2004		2	4	0.05	3				
5/6/2004		3	4	0.1	3				
5/6/2004		4	4	0.15	3				
5/6/2004		5	4	0.2	3				
5/6/2004		6	4	0.25	3				
5/6/2004		7	4	0.25	6				
5/6/2004		8	4	0.2	6				
5/6/2004		9	4	0.15	6				

APPENDIX D. CONTINUED

Date	Time	Data Point Number	Angle of Attack, α, deg.	Mach Number	Frequency, Hz	Mode	HWA Probe Position, inches	Velocity, m/sec	Comment
5/6/2004		10	4	0.1	6				
5/6/2004		11	4	0.05	6				
5/6/2004		12	4	0.05	10				
5/6/2004		13	4	0.1	10				
5/6/2004		14	4	0.15	10				
5/6/2004		15	4	0.2	10				
5/6/2004		16	4	0.25	10				
5/6/2004		17	8	0.05	3				
5/6/2004		18	8	0.1	3				
5/6/2004		19	8	0.15	3				
5/6/2004		20	8	0.2	3				
5/6/2004		21	8	0.25	3				
5/6/2004		22	8	0.25	6				
5/6/2004		23	8	0.2	6				
5/6/2004		24	8	0.15	6				
5/6/2004		25	8	0.1	6				
5/6/2004		26	8	0.05	6				
5/6/2004		27	8	0.05	10				
5/6/2004		28	8	0.1	10				
5/6/2004		29	8	0.15	10				
5/6/2004		30	8	0.2	10				
5/6/2004		31	8	0.25	10				
5/6/2004		32	14	0.05	3				Changed vibrometer x value from 4.25 to 3.85 to get back on blade.
5/6/2004		33	14	0.1	3				
5/6/2004		34	14	0.15	3				
5/6/2004		35	14	0.2	3				Moved rake wrong direction; bend center rake tube; unable to straighten with hand pressure alone; used a tube over the pressure tube to straighten. Realigned pressure tubes 5 & 6.
5/6/2004		36	14	0.15	3				Repeat DP34
5/6/2004		37	14	0.2	3				
5/6/2004		38	14	0.25	3				
5/6/2004		39	14	0.25	6				
5/6/2004		40	14	0.2	6				
5/6/2004		41	14	0.15	6				
5/6/2004		42	14	0.1	6				

APPENDIX D. CONTINUED

Date	Time	Data Point Number	Angle of Attack, α, deg.	Mach Number	Frequency, Hz	Mode	HWA Probe Position, inches	Velocity, m/sec	Comment
5/6/2004		43	14	0.05	6				
5/6/2004		44	14	0.05	10				
5/6/2004		45	14	0.1	10				
5/6/2004		46	14	0.15	10				
5/6/2004		47	14	0.2	10				
5/6/2004		48	14	0.25	10				
									Change to pitch mode to rerun DP 40-62 from 5/5/04.
5/6/2004		49	4	0.05	10				
5/6/2004		50	4	0.1	10				
5/6/2004		51	4	0.15	10				
5/6/2004		52	4	0.2	10				
5/6/2004		53	4	0.25	10				
5/6/2004		54	4	0.25	20				
5/6/2004		55	4	0.2	20				
5/6/2004		56	4	0.15	20				
5/6/2004		57	4	0.1	20				
5/6/2004		58	4	0.05	20				
5/6/2004		59	4	0.05	30				
5/6/2004		60	4	0.1	30				
5/6/2004		61	4	0.15	30				
5/6/2004		62	4	0.2	30				
5/6/2004		63	4	0.25	30				
5/6/2004		64	4	0.25	45				
5/6/2004		65	4	0.2	45				
5/6/2004		66	4	0.15	45				
5/6/2004		67	4	0.1	45				
5/6/2004		68	4	0.05	45				
5/6/2004		69	8	0.05	45				
5/6/2004		70	8	0.1	45				
5/6/2004		71	8	0.15	45				
5/6/2004		72	8	0.2	45				
5/6/2004		73	8	0.25	45				
5/6/2004		74	8	0	0				Air Off

APPENDIX D. CONTINUED

Date	Time	Data Point Number	Angle of Attack, α, deg.	Mach Number	Frequency, Hz	Mode	HWA Probe Position, inches	Velocity, m/sec	Comment
									Flap Mode
5/7/2004		1	0	0	0				Air Off
5/7/2004		2	8	0	3				
5/7/2004		3	8	0	6				
5/7/2004		4	8	0	10				
5/7/2004		5	4	0	3				
5/7/2004		6	4	0	6				
5/7/2004		7	4	0	10				
5/7/2004		8	14	0	3				
5/7/2004		9	14	0	6				
5/7/2004		10	14	0	10				
5/7/2004		11	14	0.05	0				Fixed at 14 degs. with LE closest to outside wall
5/7/2004		12	14	0.1	0				
5/7/2004		13	14	0.15	0				
5/7/2004		14	14	0.2	0				
5/7/2004		15	14	0.25	0				
5/7/2004		16	14	0.05	0				Fixed at 14 degs. with LE away from outside wall
5/7/2004		17	14	0.1	0				Rerun data files are empty; DMS sequence error
5/7/2004		18	14	0.15	0				Rerun data files are empty; DMS sequence error
5/7/2004		19	14	0.2	0				
5/7/2004		20	14	0.25	0				
5/7/2004		21	8	0.05	0				Fixed at 8 degs. with LE closest to outside wall
5/7/2004		22	8	0.1	0				
5/7/2004		23	8	0.15	0				
5/7/2004		24	8	0.2	0				
5/7/2004		25	8	0.25	0				
5/7/2004		26	8	0.05	0				Fixed at 8 degs. with LE away from outside wall
5/7/2004		27	8	0.1	0				
5/7/2004		28	8	0.15	0				
5/7/2004		29	8	0.2	0				
5/7/2004		30	8	0.25	0				
5/7/2004		31	14	0.1	0				Fixed at 14 degs. with LE away from outside wall; rerun of DP 17
5/7/2004		32	14	0.15	0				Rerun of DP 18

APPENDIX D. CONTINUED

Date	Time	Data Point Number	Angle of Attack, α, deg.	Mach Number	Frequency, Hz	Mode	HWA Probe Position, inches	Velocity, m/sec	Comment
5/7/2004		33	4	0.05	0				Fixed at 4 degs. with LE away from outside wall
5/7/2004		34	4	0.1	0				
5/7/2004		35	4	0.15	0				
5/7/2004		36	4	0.2	0				
5/7/2004		37	4	0.25	0				
5/7/2004		38	4	0.05	0				Fixed at 4 degs. with LE closest to outside wall
5/7/2004		39	4	0.1	0				
5/7/2004		40	4	0.15	0				
5/7/2004		41	4	0.2	0				
5/7/2004		42	4	0.25	0				
5/7/2004									
5/7/2004									Pitch Mode
5/7/2004									
5/7/2004		43	4	0	10				
5/7/2004		44	4	0	20				
5/7/2004		45	4	0	30				
5/7/2004		46	4	0	45				
5/7/2004		47	8	0	10				
5/7/2004		48	8	0	20				
5/7/2004		49	8	0	30				
5/7/2004		50	8	0	45				
5/7/2004		51	20	0	10				
5/7/2004		52	20	0	20				
5/7/2004		53	20	0	30				
5/7/2004		54	20	0	45				
5/7/2004		55	20	0.05	0				Fixed at 20 degs. with LE closest to outside wall
5/7/2004		56	20	0.1	0				
5/7/2004		57	20	0.15	0				
5/7/2004		58	20	0.2	0				
5/7/2004		59	20	0.25	0				
5/7/2004		60	20	0.05	0				Fixed at 20 degs. with LE away from outside wall
5/7/2004		61	20	0.1	0				
5/7/2004		62	20	0.15	0				
5/7/2004		63	20	0.2	0				
5/7/2004		64	20	0.25	0				

APPENDIX D. CONTINUED

Date	Time	Data Point Number	Angle of Attack, α, deg.	Mach Number	Frequency, Hz	Mode	HWA Probe Position, inches	Velocity, m/sec	Comment
5/7/2004		65	20	0	0				Air Off
5/10/2004		1	8	0	0				Air Off
5/10/2004		2	8	0.05	0				Fixed at 8 degs. with LE closest to outside wall
5/10/2004		3	8	0.1	0				
5/10/2004		4	8	0.15	0				
5/10/2004		5	8	0.2	0				
5/10/2004		6	8	0.25	0				
5/10/2004		7	8	0.25	0				Fixed at 8 degs. with LE away from outside wall
5/10/2004		8	8	0.25	0				
5/10/2004		9	8	0.2	0				
5/10/2004		10	8	0.15	0				
5/10/2004		11	8	0.1	0				
5/10/2004		12	8	0.05	0				
5/10/2004		13	4	0.05	0				Fixed at 4 degs. with LE closest to outside wall
5/10/2004		14	4	0.1	0				
5/10/2004		15	4	0.15	0				
5/10/2004		16	4	0.2	0				
5/10/2004		17	4	0.25	0				
5/10/2004		18	4	0.25	0				Fixed at 4 degs. with LE away from outside wall
5/10/2004		19	4	0.2	0				
5/10/2004		20	4	0.15	0				
5/10/2004		21	4	0.1	0				
5/10/2004		22	4	0.05	0				
5/10/2004		23	4	0	0				Air Off
									Removing instrumented wing. Put silver tape over hole for wing in tunnel floor Put silver tape over white can holes that wing wires and tubes went through
									Empty tunnel data
5/10/2004		24	0	0	0				Air Off
5/10/2004		25	0.05	0	0				Moved traversing rake all the forward to LE of test section (where Plexiglas started). Rake would not retract.

APPENDIX D. CONTINUED

Date	Time	Data Point Number	Angle of Attack, α, deg.	Mach Number	Frequency, Hz	Mode	HWA Probe Position, inches	Velocity, m/sec	Comment
5/10/2004		26	0.05	0	0				
5/10/2004		27	0.1	0	0				
5/10/2004		28	0.15	0	0				
5/10/2004		29	0.2	0	0				Mach number decreased the further into the section the rake went. Mach number controller was over correcting.
5/10/2004		30	0.25	0	0				Mach number decreased the further into the section the rake went. Mach number controller was over correcting.
5/10/2004		31	0	0	0				Air Off
5/14/2004									Brown Blade
									Took videotape; times are recorded to correlate CADDMAS and videotapes
5/14/2004	10:26	1	0	0	0				Air Off; day is overcast
5/14/2004	10:38	2	0.092						Flap mode, 74.3° F; probably 8 degs. Cooler than last week when ran same blade.
5/14/2004	10:47	3	0.115						Pitch mode. There was no dead zone between flap and pitch mode like there was last week when it was warmer.
5/14/2004	10:57	4	0.08 thru 0.14						Transient: rake forward just aft of Blade TE; 75.3° F
5/14/2004	11:15	5	0.24						Peak @ 7.3 Hz; 74.1° F.; @M=0.25, f=8.3 Hz peak
5/14/2004	11:22	6	0.26						approx. M=0.263 started to suddenly increase flap mode--hit side Plexiglas wall. Cap came off. Emergency shut-down, pull accelerometer off wires. Was caught on video. Was going to 0.265 trying to fine when came out of flap mode. Started into flap mode approx. M= 0.17. Gradual increase until above 0.26. Cap came off and went down tunnel.
7/19/2004									Maroon Flexible Wing (FW08 on bottom metal plate)
7/19/2004	7:45	1	0	0	0				Air Off
									Will turn on videotape and let it run. Video does not record time on the tape.
									Use delta Mach number increments of 0.005
7/19/2004	8:09	2	0	0.06					
7/19/2004	8:10	3		0.065					
7/19/2004	8:12	4	0	0.07					flap mode
				0.075					about the same as M=0.07
				0.08					less than at 0.07

APPENDIX D. CONTINUED

Date	Time	Data Point Number	Angle of Attack, α, deg.	Mach Number	Frequency, Hz	Mode	HWA Probe Position, inches	Velocity, m/sec	Comment
7/19/2004	8:21	5		0.1					Started into torsion mode approx. M=0.098
7/19/2004	8:23	6		0.105					rake data (moved rake fwd. And back)
7/19/2004	8:28	7		0.115					Rake data
7/19/2004	8:34	8		0.13					Looks the same as M=0.115
7/19/2004	8:38	9		0.14					Rake data
7/19/2004	8:42			approx. = 0.156					
7/19/2004	8:57								Changing videotape
7/19/2004	9:12	10		0.25					About half way through data point after rake was close to TE, amplitude of blade vibration increased.
7/19/2004	9:15								Air off
7/19/2004	9:21	11							Air off
									Blue Flexible Wing (FW09 on metal base plate)
7/19/2004	9:46	12							Air Off
7/19/2004	9:50								Air On
7/19/2004	9:57	13		0.1					Blade reacted every time solenoid valve was activated.
7/19/2004	10:03	14		0.105					Changed vibrator y from 4.75 to 3.75
7/19/2004	10:06			approx. 0.106					Flap mode stopped, blade canted away from outside wall.
7/19/2004	10:15	15		0.145					Blade did not react to solenoid valve operation.
7/19/2004	10:20	16		0.155					Blade straightened up.
7/19/2004	10:25	17		0.16					Mixed modes??
7/19/2004	10:28			0.17					Hit wall one, intermittent large deflections; brought back to M=0.15, started increasing M toward 0.18; at M= 0.175, hit wall 3 or 4 times. Shut down tunnel.
7/19/2004	10:35								Air Off
7/19/2004		18							Air Off

Both Views are Top Looking Down

Blade Pressure Locations

Airflow	CADDMAS Channel No.	Pressure Tap Location	Serial No. of Transducer

APPENDIX D. CONTINUED

Date	Time	Data Point Number	Angle of Attack, α, deg.	Mach Number	Frequency, Hz	Mode	HWA Probe Position, inches	Velocity, m/sec	Comment
						15	A		6725-4-96
						14	B		6725-4-95
						13	C		6725-4-94
						12	D		6725-4-93
						11	E		6725-4-92
						10	F		6725-4-91
						7	G		6725-4-90
						6	H		6725-4-89
						5	I		6725-4-87
						4	J	6725-4-85	bad, removed
						3	K		6725-4-83
						2	L		6725-4-82
	Pressure Tap Locations			Transducer Locations					Serial No. # 6725-4-86 & 6725-4-88. Don took these to test; I think they are bad.
9/28/2004									Red Flex Blade: 1/16 & 1/32 inch flex straps
									Mach number ramps to look at transients for resonants
9/28/2004		1		0.07 to 0.09					Mach number ramp; rake fixed @ location of downstream wall statics
9/28/2004		2		0.09					Steady state; rake sweep flap mode, however went to torsion mode when rake in fully retracted & then moved forward to wall statics position per DP0001 & started flapping again.
9/28/2004		3		0.08 to 0.11					Ramp, rake fixed @ downstream wall statics.
9/28/2004		4		0.105 to 0.125					Ramp, rake fixed @ downstream wall statics.
9/28/2004		5		0.125					Rake sweep
9/28/2004		6		0.120 to 0.140					Ramp, rake fixed @ downstream wall statics.
9/28/2004		7		0.120 to 0.140 to 0.120					Ramp, rake fixed @ downstream wall statics (when started originally to go from 0.135 to 0.155 ramp, saw a hysterisis, so decided to capture it.)
9/28/2004		8		0.135 to 0.155					Ramp, rake fixed @ downstream wall statics
9/28/2004		9		0.155 to 0.185					Ramp, rake fixed @ downstream wall statics (note, slight lean to west, opposite to wall statics).
9/28/2004		10		0.185 to 0.0					Ramp

APPENDIX D. CONTINUED

Date	Time	Data Point Number	Angle of Attack, α, deg.	Mach Number	Frequency, Hz	Mode	HWA Probe Position, inches	Velocity, m/sec	Comment
9/29/2004									NOTE: Accelerometers in cap of red wing (flex wing #08) for today and yesterday(9/28/2004) runs are not installed correctly; sinusoids 180 deg. out of phase in flap mode.
									NOTE: When increasing Mach number, oscillation mode changes from torsion to flap @ M=0.091 and then decreasing Mach number the oscillation changes from flap to torsion at M=0.084
9/29/2004		11							Computer reboot
9/29/2004		12		0.091					Steady state; onset of flap mode from torsion while increase Mach number. Barometer=392.7 inches of water, Temperature= 66.7 deg. F
9/29/2004		13		0.091 to 0.084					To check transition from flap to torsion mode=IT REPEATS.
9/29/2004		14		0.091 to ?					Increase Mach number to find upper Mach no. where flap transitions to torsion. Transitioned at approx. M=0.095 from flap to torsion.
9/29/2004		15		0.097 to ?					Decrease Mach number from 0.097 to find torsion to flap transition going down in Mach no. Transition at approx. M=0.094.
9/29/2004		16		0.18 to 0.200					Rake at aft wall statics position, fixed. Nothing, very steady, Slight lift to west.
9/29/2004		17		0.200 to 0.220					Rake fixed, Nothing.
9/29/2004		18		0.220 to 0.240					Rake fixed, Nothing.
9/29/2004		19		0.240 to 0.260					Rake fixed, started torsion @ just over 0.250 (approx. 0.252), mostly TE, increased at M=0.258
9/29/2004		20		0.260 to 0.270 to 0.235					Frequency of torsion + bending has increased probably due to lift stiffening. Flap violent at M=0.267. Multi modes--spectrum pretty full in 0 to 50 Hz. Stopped at M=0.2365
9/29/2004		21		0.150 to 0					Shutdown.
									Installed Green wing with telemetry.
9/30/2004		22		0.082 to 0.100					Rake at TE, transitions @ torsion to flap @ M=0.091; flap to nothing @ M=0.094; Nothing to torsion @ M=0.095
9/30/2004		23		0.100 to 0.080					Torsion to nothing @ M=0.093; nothing to flap @ M=0.092; nothing to torsion @ M=0.092; see data point (raw)
9/30/2004		24							skipped
9/30/2004		25		0.26					Steady state; time 1541 (DRB=1544); for data comparisons
9/30/2004		26		0.270 to					in varying increments.

APPENDIX D. CONTINUED

Date	Time	Data Point Number	Angle of Attack, α, deg.	Mach Number	Frequency, Hz	Mode	HWA Probe Position, inches	Velocity, m/sec	Comment
				0.080					
12/14/2004									FSI Tunnel Assessment with Hot Wire Anemometer (HWA)
									Empty Tunnel
									Changed CADDMAS inputs to eliminate Polytec positions for anemometer inputs.
									WAS: Ch25 X Position; A=2.56964, B=0 NOW: Ch25 HWA X-vel, U; A=1, B=0
									WAS: Ch26 Y Position; A=2.75254, B=0 NOW: Ch26 HWA Y-vel, V; A=1, B=0
12/14/2004		1						15	Cal point for Anemometer
12/14/2004		2						35	Cal point for Anemometer
12/14/2004		3						55	Cal point for Anemometer
12/14/2004		4						75	Cal point for Anemometer
12/14/2004		5						95	Cal point for Anemometer
12/14/2004		6						115	Cal point for Anemometer; saw significant HWA probe vibes and bending
12/14/2004		7						135	Cal point for Anemometer; saw significant HWA probe vibes and bending
12/14/2004		8							Broke anemometer wire on X-vel. Took data point on decel to show breakage signal.
									Replaced broken HWA probe, stiffened it for vibes & bending. Checked formula inputs for CADDMAS.
									Calibrating HWA from 20 to 80 m/s in 10 m/sec increments
12/14/2004		10						20	Cal point for HWA
12/14/2004		11						30	Cal point for HWA; pretty smooth Tt & HWA
12/14/2004		12						40	Cal point for HWA; pretty smooth Tt & HWA
12/14/2004		13						50	Cal point for HWA; pretty smooth Tt & HWA
12/14/2004		14						60	Cal point for HWA; pretty smooth Tt & HWA

APPENDIX D. CONTINUED

Date	Time	Data Point Number	Angle of Attack, α, deg.	Mach Number	Frequency, Hz	Mode	HWA Probe Position, inches	Velocity, m/sec	Comment
12/14/2004		15						70	Cal point for HWA; more Tt & HWA oscillations
12/14/2004		16						80	Cal point for HWA; more Tt & HWA oscillations
12/16/2004									Tunnel vertical centerline (horizontal plane dividing the tunnel into 2 equal parts above & below the centerline) is a 16.7 inch reading on probe scale Probe setting on probe scale went from 23.9 to 9.2 inches. Probe was moved one inch increments on the probe scale. HWA Probe Position column are physical inches with zero at the vertical center. Re-calibrated Pt & Ps sensors
12/16/2004		1					0	10	"0" is at tunnel centerline
12/16/2004		2					-7.22	10	Full down position
12/16/2004		3					-6.015	10	
12/16/2004		4					-4.99	10	
12/16/2004		5					-3.97	10	
12/16/2004		6					-2.97	10	
12/16/2004		7					-1.923	10	
12/16/2004		8					-0.966	10	0.35% axial turbulence @ centerline
12/16/2004		9					0.114	10	centerline = 0
12/16/2004		10					1.162	10	
12/16/2004		11					2.189	10	
12/16/2004		12					3.197	10	
12/16/2004		13					4.23	10	
12/16/2004		14					5.241	10	
12/16/2004		15					6.227	10	
12/16/2004		16					7.272	10	
12/16/2004		17					7.8	10	approx. 1.1% axial turbulence
12/16/2004		18					7.8	40	1% axial turbulence
12/16/2004		19					7.293	40	
12/16/2004		20					6.328	40	
12/16/2004		21					5.305	40	
12/16/2004		22					4.322	40	
12/16/2004		23					3.313	40	

APPENDIX D. CONTINUED

Date	Time	Data Point Number	Angle of Attack, α, deg.	Mach Number	Frequency, Hz	Mode	HWA Probe Position, inches	Velocity, m/sec	Comment
12/16/2004		24					2.316	40	
12/16/2004		25					1.294	40	
12/16/2004		26					0.265	40	centerline = 0; 0.46% axial turbulence
12/16/2004		27					-0.7786	40	
12/16/2004		28					-1.801	40	
12/16/2004		29					-2.813	40	
12/16/2004		30					-3.84	40	
12/16/2004		31					-4.857	40	
12/16/2004		32					-5.884	40	
12/16/2004		33					-7.098	40	0.54% axial turbulence; full down at 23.9 inch probe scale
12/16/2004		34					-7.105	70	Full down at 23.9 inch probe scale; some intermittent probe vibes; approx. 0.7% axial turbulence
12/16/2004		35					-5.92	70	some probe vibes
12/16/2004		36					-4.907	70	some probe vibes
12/16/2004		37					-3.93	70	probe vibes subsiding, HWA X-vel=64 m/sec; Y-vel=81 m/sec
12/16/2004		38					-2.926	70	
12/16/2004		39					-1.94	70	
12/16/2004		40					-0.944	70	
12/16/2004		41					0.108	70	centerline = 0; no vibes; 0.43% axial turbulence
12/16/2004		42					1.15	70	
12/16/2004		43					2.157	70	
12/16/2004		44					3.188	70	
12/16/2004		45					4.224	70	
12/16/2004		46					5.241	70	
12/16/2004		47					6.262	70	
12/16/2004		48					7.237	70	
12/16/2004		49					7.796	70	Full up, 9.2 on probe scale; 0.6% axial turbulence; HWA X-vel = 63.5 m/sec
12/16/2004									Shut down to position probe for corners
12/17/2004									FSI Test Section Corner HWA Investigation
									Probe position for this test is distance above the tunnel floor: Depth = 11 is 10 inches above the tunnel floor; zero is defined to be the tunnel floor. (Due angle were able to move 11 inches on the diagonal)

APPENDIX D. CONTINUED

Date	Time	Data Point Number	Angle of Attack, α, deg.	Mach Number	Frequency, Hz	Mode	HWA Probe Position, inches	Velocity, m/sec	Comment
									Using manual insertion depth settings for potentiometer (chan 5 HWA probe position)
12/17/2004		1					11	70	People door open; 0.7% axial turbulence
12/17/2004		2					11	70	People door closed; 0.7% axial turbulence
12/17/2004		3					10	70	
12/17/2004		4					9	70	
12/17/2004		5					8	70	
12/17/2004		6					7	70	
12/17/2004		7					6	70	
12/17/2004		8					5	70	Slight probe vibes
12/17/2004		9					4	70	
12/17/2004		10					3	70	More probe vibes
12/17/2004		11					2.5	70	
12/17/2004		12					2	70	Saw 28.5 Hz vibe spike, probe?
12/17/2004		13					1.5	70	
12/17/2004		14					1	70	More vibes, intermittent, 1.6% axial turbulence
12/17/2004		15					0.75	70	More steady vibes, 3.7% axial turbulence; 2.2% lateral turbulence
12/17/2004		16					0.5	70	
12/17/2004		17					0.25	70	Slight probe bending, may not yet "zero"
12/17/2004		18					0	70	Full down without probe hitting floor
12/17/2004		19					11	40	0.3% axial turbulence
12/17/2004		20					10	40	
12/17/2004		21					9	40	
12/17/2004		22					8	40	
12/17/2004		23					7	40	
12/17/2004		24					6	40	
12/17/2004		25					5	40	
12/17/2004		26					4	40	
12/17/2004		27					3	40	Slight vibes, 27 Hz peak
12/17/2004		28					2.5	40	
12/17/2004		29					2	40	
12/17/2004		30					1.5	40	
12/17/2004		31					1	40	

APPENDIX D. CONTINUED

Date	Time	Data Point Number	Angle of Attack, α, deg.	Mach Number	Frequency, Hz	Mode	HWA Probe Position, inches	Velocity, m/sec	Comment
12/17/2004		32					0.75	40	
12/17/2004		33					0.5	40	
12/17/2004		34					0.25	40	
12/17/2004		35					0	40	@ zero, 8.9% axial turbulence
12/17/2004		36					11	10	HWA probe cal looks bad at this low velocity
12/17/2004		37					10	10	HWA probe cal looks bad at this low velocity
12/17/2004		38					11	70	Moved probe to opposite corner, 0.4% axial turbulence
12/17/2004		39					10	70	nice peak at 86.5 Hz
12/17/2004		40					9	70	Peak shifted to 76.3 Hz
12/17/2004		41					8	70	Probably probe
12/17/2004		42					7	70	Peak shifted to 57.2 Hz
12/17/2004		43					6	70	Peak shifted to 47.6 Hz
12/17/2004		44					5	70	Peak shifted to 42.9 Hz
12/17/2004		45					4	70	Peak shifted to 37.7 Hz
12/17/2004		46					3	70	Peak shifted to 33.2 Hz
12/17/2004		47					2.5	70	Peak shifted to 29.3 Hz
12/17/2004		48					2	70	Peak shifted to 28.4 Hz
12/17/2004		49					1.5	70	Peak shifted to 27.8 Hz
12/17/2004		50					1	70	Hard to see
12/17/2004		51					0.75	70	Slight bowing & vibes
12/17/2004		52					0.5	70	Intermittent vibes, not as bad as other corner
12/17/2004		53					0.25	70	Last point, hitting corner; 8.7% axial turbulence
12/17/2004		54					11	40	Probe frequency = 110 Hz; 0.3% axial turbulence
12/17/2004		55					10	40	Peak at 90.7 Hz
12/17/2004		56					9	40	Peak at 71.4 Hz
12/17/2004		57					8	40	Peak at 61.85 Hz
12/17/2004		58					7	40	Peak at 52.2 Hz
12/17/2004		59					6	40	Peak at 43.4 Hz
12/17/2004		60					5	40	Peak at38.4 Hz
12/17/2004		61					4	40	Peak at 37.2 Hz
12/17/2004		62					3	40	Peak at 29.4 Hz
12/17/2004		63					2.5	40	Peak at 28.8 Hz
12/17/2004		64					2	40	Peak at 28.5 Hz
12/17/2004		65					1.5	40	Peak at 27.84 Hz
12/17/2004		66					1	40	Hard to see probe frequency

APPENDIX D. CONTINUED

Date	Time	Data Point Number	Angle of Attack, α, deg.	Mach Number	Frequency, Hz	Mode	HWA Probe Position, inches	Velocity, m/sec	Comment
12/17/2004		67					0.75	40	
12/17/2004		68					0.5	40	
12/17/2004		69					0.25	40	Elbow against wall; 9.7% axial turbulence
11/30/2005									FSI 16 Channel Orange Flex Wing Shaker Test
									Test #113005
									Barometer= 14.262 psia
									Wing chord perpendicular to shaker motion, LE facing camera
		1							Zero cal (Baseline, wing in shaker static, no shaker inputs, no pumps running (heater fan running)
		2							Keith's run #1; 1st frequency sweep: 0-200 Hz
		3							Skipped
		4							Keith's run #2; 2nd frequency sweep: 0-200 Hz; approx. 550 sec DP; approx. 69.8 G p2p on TE @30.67 Hz (39.0 G p2p LE); 19.8 G p2p on TE @ 75.32 Hz (13.86 G p2p LE
		5							Skipped; Reset accels to DC
		6							Keith's run #3; Repeat of DP004 to check Keith's plots
		7							Keith's run #3; Restart from A/D overrun error when trying to look at waterfalls (just before 2nd bending @ approx. 30.5 Hz)
		8							Skipped--Reset accels to AC
		9							Keith's run #4; Sweep 0-45 Hz only
		10							Keith's run #5; Sweep 25-35 Hz only; approx. 2025 sec DP; starts @ approx. 1st torsional w/pivot at chord/2; noticed in run 3 & run 4 very distinct edge in amplitudes of SG & accels & same on Keith's!? Actually can see on all runs @ same frequency. Note: LE & TE strain gages appear to be swapped (not wiring, but channel on board). Keith say they are correct based on tests.
12/9/2005									FSI Setup with new CADDMAS version with instrumented orange flex wing
									-from FSI signals: deleted "telemetry" & "Noise Def."
									-moved Polytec velocity--channel 17 (airfoil AOA accel)
									-moved Polytec displacement--channel 18 (airfoil flap accel)

APPENDIX D. CONTINUED

Date	Time	Data Point Number	Angle of Attack, α, deg.	Mach Number	Frequency, Hz	Mode	HWA Probe Position, inches	Velocity, m/sec	Comment
									Looks like PS9 & PS10 are swapped in wiring
		1							Baseline open tunnel after cals
									Velocity: A=39.37; B=0
									Vibrometer settings (on vib): velocity=25 mm/s/v & displacement=5120 µm/v
									Multiple gains by 2 on CADDMAS: velocity=50 mm/s/v=1.9685 in/s/v & displacement=10240 µm/v=10.24 mm/v=0.403 in/v
12/14/2005									Shakedown
									CADDMAS still gives buffer overflow error & DMA read error (this requires closing & reopening software).
									Torsion mode starts near M=0.075 torsion @ 20 Hz; very small flap mode at M=0.06
									M=0.088 transition from 1st torsion to 1st bending
									M=0.095 transition from 1st bending back to 1st torsion
									M=0.11 transition from 1st torsion to steady
									M=0.234 transition from steady to 2nd bending? (high displacement)
12/15/2005									block size 4096; fs=9766 Hz (this sampling rate not supported anymore) now using fs=15625 Hz
	9:36	1		off					Air off "zero" set
	9:39	2		0.07-0.09					Mach ramp, rake fixed, downstream of wall static
	9:49	3		0.09+/-					Rake sweep @ steady state, flap mode
	9:52	4		0.08-0.11					Mach sweep, rake downstream of wall static
	9:55	5		0.11					Rake sweep @ steady state, torsion mode
	10:00	6		0.10-0.120					Mach sweep, rake downstream
	10:05	7		0.12-0.14					Mach sweep, rake downstream
1/6/2006	7:50	1		0.14-0.16					Mach sweep (20 sec camera, CADDMAS longer)
	7:56	2		0.16-0.18					Mach sweep (20 sec camera, CADDMAS longer)
	8:01	3		0.18-0.2					Mach sweep (20 sec camera, CADDMAS longer)
	8:06	4		0.2-0.22					Mach sweep (20 sec camera, CADDMAS longer)
									Lots of CPU beeps, cold? Approx. 40 deg. F
	8:13	5		0.22-0.24					Mach sweep, rake downstream, start camera @ M=0.23
	8:14	6&7		0.24+/-					Rake sweep @ steady state flap/torsion?, no camera; DP006 stopped due to rake flutter

APPENDIX D. CONTINUED

Date	Time	Data Point Number	Angle of Attack, α, deg.	Mach Number	Frequency, Hz	Mode	HWA Probe Position, inches	Velocity, m/sec	Comment
	approx. 8:20	8		0.24-0.22					Mach descend, rake downstream
	8:29	9		0.12-0.10					Mach descend, rake downstream
	8:36	10		0.11-0.08					Mach descend, rake downstream
	8:44	11		0.09-0.07					Mach descend, rake downstream
	8:50	12		0.15-0.					Mach descend, rake downstream; Rapid kill!
	8:58	13		0.25-0.08					Mach descend, rake downstream
	9:05	14		0-0.26					Mach ascend, transient to begin increase in Mach no.; got A/D overflow error @ approx. M=0.26
	9:07	15		0.26-0.28					got weird & radical modes, hit wall
	approx. 9:30	16		0.26-0.264					Starting @ M=0.264 to 0.28, then backed down to 0.23--crazy stuff; stopped almost immediately from M=0.264
	9:38	17		0.2655					see multiple modes, 20 sec video & M=0.256 to 0.257, secondary flap is gone, more normal now, steady & min torsion @ approx. M=0.217
9/13/2006									Pitch Pot was on Ch016 (defined to be ch0 on 24 channel board) EUA=2652.6 EU/Volt EUB=156.453 DC signal cjaged tp DP synch input==EUA=1; EUB=0 Wall statics #1, 2, 3, 4, 5, 6, 8, 9 OK Wall statics #7,10,11 Look Dead (at least not connected to same ref & doesn't look same as rest #7 appears to move, but gain & offset way off. Pt Probes #2, 5, 7, 8 OK; rest bad
9/14/2006									FSI Flex Wing (Orange with telemety package) Validated Polytec ref positions with camera shots wrt ref positions (origin--see pics) X Y Depthcorr (compensates for blade curvature) -1.67 -8.2 0.2 -0.3 -8.2 0.45 1.2 -8.2 0.2 -1.67 -3.85 0.2 1.2 -3.85 0.2

APPENDIX D. CONTINUED

Date	Time	Data Point Number	Angle of Attack, α, deg.	Mach Number	Frequency, Hz	Mode	HWA Probe Position, inches	Velocity, m/sec	Comment
									-1.67 0.0 0.2
									1.2 0.0 0.2
									Note: the above X & Y values are relative to the origin. Chord length is 4.5 inches
		1							Check Data Storage via switch
		2							Check Data Storage via switch
									IRIG time on video & CADDMAS
									Rake pot appears to be off on cal, but starting at TE + 1 inch (to be safe on start up)
									Video: 10 sec shot; 20 sec down
		3		0.07					SS baseline; rake @ TE + 1 with video
									moved rake to full aft downstream
		4		0.07 to 0.125					Ramp to allow aero zero of AoA
									Note: DP didn't work because still in auto mode & did manual not via switch
		5		0.125 to 0.09					Ramp in approx 10 sec with video
		6		0.09					SS with video--torsional osc.

APPENDIX D. CONTINUED

Date	Time	Data Point Number	Angle of Attack, α, deg.	Mach Number	Frequency, Hz	Mode	HWA Probe Position, inches	Velocity, m/sec	Comment
		7		0.09 to 0.08					Ramp with video
		8		0.08					SS with video
		9		0.08 to 0.07					Ramp with video
		10		0.07					SS with video; changed video frame rate to 250 fr/sec==20 sec DP
		11		0.07 to 0.10					Ramp with video
		12		0.10					SS with video; Flap mode
		13		0.10 to 0.12					Ramp with video; starting in flap mode; osc stopped @ approx. M = 0.110
		14		0.12					SS
		15		0.12 to 0.14					Ramp
		16		0.14 to 0.16					Ramp; Very steady, slight dew on airfoil
		17		0.16 to 0.18					Ramp; Very stable
		18		0.18 to 0.20					Ramp; Very stable
		19		0.200 to 0.22					Ramp; Had CADDMAS error, aborted, return to M=o.20
		20		0.200 to 0.22					Ramp; Very steady, slight TE only twist
		21		0.22 to 0.24					Ramp
		22		0.24					SS
		23		0.24 to 0.255					Ramp
		24		0.255					SS; Large Displ: TE approx. 2X LE disp; Reduced to 0.23==stopped violent osc. @ M approx. 0.252 Increased to M = 0.255
		25		0.255 to 0.070					Ramp; turned off DP @ M= 0.115 to try for another video, but didn't recover in time Changed video to 165 frames/sec, set time for 1 minute. Restarted CADDMAS to be sure
		26		0.070 to 0.255 to 0.230					Ramp, video for 1 min., missed lower Mach no. modes--too fast of a sweep Reset M=0.70
		27		0.070 to 0.013					Ramp for 1st modes video @ 1 min., rake still full aft
		28		0.013 to 0.255 to 0.230					for second set of modes, video @ 1 min.; Banging mode starts and ends @ approx. M = 0.252
		29		0.23					Rake survey, Full aft to TE+0
		30		0.255					Rake survey with video; started @ TE + 0 to full aft
		31		0.10					Rake survey with video; started @ full aft to TE+ 0 to full aft; Torsion mode

APPENDIX D. CONTINUED

Date	Time	Data Point Number	Angle of Attack, α, deg.	Mach Number	Frequency, Hz	Mode	HWA Probe Position, inches	Velocity, m/sec	Comment
									Reduced speed to M=0.095
		32		0.095					Rake survey; started @ TE+0 to full aft: trying to get flap mode, but can't find it, though this looks like a transition
									Can't find pure flap mode again!!

NOMENCLATURE

M	Mach number
p_t	Total pressure, psi
p	Static pressure, psi
q	Dynamic pressure, psi
u	Local axial velocity, ft/s
u'	Axial perturbation velocity as standard deviation of u, ft/s
U_0	Mean axial velocity, ft/s
v	Local lateral local velocity, ft/s
v'	Lateral perturbation velocity as standard deviation of v, ft/s
γ	Ratio of specific heats